Ronny Oswald

Protein crystals

Definition and control of dissolution

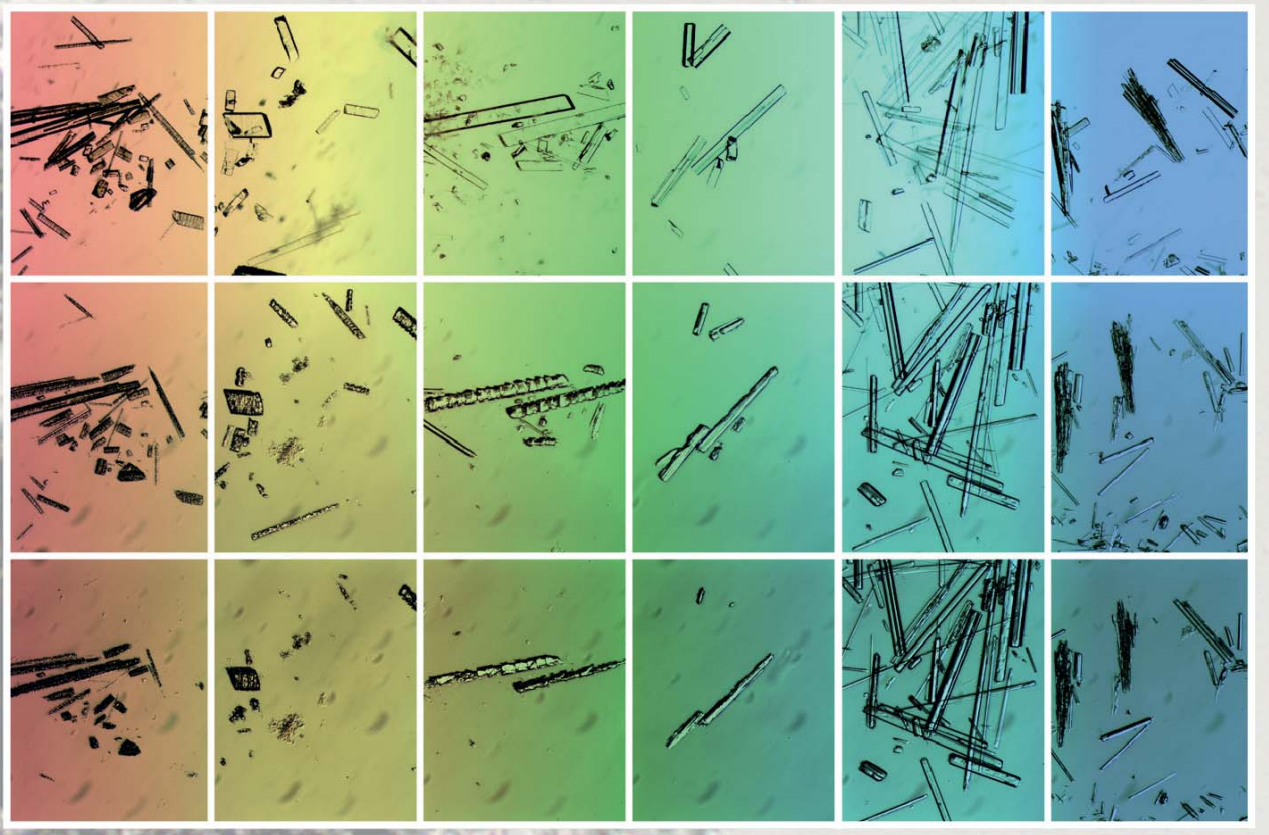

Cuvillier Verlag Göttingen
Internationaler wissenschaftlicher Fachverlag

Protein crystals
- Definition and control of dissolution -

Protein crystals
- Definition and control of dissolution -

Dissertation

zur Erlangung des
Doktorgrades der Ingenieurwissenschaften (Dr.-Ing.)

der

Naturwissenschaftlichen Fakultät I – Biowissenschaften –

der Martin-Luther-Universität
Halle-Wittenberg,

vorgelegt

von Herrn Dipl.-Chem. Ronny Oswald
geb. am 25.04.1982 in Dessau, Deutschland

Gutachter:	Prof. Dr.-Ing. Dr. h.c. Joachim Ulrich
	Prof. Dr. rer. nat. Markus Pietzsch
	Prof. Dr. Adrian E. Flood
Tag der öffentlichen Verteidigung:	Dienstag, 18.07.2017

Bibliografische Information der Deutschen Nationalbibliothek
Die Deutsche Nationalbibliothek verzeichnet diese Publikation in der Deutschen Nationalbibliografie; detaillierte bibliographische Daten sind im Internet über http://dnb.d-nb.de abrufbar.
1. Aufl. - Göttingen: Cuvillier, 2018
Zugl.: Halle-Wittenberg, Univ., Diss., 2017

Nonnenstieg 8, 37075 Göttingen
Telefon: 0551-54724-0
Telefax: 0551-54724-21
www.cuvillier.de

1. Auflage, 2018
Gedruckt auf umweltfreundlichem, säurefreiem Papier aus nachhaltiger Forstwirtschaft.

ISBN 978-3-7369-9706-6
eISBN 978-3-7369-8706-7

Acknowledgement

The research work presented was carried out during my stay at the chair of Thermal Process Technology, Center of Engineering Science at Martin Luther University Halle-Wittenberg as a research associate. My sincere thanks I would like to express to Prof. Dr.-Ing. Dr. h.c. Joachim Ulrich for the supervision of my PhD thesis and giving me the great opportunity to work on the subject of protein crystallization. Especially, the fruitful discussions on the found results.

Also sincere thanks I would like to express to Prof. Dr. Markus Pietzsch on the fruitful discussions during this work, especially "what a protein contains of", handling of the measurement of fundamental analyses, and the collaboration to prepare publication and conference distributions. Furthermore, the willingness to review my thesis.

Profs. Ulrich and Pietzsch also were part of the exam committee which was chaired by Prof. Dr. rer. nat. Reinhard Neubert, Prof. Dr. Ralf B. Wehrsporn, Prof. Dr.-Ing. René Androsch and Prof. Dr.-Ing. Hans-Joachim Radusch acted as further members of the committee. I thank all of them for their participation.

I thank Prof. Dr. Adrian E. Flood for his review of my thesis and some suggestions to improve the English grammar.

Furthermore, I have to say thanks to Ms. Andrea Alles and Ms. Bettina Karger from ITA Instruments KG Hettenleidelheim for the provision of prototype lab equipment during the development of this devices and the implementation of some of my ideas developed during this work, especially, the "Vision" probe.

I like to thank all of the students who worked with me on the topic of protein crystallization. Especially Guilherm, Martin, Qingkai, Ralf, Susi and Yassin.

I would like to thank all my TVT colleagues and friends, for the unforgettable time that I had with them during these years. I thank them for all of their help and support. Especially Ahmed, Anne, Claudia, Dan, Felix, Franzi, Gerhard, Haihao, Hamid, Isabel, Jiting, Julia H., Julia S., Kati, Kristin, Lydia, Martha, Maryam, Miaomiao, Mohammad, Patrick, Phuong, Sandra, Steffi, Viviana, Xiaoxi, Yi , Ms. Höser and Mr. Kleinert.

I am also grateful for the support of the Chinese-German Center to Promote Science (GZ: 935), which gave me also the opportunity of travel to China.

I would, especially, like to thank my family who supported me always.

Contents

1 Introduction

Crystallization of proteins was in past decades mostly used to prepare large and highly pure crystals, to determine the structure of the protein crystals by X-ray measurements [Des11]. With the increase of industrial applications of proteins [Bre08], the desired amount of high purity proteins is increasing, too. Crystallized proteins offer an improved shelf life with a very high degree of preservation of the protein enzyme activity. A further important advantage of protein crystallization is purification at low cost in industrial mass production [Hun03; Jon14]. A large number of studies on the crystallization of proteins with the aim to optimize purity, yield, shape or activity were performed, e. g. by Durbin and Feher [Dur96] or McPherson [McP90]. In research papers on protein crystallization, lysozyme is the most often described protein because it is easily available and it is of fairly low cost. In most cases, however, only the crystallization processes are investigated, the dissolution is neglected even though dissolution of crystals is of most importance for the use of the proteins after storage. Dissolution with respect to the mechanism is known to be the reverse of the crystal growth process (see e. g. Ulrich and Stelzer [Ulr11]).
Müller and Ulrich [Mül12a] described the first time an unusual dissolution behavior for protein crystals which is different from a conventional dissolution behavior, and cannot be explained in the same way as the traditionally known dissolution processes. For a better controlled use of crystallized proteins in future, it is necessary to observe and understand those dissolution mechanisms. One reason for the importance of an understanding of the prediction of the dissolution behavior is bioavailability of pharmaceuticals. Due to the high price most proteins could be examined in only a low quantity. Therefore, new technologies of the examination need to be developed. Furthermore, the term “protein crystal” is not well understood. Usually it is assumed that the crystallization of a protein follows the same rules as a crystallization of conventional crystals. A protein crystal contains, how-

ever, not only protein but also water, buffer and salt (see e. g. Ulrich and Pietzsch [Ulr15]). Also, the molecule size of a protein is much larger than inorganic and even most of the organic compounds. A protein delivers many functional groups distributed over the molecule chain length.
All different components in a crystal, when they are a matter of change, can if big enough change the crystal lattice. Definitely, a change of the amount of a component in a crystal will change its chemistry. This is very much like in solvates or hydrates, but it can also be imagined that the change of the environment (composition of the *liquid phase* around the crystal) of a protein crystal might not change its chemistry but just its lattice, then a classical polymorph would be faced. In both cases (solvate or polymorph) the physical properties (density, solubility, dissolution rate, color, hardness, etc.) can be changed. A phase diagram would be extremely helpful in order to determine the stability ranges (the respective metastable zones). There are, however, not much of such data known.
It is necessary to know whether a crystal pattern of one crystal modification stays the same even if there is e. g. a slight deviation in pH value existing during crystal growth or not. With all of these information's it should be possible to present a new understanding in the crystallization of proteins and on the dissolution mechanism, too, as well as their metastable zone widths.

2 State of the art

The number of papers on protein research respectively protein crystallization, is large. In this Chapter only the literature is cited which is necessary to explain and understand the crystallization of the protein lysozyme and the chemistry to understand structural conditions. This Chapter introduces the fundamentals in order to be able to follow the discussion in this work. Most of the information can be found in textbooks (e. g. [Wie02; Jon14; Mul01]).

2.1 Proteins

A protein is a biological macromolecule. Those macromolecules are built of amino acids connected by peptide bonds. All proteins are built based on 20 different amino acids (e. g. see Karlson et al. [Kar94]). The resulting protein is a long peptide chain of amino acids with varying number and sequence.
The structure of a protein is not only a long straight line. The protein structure is described by the primary, secondary, ternary and quaternary structure. The primary structure is the sequence of amino acids. The secondary structure describes the local substructure due to hydrogen bonds between CO and NH groups. The ternary structure describes the three-dimensional structure of a protein molecule. In addition to the hydrogen bonds of the secondary structures, some more bonds are responsible for the formation and stabilization of such a structure. Those bonds are hydrophobic interactions, disulfide bonds between cysteine groups by dehydration of HS groups, and some ion bonds due to positive and negative charged side chains. The quaternary structure is formed by the arrangement of more than one protein molecule. Existing complexes of two domains as dimers and of several domains are called multimers. Depending on the properties of the side chains, e. g. the charges of side chains, the domains

are organized in a specific order. Many proteins do not build a quaternary structure, they function as monomers. An overview of the build-up of the different structure elements of a protein can be seen in Figure 2.1 according to Karlson et al. [Kar94].

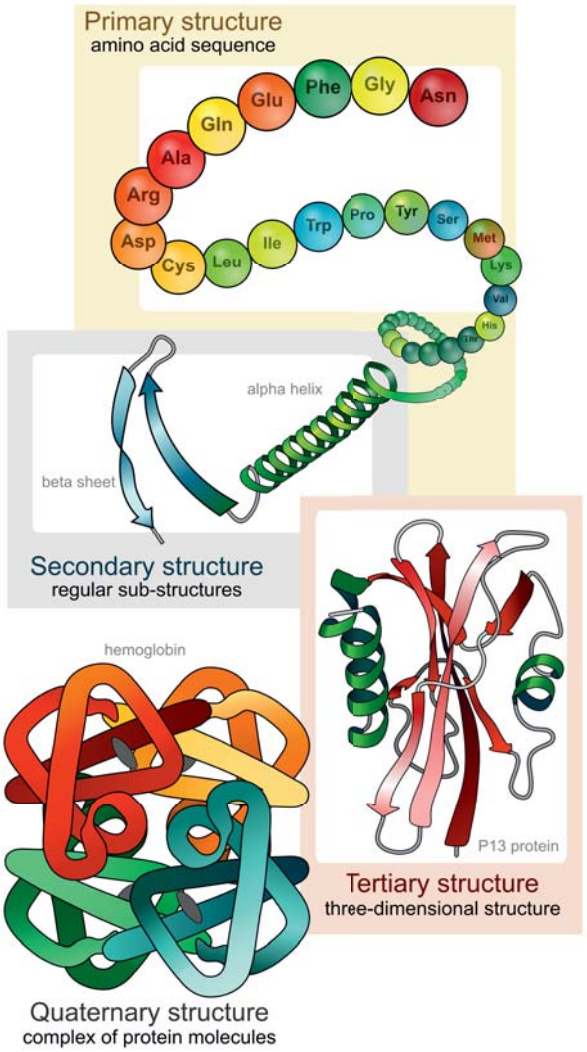

Figure 2.1: Overview of the structure of proteins according to Karlson et al. [Kar94]

2.1.1 Amino acids

Amino acids consist of a central alpha carbon atom which connects an amino group, a carboxyl group and a mutable side chain to each other. This can be seen in the structural Formula 2.1. The residue side chain

is characteristic for different amino acids. There are non-polar aliphatic and aromatic amino acids, and amino acids with uncharged polar residual groups available. But there are also amino acids existing with positive and negative charged side chains.

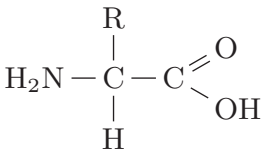

R=mutable side chain (2.1)

The charge of this side chains is impressionable by pH value. The equilibrium of each charge is defined by the pKa value. The effect of changed charges by the pH value on the ends of the protein chain is shown in reaction Equation 2.2. Also, the residual is often able to be charged.

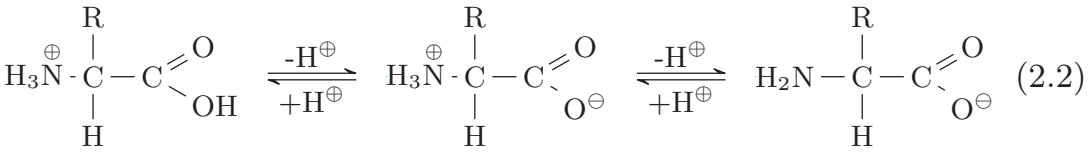

(2.2)

positive charged neutral negative charged

2.1.2 Peptide bond

A peptide bond which is used to form the primary structure of a protein is a strong covalent bond. The formation of a peptide bond is shown in the reaction Equation 2.3.

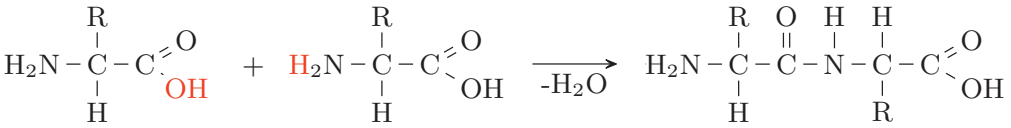

(2.3)

2.1.3 Surface charge

Based on the above stated it is possible to assume that if an amino acid is able to have a point which can be electrostatically charged, the built

protein molecules have several charges distributed over the whole molecule chains due to the formation of polypeptide bonds between the amino acids. In science this is called a polyelectrolyte [Pod06].
The different charges with different polarity, and a formation of disulfide and hydrogen bonds, form the secondary and ternary structure of the protein molecules. Some of the charges of different polarity neutralize each other already, other charges are located at the exterior of the protein molecule. Those have to be neutralized by the solvent molecules in the *liquid phase*, or so called "counter ions" in the *solid state*.

2.1.4 Isoelectric point

The pI (isoelectric point) describes the pH value at which the positive and negative charges will balance and the net charge will be zero. Usually in literature the protein solubility is minimal at the protein's isoelectric point [Ric92]. If there is a charge at the protein surface, the protein prefers to interact with water, rather than with other protein molecules. The charge makes the protein more soluble.

2.1.5 Active site

In chemistry, an active site is called the point at which the catalyzed reaction of a catalyst occurs. In the field of enzymes, it describes the area of the enzyme which is responsible for the catalyzed reaction. Catalytic residues of the site interact with the substrate to lower the activation energy of a reaction and therefore to make it proceed faster. There are two models of binding the substrate to the enzyme, the "lock and key hypothesis" and the "induced fit" [Sul08]. Due to this property, a protein molecule is able to increase the reaction rate of a specific reaction. This is called the "activity of a protein" which can be measured by methods depending on the chosen protein. If the structure of a protein is influenced by the pH, the activity of a protein is affected, too. Here are still some open questions. If there are different modifications existing which are crystallized at different pH regions, is also the enzymatic activity influenced by the modification? Will the modification have an influence on the shelf life of the activity? Furthermore, there are no reasonable information about

the shelf life of crystallized proteins by means of activity preservation with changing humidity and temperature conditions in literature given yet.

2.1.6 UV/Vis activity

UV/Vis activity describes a phenomenon of a substrate, which will be illuminated by light with a wavelength in region of UV up to visible light, is able to decrease the light emission at a small wavelength region. This is due to movement of electrons from a lower energy level to a higher level. The wavelength can be calculated by use of the plank constant and the energy difference between both levels. Different energy levels exist for organic molecules which are unsaturated. Depending on the concentration of those substrate the absorbance is changed. With use of several substrate concentration a calibration curve can be plotted, to subsequently measure the concentration of any substrate with a UV/Vis spectrophotometer. In 1969, Aune and Tanford [Aun69] described this phenomenon for the first time for the protein lysozyme. In 1989, Gill and von Hippel [Gil89] presented a method to calculate the extinction coefficient of any protein by the known amino acid sequence. This is possible due to the fact that many of the known amino acids are able to be UV active depending on the residual chain. A protein is a combination of those amino acids (see above) and by formation of the peptide bond between amino acids and therefore also UV active.

2.2 Buffersystems in protein crystallization

2.2.1 pH buffer

Per definition a buffer is a mixture of substances with a pH which changes very little when a small amount of strong acid or base is added to it, and thus it is used to prevent changes in the pH of a solution. A buffer solution (also called pH buffer) is an aqueous solution consisting of a mixture of weak acid and its conjugated base, or vice versa.
With use of the Handerson-Hasselbalch equation, the context between the pH value and the point of the equilibrium of the acid-base-reaction of an acid and its corresponding base is described. With this equation, it is

possible to calculate the pH value out of the concentration of buffer components. More information on the concept of acid and base can be found in textbooks (e. g. see Holleman and Wiberg [Hol07] or Riedel [Rie04]).

2.2.2 Precipitants

With precipitants, the solubility of proteins can be affected in different ways depending on the used ions. Hofmeister ranked the efficiency of a variety of electrolyte types to salt-in and salt-out of proteins in 1888 [Hof88]. Due to this effect, a new solvent system is created and thus has a different solubility on the solved protein and other substances.

Salting-in

The salting-in can be explained by the Debye-Huckel theory. The electrolyte concentration affects the value κ, the inverse Debye length. An increase of the electrolyte concentration causes an increase in the ionic strength, which increases κ and thus, protein solubility. This theory is working with low ionic strength but fails for moderate and high electrolyte concentrations. Also, it fails to predict the commonly observed salting-out behavior of proteins [Wie02].

Salting-out

A popular explanation for this effect relies on the relative hydration of the protein versus bulk electrolyte. The electrolyte is assumed to bind bulk water, as water of hydration near the ions surface. The bulk electrolyte and the protein molecules compete for bulk water to hydrate their respective surfaces. The dehydrated protein molecules fill such exposed dehydrated surface with other protein molecules. Thus, the solubility of the protein is reduced [Wie02].

2.2.3 Anti-solvent

An anti-solvent is the addition of a small polar organic solvent, as an example methanol or ethanol. It works in a similar manner as electrolytes do and competes with the protein for water molecules. Furthermore, the solvent tends to lower the dielectric constant of the water and enhances

electrostatic interactions between protein molecules, which reduces their solubility. The lower dielectric constant tends to solubilize the hydrophobic core of the protein molecule. This results in unfolding and denaturation of the protein. (see e. g. Wiencek [Wie02])

2.2.4 Polymers

Polymers are also often used to lower the solubility. Especially polyethylene glycols (PEGs) of different molecular weight are used. The molecular weight must be optimized for each protein. At the moment it is not clear how it is working, but it tends to be a similar way as an anti-solvent. It will hydrate and change the dielectric constant of the solvent also. (see e. g. Wiencek [Wie02])

2.3 Crystallization

2.3.1 Metastable zone

The metastable zone covers the region between two lines in the plot of concentration versus temperature. The first line in this plot is the solubility line. The solubility line is a thermodynamic value, it covers the maximum amount of a substance which can be dissolved in the used solvent. The second line is the nucleation line. This is a kinetic value. This means the position of the nucleation line is influenced by the method which is used to determine this value, and it is depending on process parameters.
The first major investigation on solubility of proteins was presented by Howard et al. [How88]. It covers the temperature dependence over a range of pH values between 4 and 7.5, and also the amount of salt was investigated. The data show that the solubility of lysozyme is strongly dependent upon the sodium chloride concentration. This behavior is consistent with the inverse Hofmeister series behavior (e. g. see Riès-Kautt and Ducruix [Riè91] and Zhang and Cremer [Zha09]) as expected for a basic protein [Jon14].
A more comprehensive study of lysozyme chloride solubility was carried out by Pusey's group [Pus88; Cac91a; Cac91b; For96; For99a] using the column method presented in 1988 [Pus88]. The results show clearly that

protein solubility behaves in a similar manner when compared to the majority of small molecule organic compounds, in that the solubility increases with temperature [Jon14]. The behavior of the solubility as function of the precipitant concentration decreases with increasing salt concentration. For the acetate buffer concentration in the range of 0.01 up to 0.5 M the solubility appears to have a minimum for an acetate concentration of 0.1 M. Already Cacioppo and Pusey [Cac91b] in 1991 showed in their 3D plots the influence by the pH value at a higher solubility at certain pH values. The influence by the pH value is not straight-forward as oscillations were observed within the small observed pH intervals. The overall data show, however, the expected trend for a solubility decrease as the pH value approach the pI (see Chapter 2.1.4). In the paper of Forsythe et al. [For99a], the following sentence is written: *"The effect of pH is not clearly seen and varies unpredictably with pH"*. There is a lack of information on the influence of the pH value on the solubility of protein crystals, since there is no mechanism known to explain the results based on a scientific background. An overview of the effects of the pH value in the field of crystallization (except protein crystals) can be found in the work of Mohameed [Moh96b]

2.3.2 Kinetics

The growth rates of protein crystals are typically measured via a microscope with controlled image capturing systems. The crystals grow in a temperature controlled cell. A capturing system takes images and from the length difference of a growing crystal over a period of time. Therefrom, the growth rate is calculated [Dur86]. Due to the limited amount of mother liquor in such a cell and the small space the microscope system is able to capture, only a small portion of crystals can be measured at the same time. But there is GRD (growth rate dispersion) existing, which means each crystal is different from each other, some crystals are growing fast, others are growing slow. An automated computer supported growth rate measurement system is presented by Pusey [Pus93]. This system is able to measure 40 crystals at the same time within one cycle. If 40 crystals can be placed and measured at the same time in such a system, still it is not clear if these are fast or slow growers? To determine the average rates, much more crystals must observed. An overview about this phenomenon

is given in the review of Ulrich [Ulr89]. But not only the growth rate, also the dissolution rate is affected by a dispersion [Fab93]. It is clear at this moment that the average growth and dissolution rates are of extremely high interest for an industrial protein crystallizer design. Other techniques have to be used for their determination. At this point the fluidized bed technique delivers a quite good method for the measurement of an average growth rate in crystallization. Information on this technique can be found e. g. in the work of Ulrich and Stepanski [Ulr87] or Mohameed and Ulrich [Moh96a].

2.3.3 Protein crystals

The research and definition process of "what is a protein crystal" is still in progress. It is known that a protein crystal consists of several components. To crystallize a protein, the components needed are:

- the protein itself
- the solvent to form a hydrate, e. g. water
- the precipitant, e. g. sodium chloride
- the buffer substance to control and maintain a fixed pH value

An overview is given by Ulrich and Pietzsch [Ulr15]. There are several pieces of information about the water and the salt content in a protein crystal given, but no quantification of the ingredients yet. Also, a protein is able to be crystallized in a wide range of pH values (for the lysozyme chloride e. g. 4 to 10), but only some modifications (for lysozyme LTO [Low Temperature Orthorhombic], HTO [High Temperature Orthorhombic], tetragonal, monoclinic and triclinic) are known [Nad96; Saz99; Oki99; Art82; Wie02; Ald09b; Wan07]. Here some structural information would be useful. By the end there is a big field of unknown information, which are of fundamental interest in the field of protein crystallization. Especially an accurate naming of protein crystals with information on the substances that were incorporated in the crystal during crystallization.

2.3.4 Dissolution of crystals

The dissolution of crystals is widely neglected in research. This is due to the assumption that the dissolution of a crystal is exactly the reverse of crystal growth [Ulr11]. Somasundaran and Hubbard [Som06] stated: *"Generally, there is no conceptional difference between crystal growth and crystal dissolution in the crystal-solution system... These processes are believed to be reverse process, although, in many cases, different elementary steps control the rate of the two processes. Crystal dissolution can be considered to be crystal growth in undersaturated solution, involving the same elementary processes, with net fluxes of ions or molecules in the opposite direction."*. Müller and Ulrich [Mül12a] described an unusual dissolution behavior for protein crystals, which is different from a conventional dissolution behavior, and cannot be explained in the same way as the known dissolution processes. In literature, [Mat88; Bei01; Pau07] describe a similar "falling apart" mechanism as shown by Müller and Ulrich [Mül12a] for proteins. This behavior appears in the case of binary systems at conditions when only one of the components will dissolved, or will partially be molten. Still the question remains, is it possible that the dissolution is the same process as the reverse of crystal growth? By Müller [Mül12b] the dissolution experiments where conducted in a non-systematic way since the focus of her work was on different topics. Often more than one parameter was changed during a measurement series. There is also no information given on the crystallization and harvesting process of the protein crystals, which afterwards will be dissolved. No information on wet or dried crystals is given. Based on her work it is not possible to understand the dissolution behavior of the protein crystals, and to determine a mechanism or to show reasons for different dissolution phenomena.

3 Aim of the work

In Chapter 2, an overview of some fundamentals, and the state of the art in the field on the crystallization of proteins are given.
Based on that information it is possible to conclude that the following questions remain open:

- The solubility line of the protein lysozyme with sodium chloride as precipitant is well examined for some pH values. The nucleation line is still not so clear due to the influence of the used detection methods. Both lines are plotted versus several parameters (e. g. concentration and substance of precipitant or buffer, temperature etc.) with quite good explanations on the shape of the curve, and the order of the curves with respect to each other. But there is still the effect of the pH value which is not completely understood. As it is said by Forsythe et al. [For99a]: *"The effect of pH is not clearly seen and varies unpredictably with pH."*

- Since proteins are mostly expensive, only small amounts can be used in microscope cells to determine the crystallization kinetics. The phenomena of growth and dissolution rate dispersion are, however, present. New methods must be developed, for an easy measurement of the average growth and dissolution rates considering the dispersion.

- An interesting dissolution mechanism of protein crystals exists besides the classical dissolution mechanism (rounding and shrinking homogeneously) [Mül12b]. However, there is no explanation of this behavior given yet.

- The conditions of humidity and temperature where the crystallized proteins remain stable, concerning the enzymatic activity during storage, should be determined.

- Protein crystals are known to be multi component systems in literature [Ulr15]. But a lack of several fundamental information on protein crystals is still remaining. This is also true for their names. To identify their chemical composition and their chemical modification, the naming needs more information than just to be named by the proteins name (e. g. “lysozyme” crystal).

4 Materials and methods

4.1 Crystallization conditions for lysozyme

Lysozyme is often used as model substance in fundamental protein crystallization research. It is easy to crystallize compared to other proteins, and has fairly low cost if it is purchased by professionals at high purity. Lysozyme crystals can be produced in six different crystal modifications (tetragonal, HTO [High Temperature Orthorhombic], LTO [Low Temperature Orthorhombic], monoclinic, triclinic, hexagonal [Nad96; Saz99; Oki99; Art82; Wie02; Ald09b; Wan07; Bri06]). The conditions of the crystallization for the three different modifications used in this work are shown in Table 4.1. The table shows the conditions after mixing two kinds of solutions. The first solution is the buffer with a defined pH value, and double the concentration of the salt sodium chloride than shown in Table 4.1. The second solution is the same buffer, however, containing no salt, but it contains the double concentration of the protein lysozyme than shown in Table 4.1. The salt which acts as precipitant is lowering the solubility of the lysozyme. Nucleation will occur and crystals will grow within one day to a reasonable size. This procedure in crystallization is called "salting-out" [Wie02] and is explained in Chapter 2.2.2.

Table 4.1: Lysozyme crystallization conditions according to Müller [Mül12b] and Aldabaibeh [Ald09a]

	tetragonal	HTO	LTO
lysozyme concentration	$50\,\mathrm{mg\,ml^{-1}}$	$100\,\mathrm{mg\,ml^{-1}}$	$50\,\mathrm{mg\,ml^{-1}}$
buffer type (components)	acetate	acetate	glycine
buffer concentration	0.1 M	0.1 M	0.05 M
pH	5.0	5.0	9.8
salt type	NaCl	NaCl	NaCl
salt concentration	4 wt%	6 wt%	4 wt%
temperature	4 °C	40 °C	20 °C

4.2 Width of the metastable zone

For the determination of the metastable zone width, the ”Incentive” parallel reaction station from ITA Instruments KG Hettenleidelheim was used. The connected computer system is able to control the speed of the stirrer, and the management of temperature profiles in each of the reaction vessels. The ”Vision” probe combines the known turbidity measurement (in the field of protein crystallization see e. g. Maosoongnern et al. [Mao12]) which is carried out at narrow IR wavelengths, with additional wavelengths for inline measurements. In the field of protein crystallization, the wavelength 280 nm is of interest to calculate the concentration by the method published by Gill [Gil89]. This is already described in Chapter 2.1. The ”Vision” probe has summarized the function of an inline UV/Vis photometer.

To measure a cloud point (nucleation) and a point of the solubility line, volumes of approximately 1 mL are necessary. An insert (see Figure 4.2) is used to measure in small HPLC tubes as sample vessel. The infrared light goes directly through the HPLC tube and the containing sample (see scheme in Figure 4.1).

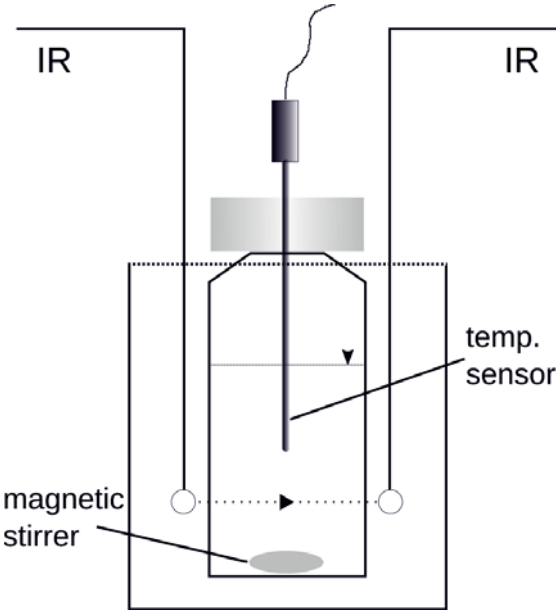

Figure 4.1: Scheme of turbidity measurement insert for HPLC tubes

Figure 4.2: Image of turbidity measurement insert for HPLC tubes

With the turbidity technique it is possible to determine the width of metastable zone. A solution with known concentration will be placed in one of the reaction seats. A program with a temperature profile as shown in Figure 4.3 is executed. During the cooling, the turbidity shows the point of nucleation by a decrease in intensity. After cooling to a given point the solution is heated up again. At the temperature where the intensity increases again is the point of solubility, the crystals are dissolved. The intensity versus time of one of those cycles is shown in Figure 4.4. The Figure 4.4 shows also the used curve area for the calculation of the temperature of nucleation and solubility. The first point is the start of the turbidity decrease which is the point where nucleation occurs. The start of the turbidity increase locates the point where the crystals starts to dissolve. The point at which the crystals are completely dissolved, is not used for the calculations. The heating rate allows to calculate a higher temperature for the solubility. In the case of an infinitely slow heating rate both points have the same temperature, since the crystals will dissolve already at the point where the turbidity signal starts to increase!
Exact points, which means the right temperature of the intensity versus time plot is determined by the numerical second derivation. The first derivative shows several peaks which correspond to the reversal points and are shown in Figure 4.5. The second derivative shows the desired points. This points were found by a ”peak search” function in the software ”Origin”. The second derivative is shown in Figure 4.6. The time found by the function ”peak search” of Origin software is used to read the measured temperature of nucleation and solubility line out of the temperature versus time plot. This method is used for each concentration to plot the thermodynamic diagram of solubility including the nucleation line.

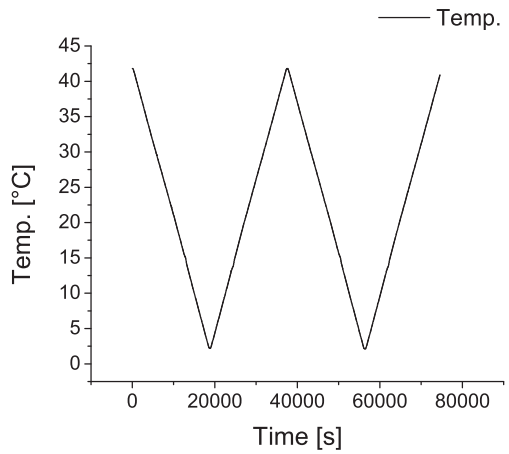

Figure 4.3: Incentive plot of temperature versus time

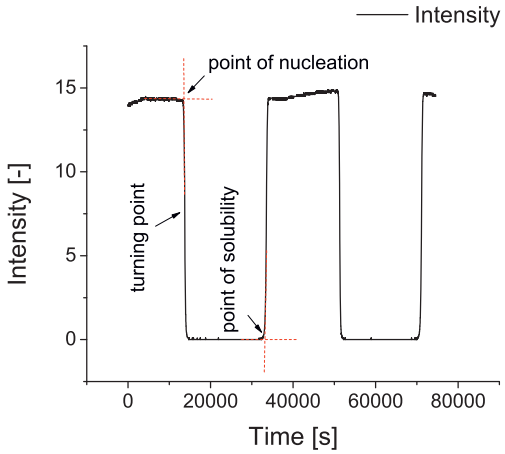

Figure 4.4: Incentive plot of IR signal versus time

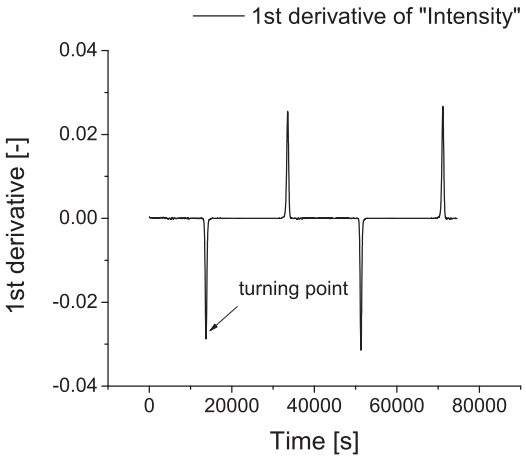

Figure 4.5: First derivative plot of IR signal versus time

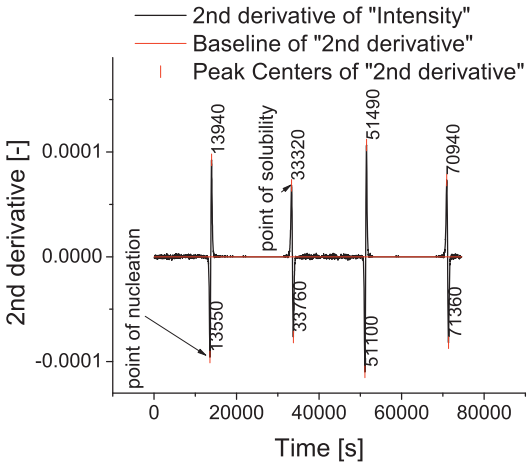

Figure 4.6: Second derivative plot of IR signal versus time

4.3 Kinetic measurements

To determine the crystallization kinetics of protein crystals, three different methods were developed in this work. Not all of these methods were verified to work as measures for the growth and dissolution rate determination. The major points to be considered in the development of this methods were:

- Only low amounts of substances should be required to determine the kinetics due to the high price of the proteins.
- Kinetic measurements considering growth and dissolution rate dispersion should be possible.

- The method should be reasonably fast to determine each point in less than two days.

4.3.1 Modified solubility measurement set-up

To measure crystal growth rates, one of the best-known methods is a fluidized bed technique. In comparison to a measurement in a microscope cell, an average growth rate of many crystals is measured in a fluidized bed. Also, a continuous stirred reactor can be used to measure kinetic rates with respect to the rate dispersions, but the stirrer might grind the crystals which distorts the measurement. A perfect mixing (temperature and concentration) in a stirred tank is also a problem. In a fluidized bed, the crystals in a suspension are mixed automatically. The crystals will be suspended by the flow rate of the supersaturated liquid and not by a stirrer. The supersaturation in such a conventional fluidized bed is realized by lowering the temperature of saturated solution (see e. g. Omar et al. [Oma10]). However, due to the high amount of solution necessary to use such an equipment in its conventional design, and due to the high price of the protein, such a technique can unfortunately not be used unchanged here. A modified measuring technique is therefore required.
From Chapter 2.2.2 the salting-out technique is known and already used in the preparation of the lysozyme crystals (see Chapter 4.1). By mixing two components it is possible to produce a supersaturated solution. A dosing unit with two separate channels is required. By such an unit, the same amount of buffer containing salt, and buffer containing the protein, can be mixed to form a supersaturated solution. The level of supersaturation can be measured on-line with a spectrophotometer at the wavelength of 280 nm. The flow inside the new type fluidized bed circuit is driven by a peristaltic pump. The diameter of fluidized bed is 6.6 mm. A mixer to feed the supersaturated solution in the circuit is realized by a small batch reactor with stirrer. The whole circuit contains approximately 3 mL of liquid and is temperature controlled. In Figure 4.7 the flow chart of the new type of fluidized bed is shown. At the start of the experiment the measurement system is in equilibrium. The solubility concentration of a fixed temperature can be calculated by the photometer data at 280 nm. A fixed amount of crystals (200 mg, larger amounts for a bigger accuracy)

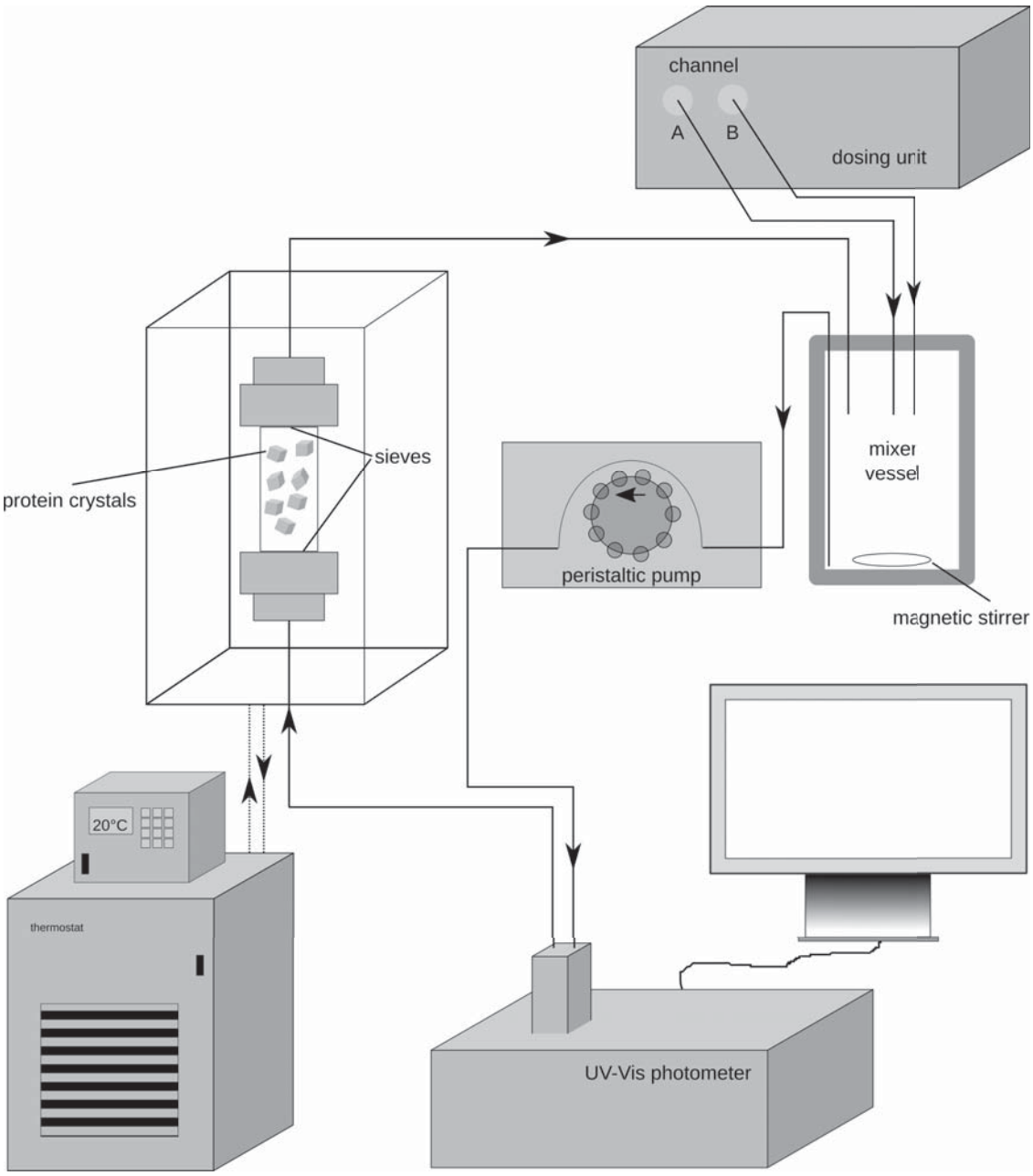

Figure 4.7: Modified solubility measurement circuit to determine kinetic studies

will be placed inside the column and the dosing unit will be started. After a period of time, the photometric measurement at 280 nm will settle to a steady state. The difference between solubility concentration (equilibrium) and the new achieved steady state is the calculated level of supersaturation during crystal growth. By different dosing rates different equilibria, for values of different levels of supersaturation (see e. g. Figure 4.8) can be set.

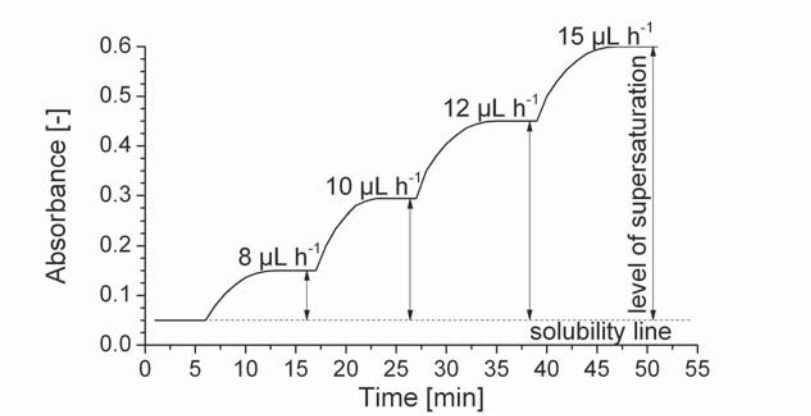

Figure 4.8: Example diagram of modifyed kinetic measurement

$$growth\ rate(t) = \frac{\mathrm{d}m_{cryst}(t)}{\mathrm{d}t} = m_{cryst_0} + \dot{V}_{dos}(t) * (\beta_{dos} - \beta_{circuit}(t)) \quad (4.1)$$

$$growth\ rate = \frac{\Delta m_{cryst}}{\Delta t} = m_{cryst_0} + \dot{V}_{dos} * (\beta_{dos} - \beta_{circuit}) \quad (4.2)$$

$$growth\ rate_{normalized} = \frac{\Delta m_{cryst}}{\Delta t * m_{cryst_0}} \quad (4.3)$$

$\dot{V}_{dos}(t)$	volume rate of dosing in relation to time
$\dot{V}_{dos}$	constant volume rate of dosing
β_{dos}	protein mass conc. of dosing liquid
$\beta_{circuit}(t)$	protein mass conc. of circuit in relation to time
$\beta_{circuit}$	protein mass conc. of circuit at steady state in relation to time
m_{cryst_0}	mass of crystals at time zero (weighted crystals for measurement)
Δm_{cryst}	mass increase of crystals in column
Δt	measurement time interval
$\mathrm{d}m_{cryst}$	infinitesimal mass increase of crystals in column
$\mathrm{d}t$	infinitesimal measurement time

The limit is the point at which nucleation occurs where the mixing of both channels takes place. By the volume rate and the concentration of dosing, the increase of the crystals inside the column in mass versus time can be calculated by Equation 4.1. Due to the steady state (volume rate kept constant and thus the mass concentration of circuit remains the same), the Equation 4.1 can be simplified to Equation 4.2. Due to mass tolerances of weighting of crystals, the crystal mass in the column has to be included in the growth rate following Equation 4.3 to compare the measurements, and calculate a value independent from the appointed crystal mass.

4.3.2 Vision probe

This technique using a "Vision" probe was already introduced in Chapter 4.2. The probe acts in this technique as a photometer, and detects the absorbance at 280 nm in wavelength. A vessel is used as batch crystallizer. Crystals with known mass (here 20 mg) were placed inside the vessel. The undersaturated solution (without any content of protein) was added into the vessel as fast as possible, and the "Vision" probe detects the concentration of the protein in the solution in the volume above the sieve and the stirrer. A grinding of the crystals by a stirrer must be avoided since it will influence the results. Also, the crystals have to be shielded from the probe window of the "Vision" probe. The crystals will block the pathway of light and will act as turbidity and again the results will be distorted. Some tests were done in 2 mL Eppendorf tube without stirrer. Experiments with stirrer were tried with two different mesh sizes of metal sieves to prevent problems by separating probe or stirrer on the one hand and the crystals on the other hand (Figure 4.9). Some problems with gas bubbles under-

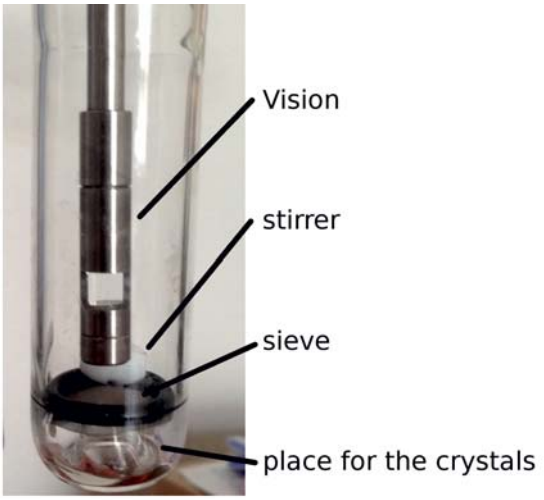

Figure 4.9: Picture of the vessel to determine crystallization kinetics by a Vision probe.

neath the sieve might occur. Furthermore, a measurement without sieve but with a prevention of crystals being grinded by the stirrer through a "nose" in the glass vessel (same used in Figure 4.9 without the sieve) gives the best results. The stirrer will sit on this "nose" and cannot come in contact to the crystals.

4.3.3 UV/Vis photometer

A UV/Vis photometer was also used to determine kinetic values of the dissolution of protein crystals. The beam of the photometer has its pathway approximately 10 mm above the bottom of the cuvettes. Again, the crystals were placed on the bottom of the cuvettes. No stirrer was used in these experiments to prevent the crystals from being grinded. The solution to dissolve the crystals were instantly added, and the photometer detects the absorbance at 280 nm to calculate the concentration of solution in the upper part of the cuvettes. As photometer the analytikjena SPECORD 40 UV/VIS was used.

4.3.4 Calculation example of dissolution rate measurements

The measurement with both devices gives diagrams (if the absorbance is already calculated into concentration) of concentration plotted versus time (shown in Figure 4.10). The concentration should start with a value of zero at time zero, and increase with time depending on dissolution rate and amount of crystals. For data preparation, in the first step the mass loss of protein crystals versus time is calculated according to Equation 4.4.

$$dissolution\ rate(t) = \frac{\mathrm{d}w_{cryst}(t)}{\mathrm{d}t} = \frac{m_{cryst_0} - V_{solution} * \beta_{solution}(t)}{m_{cryst_0}} \tag{4.4}$$

$w_{cryst}(t)$	mass fraction of crystals in relation to time
m_{cryst_0}	mass of crystals at time zero (weighted crystals for measurement)
$V_{solution}$	volume of solution to dissolve crystals
$\beta_{solution}$	mass conc. of solution to dissolve crystals (measured versus time)
$\mathrm{d}t$	infinitesimal measurement time

From this calculation, a plot of the remaining crystal mass versus time is possible (shown in Figure 4.11). Compared to the growth rate measurement in Chapter 4.3.1, the mass concentration is not constant and thus a calculation of the first derivative of $\frac{\mathrm{d}w_{cryst}(t)}{\mathrm{d}t}$ (crystal mass fraction versus time) is necessary since the dissolution rate changes with time respectively mass concentration. The plot of this first derivative versus time and the measured mass concentration (the mass concentration increases with time), results from the dissolution rates measurement of a big range of mass con-

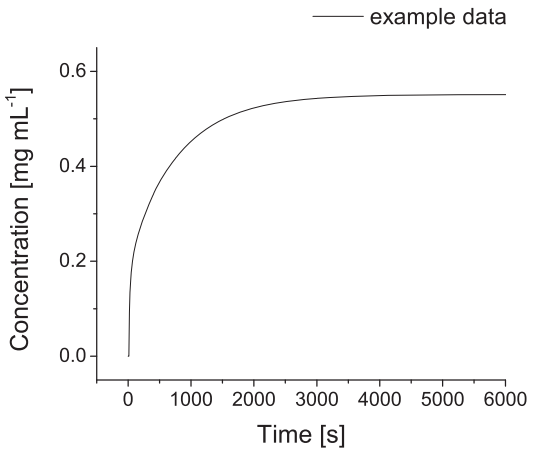

Figure 4.10: Example diagram, dissolution of protein crystals

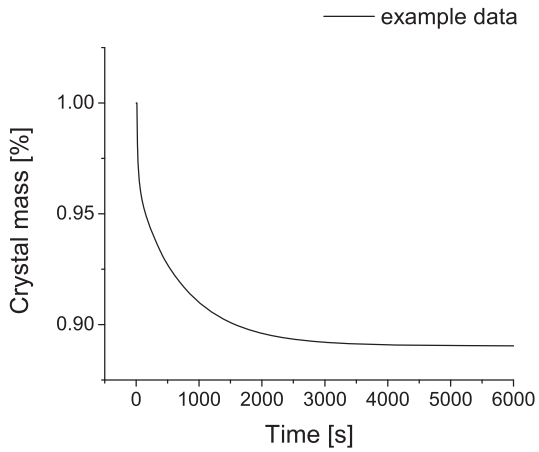

Figure 4.11: Calculated crystal mass versus time

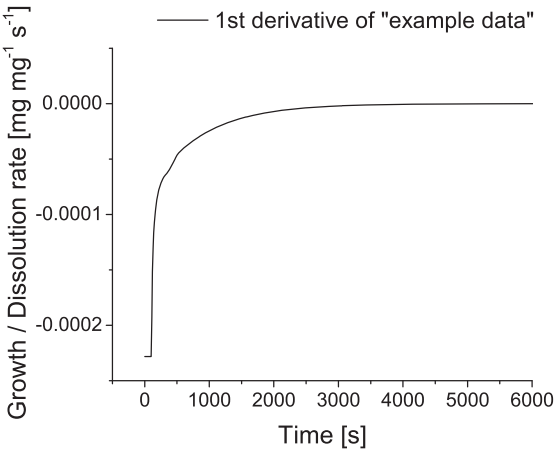

Figure 4.12: First derivative (dissolution rate) versus time

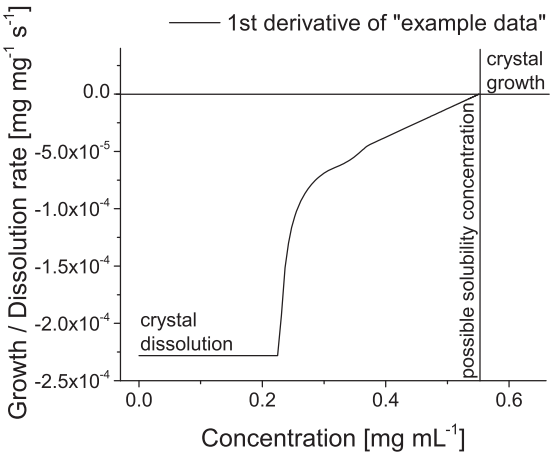

Figure 4.13: First derivative (dissolution rate) versus concentration

centrations, is shown in Figures 4.12 and 4.13. The constant zone of the start concentration is due to the photometer needs some time to give the first data point. Due to the derivative versus concentration calculations, some smoothing of the data during calculation is needed.

4.4 X-ray measurement

X-ray measurement is used to determine the structure of substances which have an ordered structure. A crystal has an ordered structure, the so called ”unit cell”. With the X-ray analysis, it is possible to calculate the lattice

constants of the unit cell. It gives information on the atom arrangement of a crystal. A monochromatic X-ray radiation beam is directed towards the crystalline sample. The crystal layers will reflect the X-ray, which can cause interferences. These interferences can be described by Bragg's law equation which is shown in Equation 4.5. In Figure 4.14 an example diagram of Bragg law equation is shown. More information on X-ray measurements can be found in textbooks, for example: Rudolf Allmann [Rud02] or Walter Borchardt-Ott [Wal13].

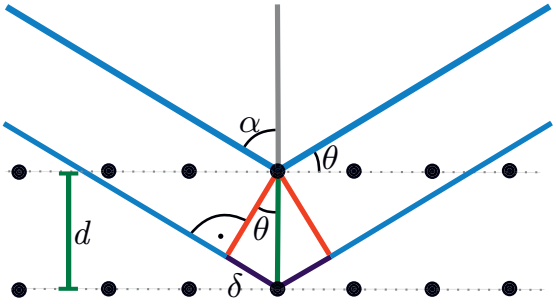

Figure 4.14: Example diagram of Bragg law equation

Figure 4.15: Image of XRPD sample preparation

$$n * \lambda = 2d * sin\theta \tag{4.5}$$

d	distance between lattice planes
λ	wavelength of X-ray radiation
θ	bragg angle
n	order of diffraction

The angle of 2θ between 10 and 50° were measured by Bruker D4 X-ray powder diffraction (XRPD) device (Figure 4.15). The samples were slightly grinded and placed on PMMA sample holders, covered by a special X-ray foil. The background from the sample holder was substracted. In the 2θ angle between 1 and 12° a capillary optics X-ray device was used to measure the tetragonal modification of the lysozyme crystals of the pH values 4.70, 4.85, 5.00, 5.15, 5.30 with an area detector.

4.5 Microscopy

Present images of the different crystal morphology's and dissolution experiments are carried out using a Keyence VHX 500F digital microscope, and an Olympus BH2 light microscope. Both types of microscope have a "coordinates table" to move the microscope cell (Figure 4.16) or the microscope slide.

4.5.1 Olympus BH2

The Olympus BH2 is a classical light microscope (Figure 4.17). An Olympus ocular NFK 3.3x LD 125 and the lens MDPlan5 / 0.1 is used. Due to a crop factor of the USB camera "Altra 20" and due to a malfunction of this camera type, later the USB camera "SC30", the total magnification of this microscope is: 53 times. This microscope can take images in short time cycles and also take videos, but time critical measurements to observe the beginning of the reaction are hard to handle. The first captured image of the instantly on the screen displayed images have a delay, which detains the location of crystals in the cell or the microscope slide.

Figure 4.16: Vessel and lid (microscope cell) with static inner volume, heat exchanger temperature controlled by thermostat

Figure 4.17: Olympus BH2 microscope with video camera and evaluation system

4.5.2 Keyence VHX 500F

The Keyence VHX 500F microscope (Figure 4.18) uses a lens with an optical magnification factor of 100 to 1000 times. The images are displayed instantly on the screen. The software is able to capture images in time steps over 15 s. With this microscope, it is more easy to find the crystal location by microscope slide in time.

Figure 4.18: Keyence VHX 500F digital microscope

Figure 4.19: Keyence VHX 500F control unit with screen

4.6 Enzymatic activity measurement

The enzymatic activity test was carried out according to Shugar [Shu52] by UV/Vis photometer. The photometer detects the turbidity of the sample Micrococcus luteus at a light wavelength of 450 nm. The protein lysozyme will break up the cell walls (lysis, see reaction Equation 4.6) of Micrococcus lysodeicticus which can be detected by a decrease of the turbidity intensity with time.

$$\textit{Micrococcus luteus}\ \text{Cells (Intact)} \xrightarrow{lysozyme} \textit{Micrococcus luteus}\ \text{Cells (Lysed)} \quad (4.6)$$

The enzymatic activity is given by $\mathrm{U\,mL^{-1}}$ (Units per mL). After some steps, the specific activity related to the protein concentration is calculated in $\mathrm{U\,mg^{-1}}$ (Units per mg). One unit of lysozyme will produce a ΔA450 of 0.001 per minute at pH 7.00 and 25 °C using a suspension of Micrococcus luteus as substrate in a 1.0 mL reaction mixture in a photometric cell with

1 cm path length. A short overview of these procedure is shown in Figure 4.20. To measure the activity the photometer analytikjena SPECORD 40 UV/VIS was used.

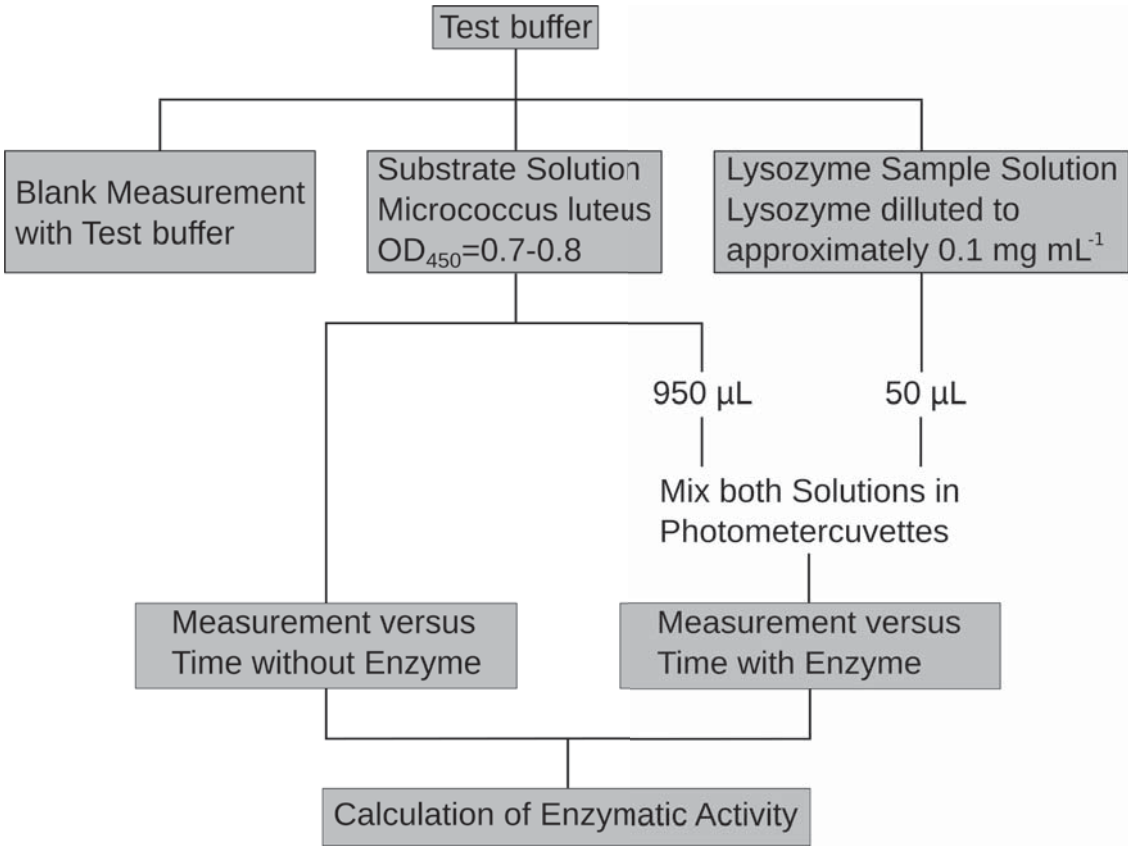

Figure 4.20: Scheme of enzymatic activity test according to Shugar [Shu52]

4.7 Water content measurements

4.7.1 TGA coupled MS

Thermogravimetric analysis

Thermogravimetric analysis (TGA) means the continuous registration of the mass of a substance during the heating up by a profile. These measurements gives a mass loss in substance of a gas which is evaporated out of the sample. The sensitivity of the balance is given for 5 µg [Mül12b]. The balance is located inside an oven. The atmosphere in the oven is purged by an inert gas (helium). For the experiments as an TGA coupled MS system, helium with a flow rate of 30 mL min^{-1} is chosen. The pre-dried crystals

were placed in alloy crucibles for measurements with a Netzsch STA-409 thermogravimetry measurement device. The temperature profile starts at 50 °C with a 30 min isothermal step, followed by a heating up to 400 °C at a rate of $2\,\mathrm{K\,min^{-1}}$. The TGA is coupled with a mass spectrometer (MS) to determine the released components and calculate the mass of water inside the crystals.

Mass spectrometry

A mass spectrometer is assembled of an ion source, an analyzer and a detector. Each of the parts exist in several different implementations. The task of the ion source is the ionization of the sample. The analyzer separates the ionized particle by size versus charge. The detector determines the ionized particles after separation. The mass spectrometer was adjusted to gather the ion mass of: 16 (oxygen or amines), 17 (carboxylic acid or amines), 18 (water), 28 (nitrogen), 32 (oxygen, sulfur of sulfides) and 44 (carbon dioxide of carboxylic acid). The main task of the MS coupled to a TGA in this works was, the detection of the decomposition of protein crystals to calculate the amount of bounded water. Further information on mass spectrometry can be found in textbooks, see e. g. Gross [Gro12] or Budzikiewicz and Schäfe [Bud12].

4.7.2 Karl-Fischer-Titration

The principle of the Karl-Fischer-Titration to determine the water content of a sample is the ability that iodine and sulfur dioxide will only combine to iodide and sulfate if water is present (see reaction Equation 4.7).

$$2\,\mathrm{H_2O} + \mathrm{SO_2} + \mathrm{I_2} \xrightarrow{H2O} {\mathrm{SO_4}}^{2-} + 2\,\mathrm{I^-} + 4\,\mathrm{H^+} \tag{4.7}$$

The water comes from the sample and the reaction is carried out in dry methanol as solvent. The device Mettler Toledo DL-35 Karl-Fischer Titrator realizes an automatic titration and calculation of the resulting water content of the sample. The point of change will be detected by a biamperometric method with use of two platinum electrodes. This is called Dead-stop End-point [Cli39]. More informations about this method can be found e. g. in the textbook of Scholz [Sch84].

4.8 Fundamental analysis

A fundamental analysis was carried out for the elements carbon, hydrogen, nitrogen and sulfur by a LECO CHNS-932 device. This device analyses an aliquot of 0.6 to 1.6 mg of the sample inside a capsule. During the measurement, a capsule is dropped inside a furnace with a temperature of 1000 °C. At the same time the sample drops into the furnace, a dose of oxygen is added. The sample combusts and forms CO_x, H_2O, N_2 and SO_x. The device is able to calculate the weight percentage by the infrared detection of CO_2, H_2O and SO_2, and by conductivity measurement of N_2. The element chloride was determined by the "Schöniger oxidation" [Sch55]. The element sodium was determined by optical emission spectrometry coupled by inductive plasma (ICP-OES). The ICP forms a stable high temperature argon plasma of about 7000 K. The sample will be ionized in the plasma and the optical emission will be detected to measure, and afterwards calculate the amount of several atoms, in this work sodium. More information about this analyze techniques can be found e. g. in the books of Nölte [Nöl02] and Harris [Har14].

4.9 Particle size distribution

The LALLS (low angle laser light scattering) can determine the particle size distribution of particles between 0.02 and 2000 µm in size [Kec12]. The determination uses an approximation process and assumes that the particles are spherical. The laser light of different wavelengths (lower wavelengths are able to detect particles with a smaller size) goes through the sample and creates a diffraction pattern which will be detected by an optoelectrical sensor (see Figure 4.21). The diffraction pattern is correlated to the particle size (see Figure 4.22 and Figure 4.23). A transformation during calculation results the size of the particles in the form of a size distribution. In this work, a Mastersizer-Hydro2000S was used to determine the particle size distribution after the batch crystallization presented in Chapter 4.1. Approximately 10 mg of the lysozyme crystals were suspended in a buffer solution of pH 5.0 containing 12 wt% sodium chloride, to prevent crystals from dissolving.

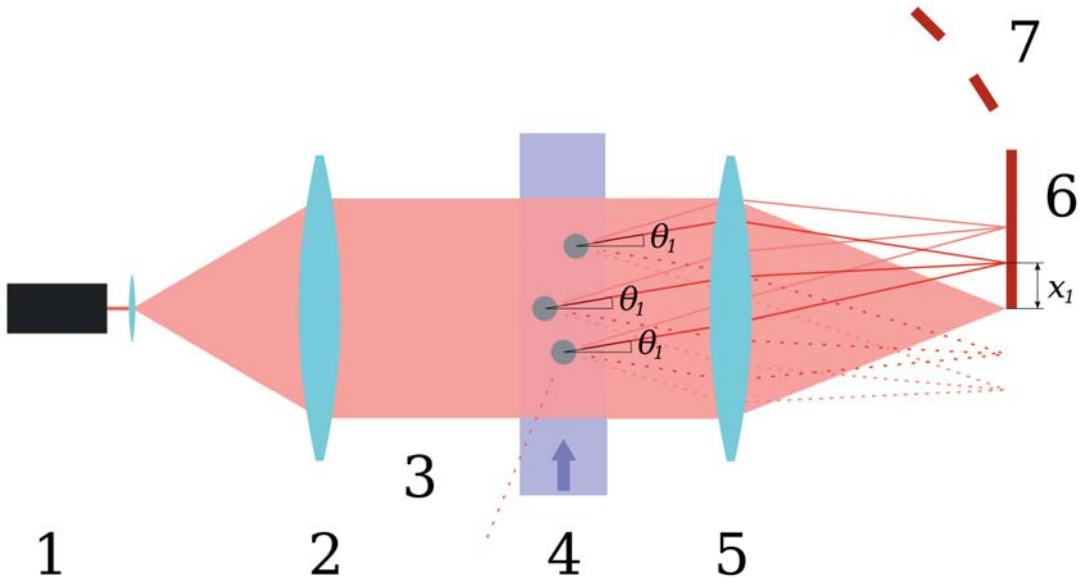

Figure 4.21: Particle size analysis by laser diffraction, 1=laser 2,5=lenses, 4 dispersion of particles flowing through 6=photo detector, semi-circular 7=photo detector, θ_1=angle of first Airy ring around the central spot, x_1=distance thereof on the detector [Sun14].

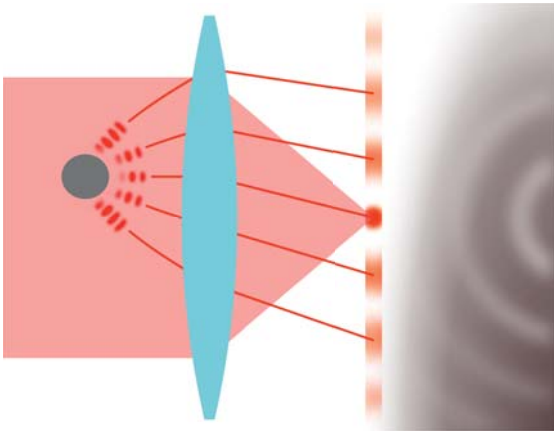

Figure 4.22: Particle size analysis by laser diffraction, single round small particle making fewer rings (than big ones) [Sun14].

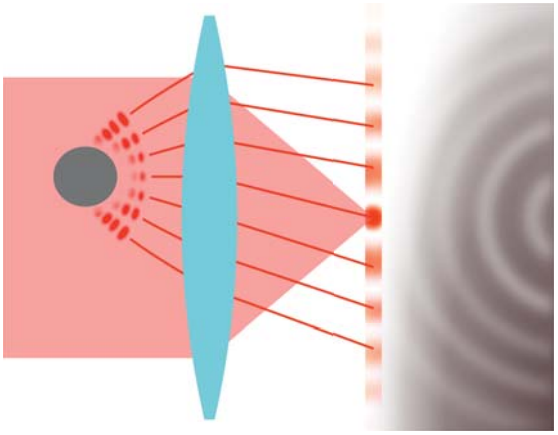

Figure 4.23: Particle size analysis by laser diffraction, single big round particle making more rings (than small ones) [Sun14].

4.10 Coloration experiment

During the work, some of the results gave the opportunity to use the coloration of protein crystals. The coloration and discoloration was already described and tested by Müller [Mül12b]. In this work, a pH active colorant was chosen to see if crystals placed inside a solution with different pH conditions will also diffuse into the crystals. Several colorants were chosen and are listed in Table 4.2. The colorants were chosen according to their estimated steric size (estimated by images of structure printed in the book of Sabnis [Sab]), pH value, of color shift reaction and a significant changing color. An amount of 30 mg of desired colorant to the already in Chapter 4.1 described method of crystallization of lysozyme crystals were added to the solutions. The resulting colorized crystals were observed by the methods presented in Chapter 4.5.

Table 4.2: Indicators used as colorants [PhI1], [PhI2], [Sab]

colorant	color	pH
calmagite	red to blue	8.1-10.2
resazurin sodium salt	orange to dark violett	3.8-6.4
alazarin red s	yellow to red	4.6-6.0
bromcresol green	yellow to blue	3.8-5.4
methyl red	red to yellow	4.4-6.2
neutral red	red to amber	6.8-8.0

5 Results

5.1 Dissolution experiments

Prior to dissolution experiments shown in the following Chapter, a test sequence to find the best operation techniques to dissolve crystals were carried out. The pre-dried crystals were dissolved. Here the first problem occurs, the dried crystals will swim on the surface of the liquid (e. g. buffer). A swimming crystal cannot be observed by a microscope, since its position will change permanently. The dissolution experiments were therefore carried out by harvested crystals. The edge of a spatula was used to gather crystals out of the mother liquor. The crystallization procedure was already presented in Chapter 4.1. The crystals were tipped on, when swimming on the surface of the solution and will sink to the ground. This solution is already temperature controlled inside the microscope cell (see Chapter 4.5). With the ”coordinate table” the crystals will be found and the automatically working capturing process of the image analysis system was started.

5.1.1 Dissolution in pure water

The starting point for all the dissolution experiments was the dissolution of crystals in pure water at a constant temperature. The dissolution was fast responding. The crystals of the tetragonal and HTO modification disintegrate into small particles very fast who will swim away from the center of the crystal as in an explosion. This is shown in Figures 5.1a to 5.1f and Figures 5.2a to 5.2f. The LTO modification showed a different dissolution behavior. It seems the crystals disintegrate after a long period of time into small needles with the orientation of the initial crystal habit. The ends of the elongated needle-like crystals seem to have peaks. The crystals look like a comb on each of the elongated sides. The rate at which

the LTO form of lysozyme chloride crystals dissolved was much slower compared to the tetragonal and HTO form.

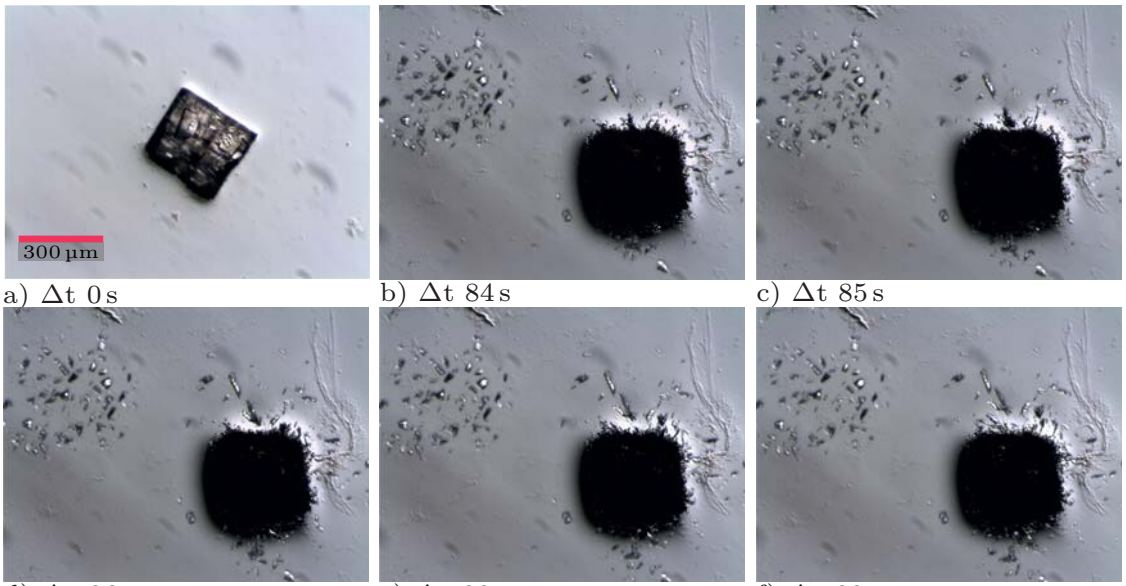

a) Δt 0 s b) Δt 84 s c) Δt 85 s

d) Δt 86 s e) Δt 88 s f) Δt 89 s

Figure 5.1: Tetragonal lysozyme chloride crystals dissolving in pure water (scale-bar in Figure 5.1a is applicable for all images in this Figure)

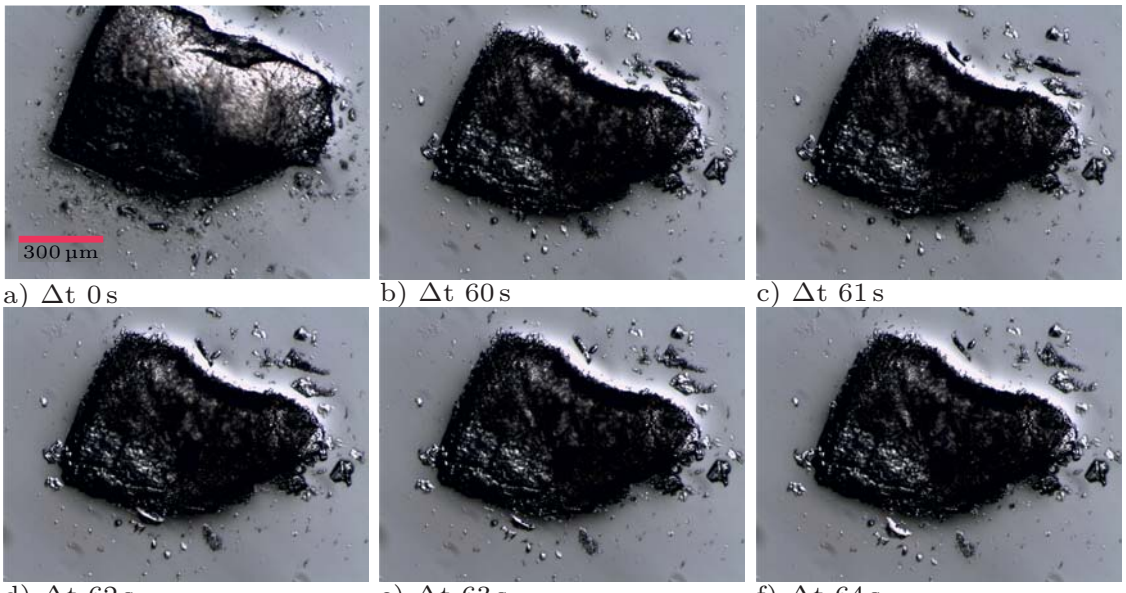

a) Δt 0 s b) Δt 60 s c) Δt 61 s

d) Δt 62 s e) Δt 63 s f) Δt 64 s

Figure 5.2: HTO lysozyme chloride crystals dissolving in pure water (scale-bar in Figure 5.2a is applicable for all images in this Figure)

a) Δt 0 s b) Δt 120 s c) Δt 240 s

d) Δt 360 s e) Δt 480 s f) Δt 1800 s

Figure 5.3: LTO lysozyme chloride crystals dissolving in pure water (scale-bar in Figure 5.3a is applicable for all images in this Figure)

5.1.2 Influence of the pH value

In order to maintain a pH value of a solution, a buffer substance is needed, see Chapter 2.2.1. To control the dissolution rate, the undersaturation level must be controlled. The dissolution conditions were first observed at a constant temperature of 20 °C, and at the same pH value that was used for the crystallization of the observed crystal modification. The images of these results are shown in Figures 5.4a to 5.4c for the HTO, Figures 5.5p to 5.5r for the LTO and Figures 5.6d to 5.6f for the tetragonal lysozyme crystals. The crystals dissolved just as expected. As known, e. g. from inorganic salts, the edges were rounded and the crystals shrunk in size by time (see Figures 5.6a to 5.6c for the tetragonal lysozyme crystals). Sometimes, it looked like HTO lysozyme crystals are “falling into pieces” (see Figures 5.4a to 5.4c). This is only due to the non-perfect generation of these crystals from agglomerates. If agglomerated crystals dissolve, at one point they fall apart into separate crystals. The LTO lysozyme crystals shown in Figures 5.5p to 5.5r shrunk homogeneously. On the elongated ends the LTO crystals looked like a comb with its teeth aligned in the direction away from the elongated crystal ends.

Some seconds after the start of a dissolution experiment where the pH value has been changed strongly, the transparent HTO and tetragonal crystals had already changed to be opaque as to be seen e. g. in Figure 5.4h or 5.6n. The microscope showed black shades and the time until these shady state was reached depends on the rate of dissolution and the change of pH value. When the crystals are falling apart into small particles, those dissolved separately. Then due to the created high surface area, the overall rate of dissolution was increased. The LTO crystals showed fasciated bars after a few seconds (see Figure 5.5g), thereafter those crystals were falling apart (Figure 5.5i). It seems the dissolution started at several points at the same time, which created separated particles if the starting points were enlarged during the dissolution process. The amount of fasciated bars were increased if the pH value was changed stronger. The gap between these bars were decreased but the gap had no constant size. A number of the gaps related to the pH of the solution is shown in Table 5.1. The dissolution mechanism was suddenly changed at a certain pH value. For crystals grown at pH value of 5.0 (HTO and tetragonal lysozyme crystals), a change in pH to approximately 7.0 was required to see that change in the dissolution mechanism from shrinking homogeneously to "falling into pieces". LTO crystals crystallized at pH 9.8 needed a lower pH value than approximately pH 7.8 in order to show a change in the dissolution mechanism.

Table 5.1: Measurement gap of fasciated bars

abs. pH	pH change	minimal gap	maximal gap	average gap
9.80	0.00	0.00 µm	0.00 µm	0.00 µm
8.40	1.40	0.00 µm	0.00 µm	0.00 µm
8.05	1.75	29.72 µm	230.98 µm	94.49 µm
7.70	2.10	16.10 µm	102.93 µm	43.83 µm
7.20	2.60	3.42 µm	12.68 µm	6.41 µm
5.00	4.80	1.66 µm	6.68 µm	4.32 µm

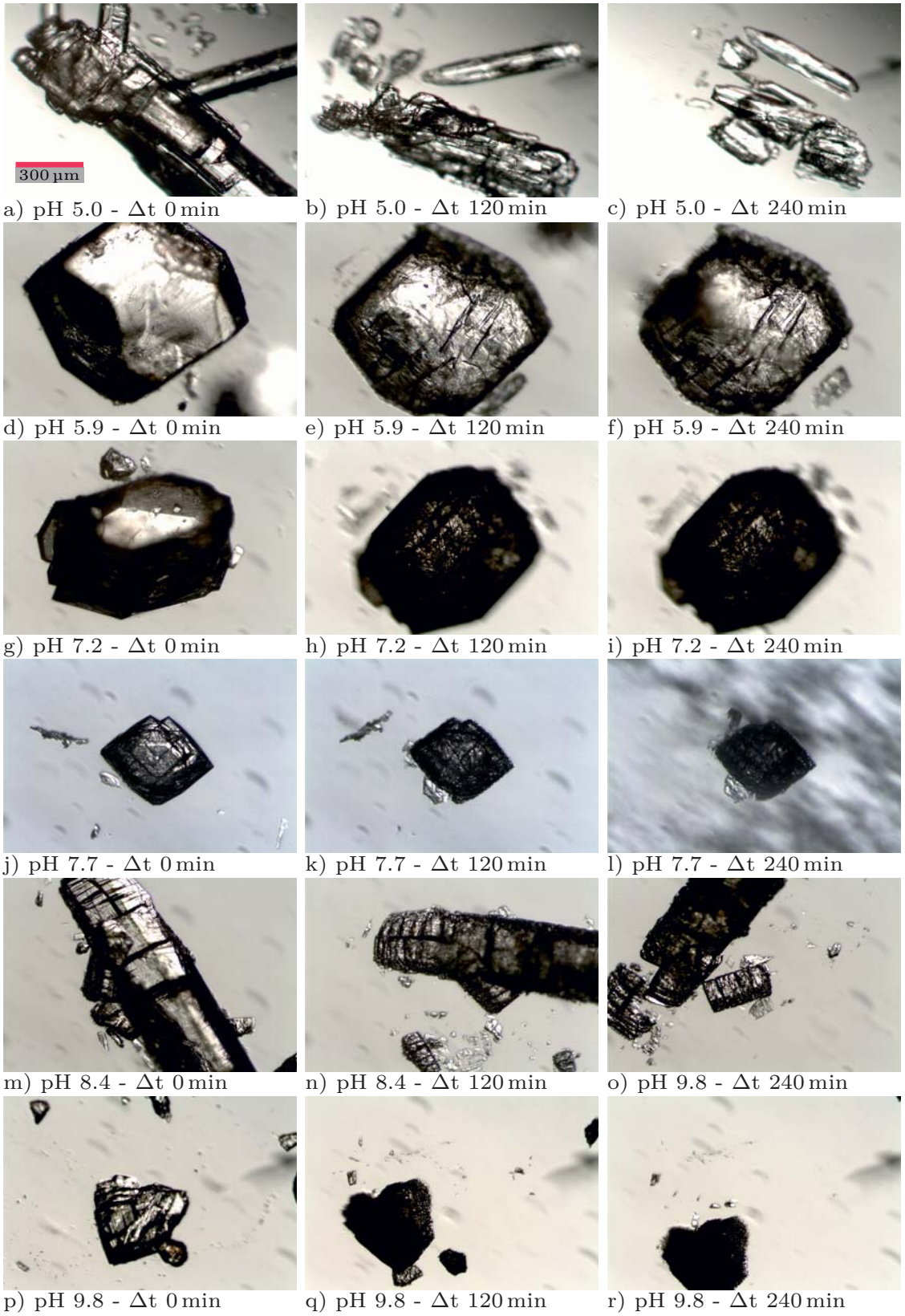

a) pH 5.0 - Δt 0 min b) pH 5.0 - Δt 120 min c) pH 5.0 - Δt 240 min
d) pH 5.9 - Δt 0 min e) pH 5.9 - Δt 120 min f) pH 5.9 - Δt 240 min
g) pH 7.2 - Δt 0 min h) pH 7.2 - Δt 120 min i) pH 7.2 - Δt 240 min
j) pH 7.7 - Δt 0 min k) pH 7.7 - Δt 120 min l) pH 7.7 - Δt 240 min
m) pH 8.4 - Δt 0 min n) pH 8.4 - Δt 120 min o) pH 9.8 - Δt 240 min
p) pH 9.8 - Δt 0 min q) pH 9.8 - Δt 120 min r) pH 9.8 - Δt 240 min

Figure 5.4: Dissolving of HTO modification of lysozyme, crystallized at a pH of 5.0 (scale-bar in Figure 5.4a is applicable for all images in this Figure)

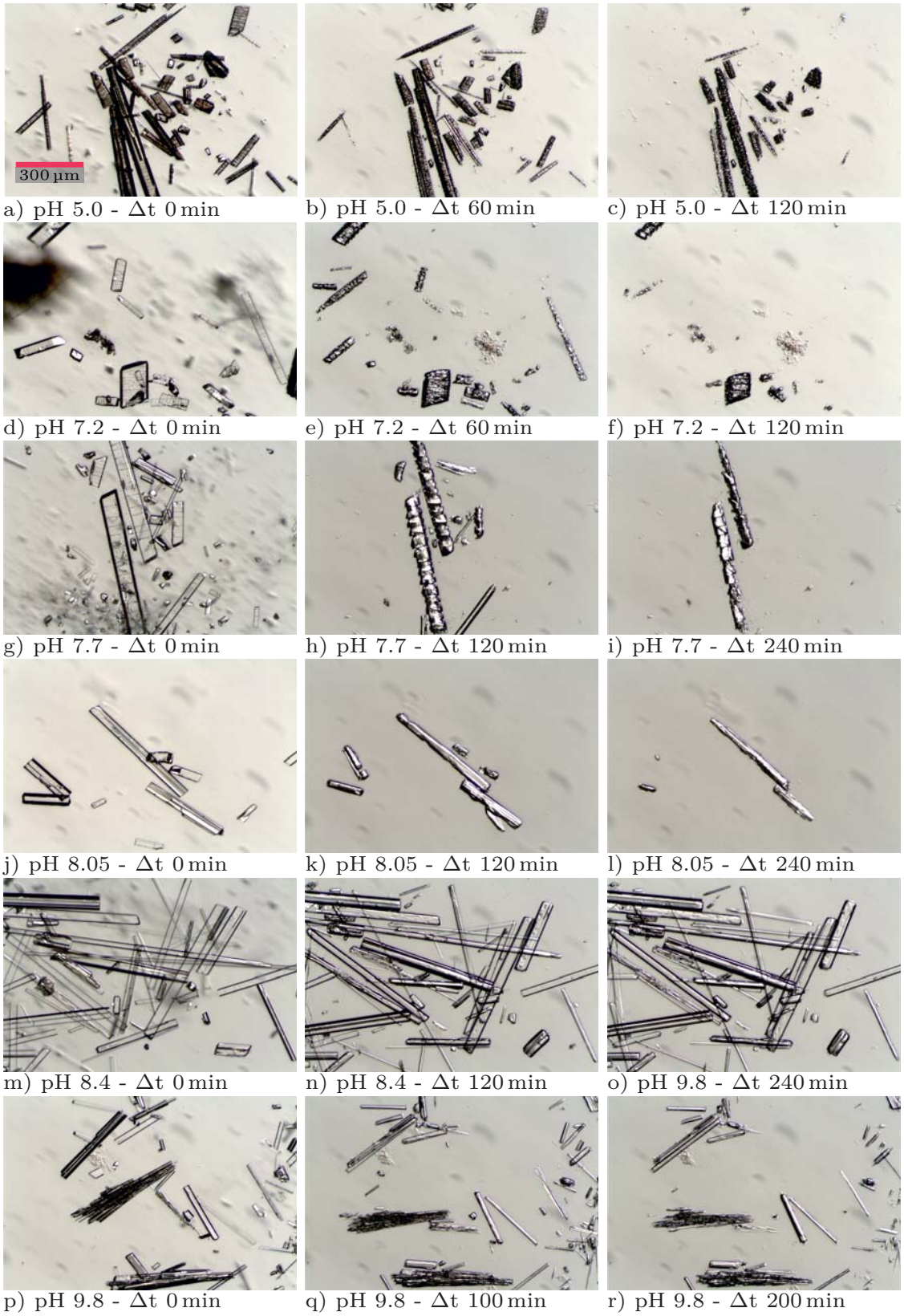

a) pH 5.0 - Δt 0 min b) pH 5.0 - Δt 60 min c) pH 5.0 - Δt 120 min
d) pH 7.2 - Δt 0 min e) pH 7.2 - Δt 60 min f) pH 7.2 - Δt 120 min
g) pH 7.7 - Δt 0 min h) pH 7.7 - Δt 120 min i) pH 7.7 - Δt 240 min
j) pH 8.05 - Δt 0 min k) pH 8.05 - Δt 120 min l) pH 8.05 - Δt 240 min
m) pH 8.4 - Δt 0 min n) pH 8.4 - Δt 120 min o) pH 9.8 - Δt 240 min
p) pH 9.8 - Δt 0 min q) pH 9.8 - Δt 100 min r) pH 9.8 - Δt 200 min

Figure 5.5: Dissolving of LTO modification of lysozyme, crystallized at a pH of 9.8 (scale-bar in Figure 5.5p is applicable for all images in this Figure)

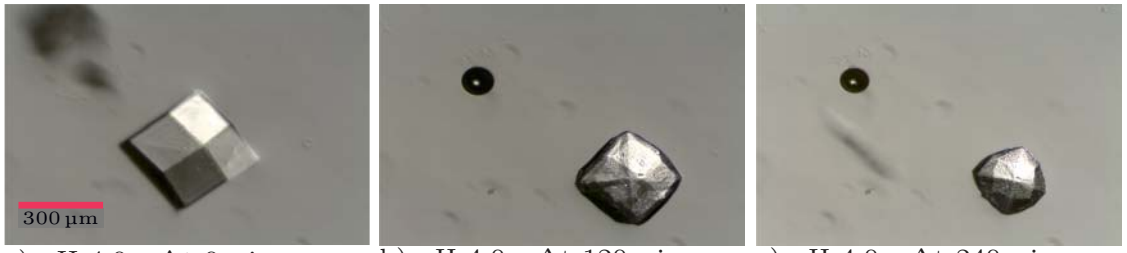

a) pH 4.0 - Δt 0 min b) pH 4.0 - Δt 120 min c) pH 4.0 - Δt 240 min

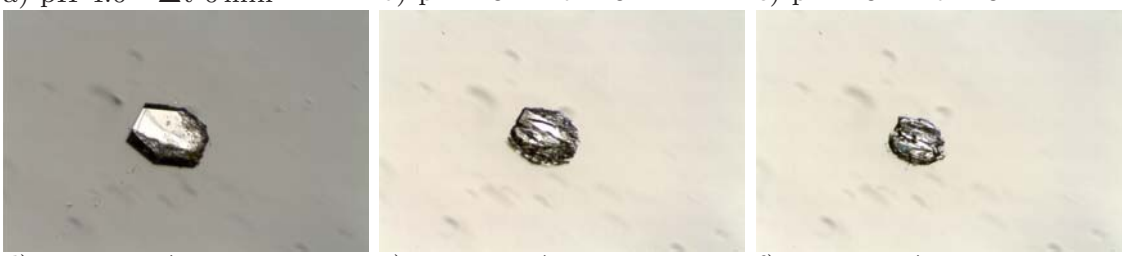

d) pH 5.0 - Δt 0 min e) pH 5.0 - Δt 120 min f) pH 5.0 - Δt 240 min

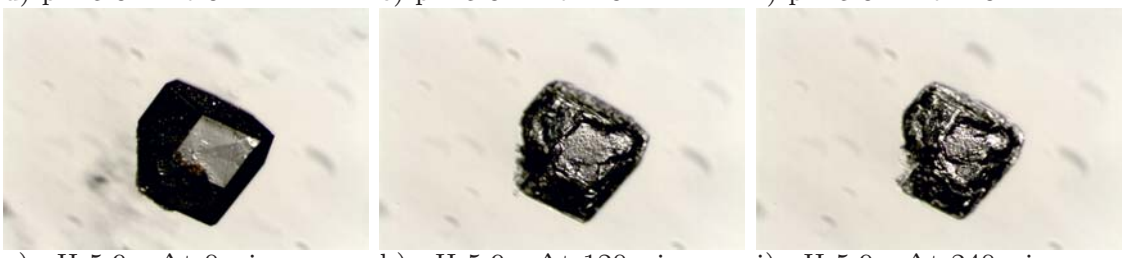

g) pH 5.9 - Δt 0 min h) pH 5.9 - Δt 120 min i) pH 5.9 - Δt 240 min

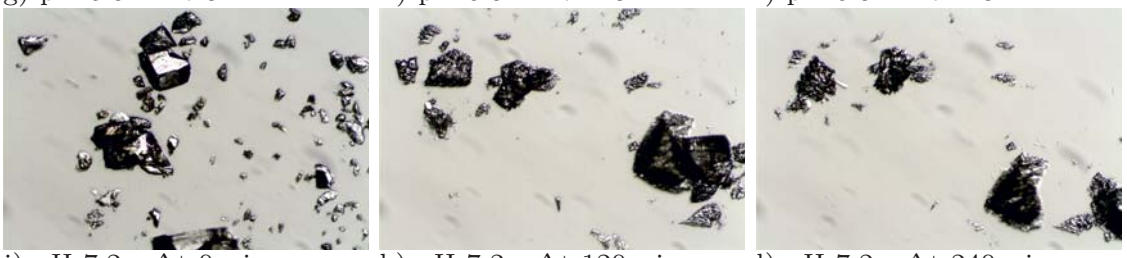

j) pH 7.2 - Δt 0 min k) pH 7.2 - Δt 120 min l) pH 7.2 - Δt 240 min

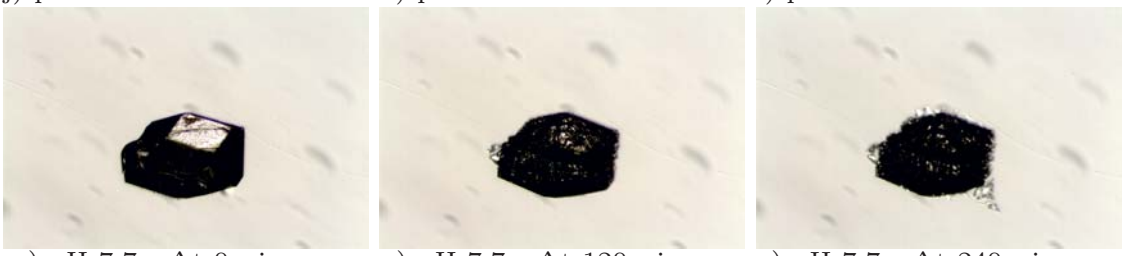

m) pH 7.7 - Δt 0 min n) pH 7.7 - Δt 120 min o) pH 7.7 - Δt 240 min

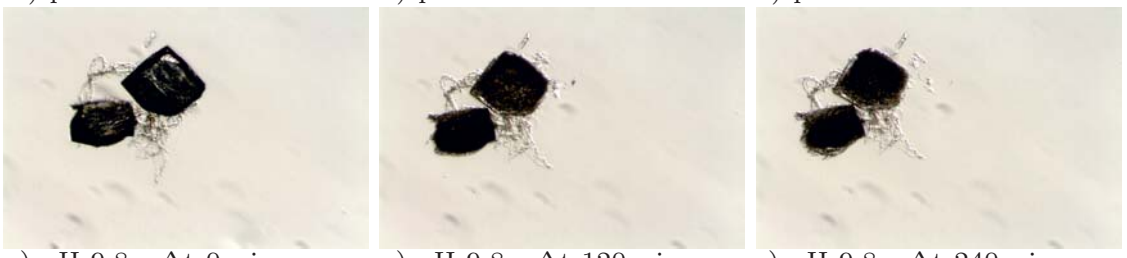

p) pH 9.8 - Δt 0 min q) pH 9.8 - Δt 120 min r) pH 9.8 - Δt 240 min

Figure 5.6: Dissolving of tetragonal modification of lysozyme, crystallized at a pH of 5.0 (scale-bar in Figure 5.6a is applicable for all images in this Figure)

5.1.3 Influence of the buffer components and concentration

As already known from Chapter 2.2.1, each buffer substance has only a small pH value range where it is working as buffer of acceptable capacity. By definition a buffer substance is able to act as a buffer composition in the range of ±1.0 pH around the pKa value. In Chapter 5.1.2 of this work a pH range of 5.0 up to 9.8 was used. This means there were several buffer compositions used. To predict that the pH influence (Chapter 5.1.2) was only affected by the pH and not by the buffer components nor concentration, measurements with constant pH value but changed components and concentration were investigated in a microscope cell (Chapter 4.5).
To observe the dissolution influence by the buffer, the method presented in Chapter 4.1 for the teragonal modification was modified by the use of propionate, pyridine and citrate prior to acetate buffer. With a citrate buffer it was not able to form crystals. The other buffers formed good shaped crystals with a size of up to 250 µm in length of reasonable quality. Furthermore, the influence of the buffer concentration was investigated. Lysozyme crystals with use of an acetate buffer of the concentrations of 0.05, 0.1 and 0.5 M were crystallized. Also different concentrations of the same buffer substance were afterwards dissolved.
The different buffer components and concentrations of the buffers had no influence on the dissolution mechanism. The images are not shown. Due to the normal rounding of edges and shrinking with time mechanism which was already shown by other images in this work, no new information can be given.
Due to the different buffer components with the same pH value it can be assumed, that the changed dissolution mechanism presented in Chapter 5.1.2 result only from the changed pH value. There is no influence by the buffer components or buffer concentrations at all.

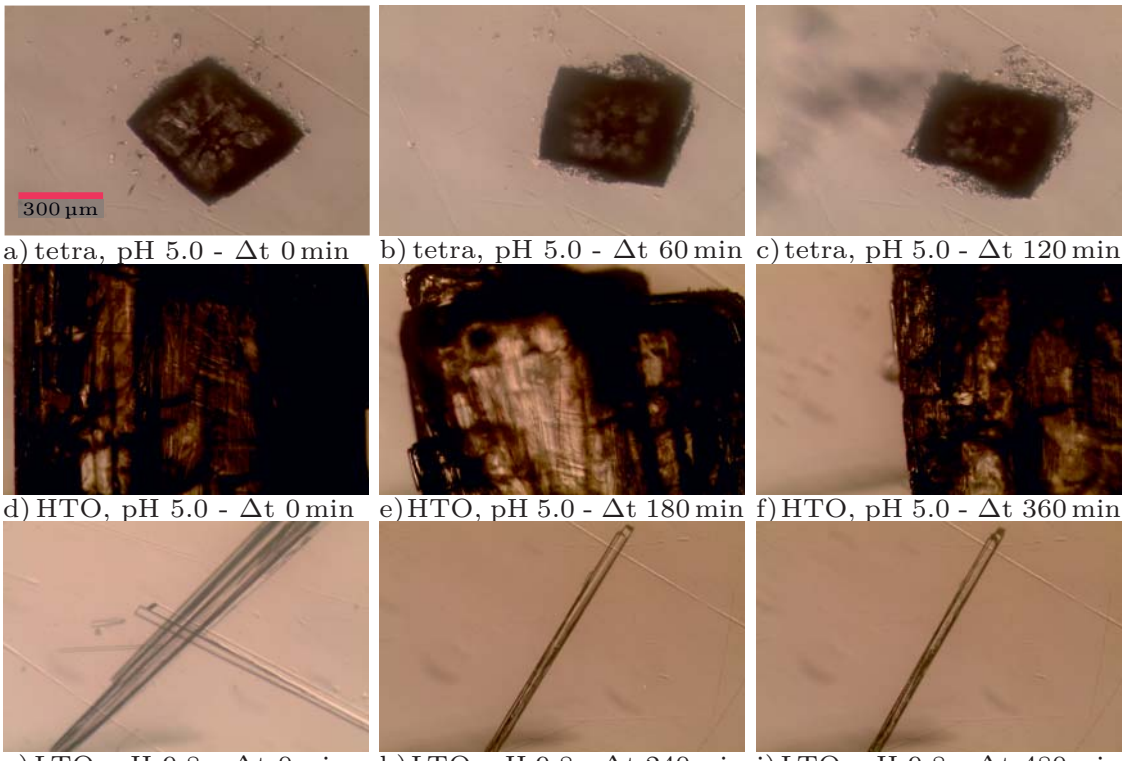

a) tetra, pH 5.0 - Δt 0 min b) tetra, pH 5.0 - Δt 60 min c) tetra, pH 5.0 - Δt 120 min
d) HTO, pH 5.0 - Δt 0 min e) HTO, pH 5.0 - Δt 180 min f) HTO, pH 5.0 - Δt 360 min
g) LTO, pH 9.8 - Δt 0 min h) LTO, pH 9.8 - Δt 240 min i) LTO, pH 9.8 - Δt 480 min

Figure 5.7: Dissolving in 2 wt% sodium bromide solution (scale-bar in Figure 5.7a is applicable for all images in this Figure)

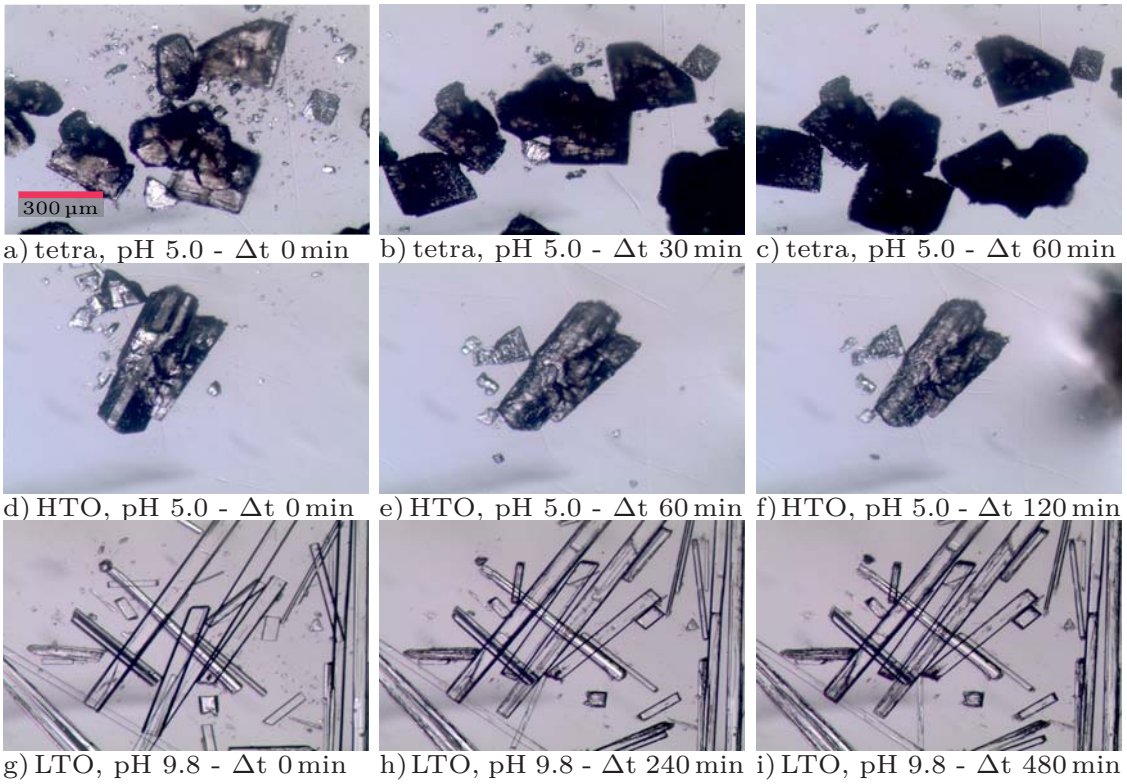

a) tetra, pH 5.0 - Δt 0 min b) tetra, pH 5.0 - Δt 30 min c) tetra, pH 5.0 - Δt 60 min
d) HTO, pH 5.0 - Δt 0 min e) HTO, pH 5.0 - Δt 60 min f) HTO, pH 5.0 - Δt 120 min
g) LTO, pH 9.8 - Δt 0 min h) LTO, pH 9.8 - Δt 240 min i) LTO, pH 9.8 - Δt 480 min

Figure 5.8: Dissolving in 0.2 M sodium nitrate solution (scale-bar in Figure 5.8a is applicable for all images in this Figure)

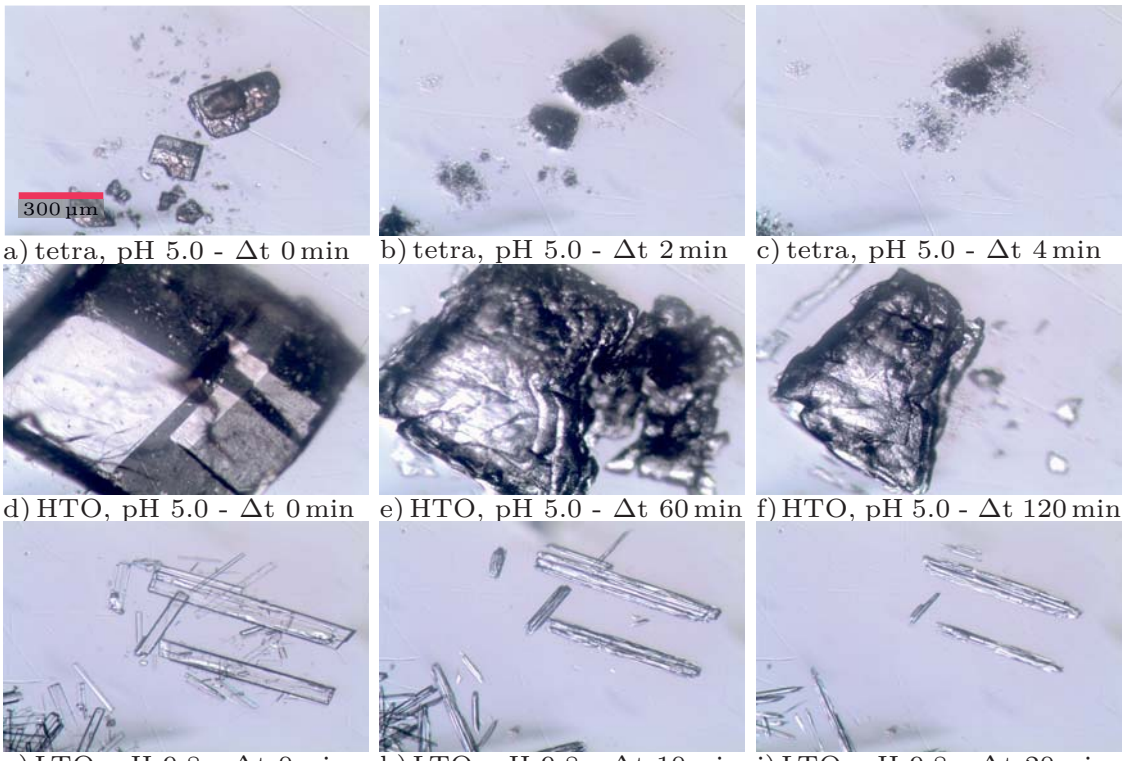

a) tetra, pH 5.0 - Δt 0 min b) tetra, pH 5.0 - Δt 2 min c) tetra, pH 5.0 - Δt 4 min
d) HTO, pH 5.0 - Δt 0 min e) HTO, pH 5.0 - Δt 60 min f) HTO, pH 5.0 - Δt 120 min
g) LTO, pH 9.8 - Δt 0 min h) LTO, pH 9.8 - Δt 10 min i) LTO, pH 9.8 - Δt 20 min

Figure 5.9: Dissolving in 2 wt% ammonium sulfate solution (scale-bar in Figure 5.9a is applicable for all images in this Figure)

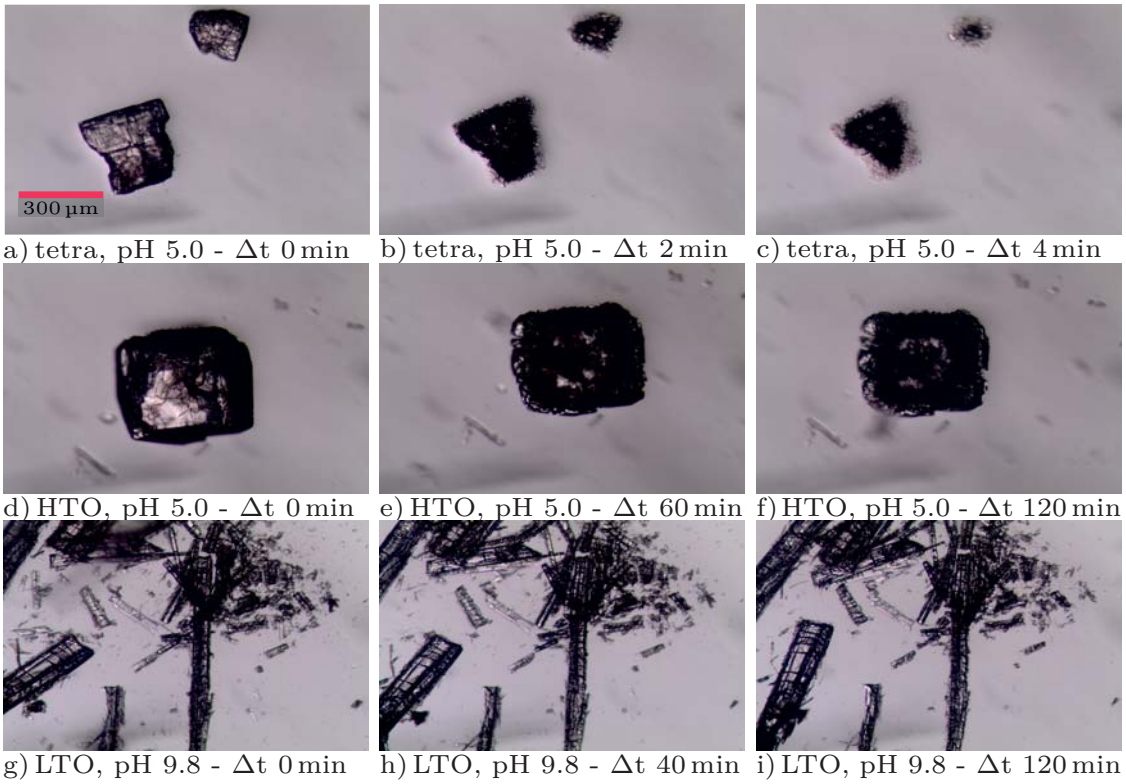

a) tetra, pH 5.0 - Δt 0 min b) tetra, pH 5.0 - Δt 2 min c) tetra, pH 5.0 - Δt 4 min
d) HTO, pH 5.0 - Δt 0 min e) HTO, pH 5.0 - Δt 60 min f) HTO, pH 5.0 - Δt 120 min
g) LTO, pH 9.8 - Δt 0 min h) LTO, pH 9.8 - Δt 40 min i) LTO, pH 9.8 - Δt 120 min

Figure 5.10: Dissolving in 20 wt% PEG_{6000} solution (scale-bar in Figure 5.10a is applicable for all images in this Figure)

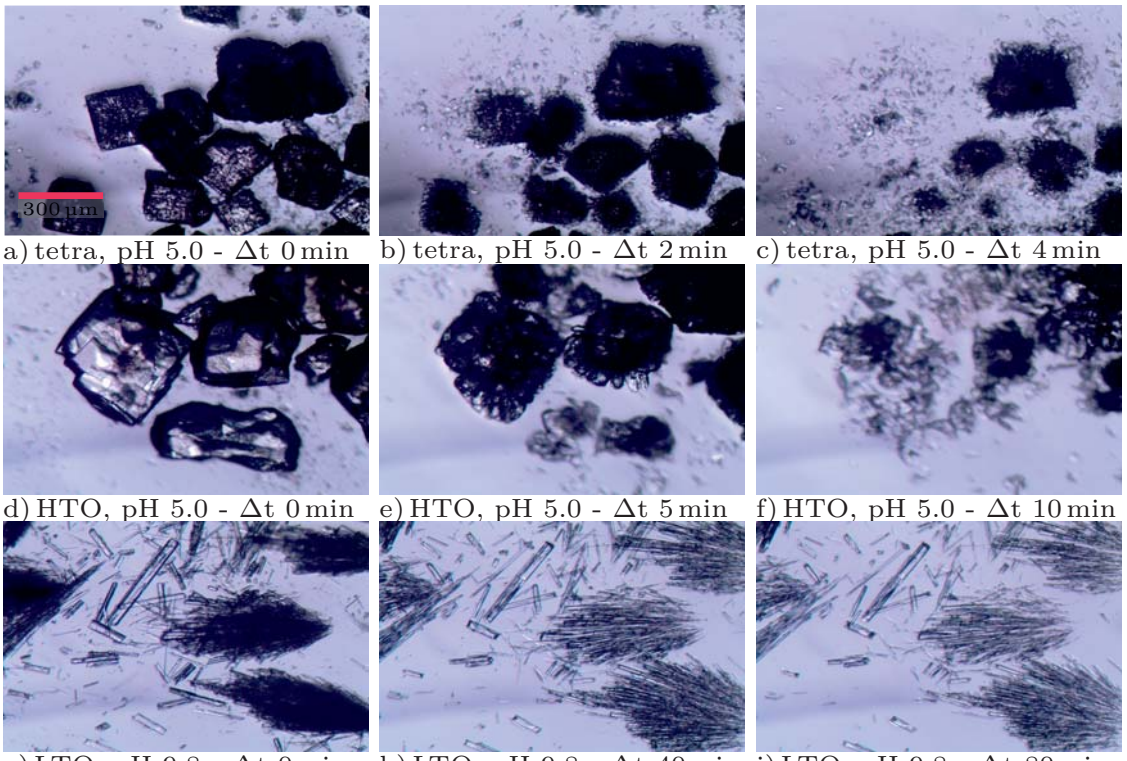

a) tetra, pH 5.0 - Δt 0 min b) tetra, pH 5.0 - Δt 2 min c) tetra, pH 5.0 - Δt 4 min
d) HTO, pH 5.0 - Δt 0 min e) HTO, pH 5.0 - Δt 5 min f) HTO, pH 5.0 - Δt 10 min
g) LTO, pH 9.8 - Δt 0 min h) LTO, pH 9.8 - Δt 40 min i) LTO, pH 9.8 - Δt 80 min

Figure 5.11: Dissolving in 2 wt% acetone solution (scale-bar in Figure 5.11a is applicable for all images in this Figure)

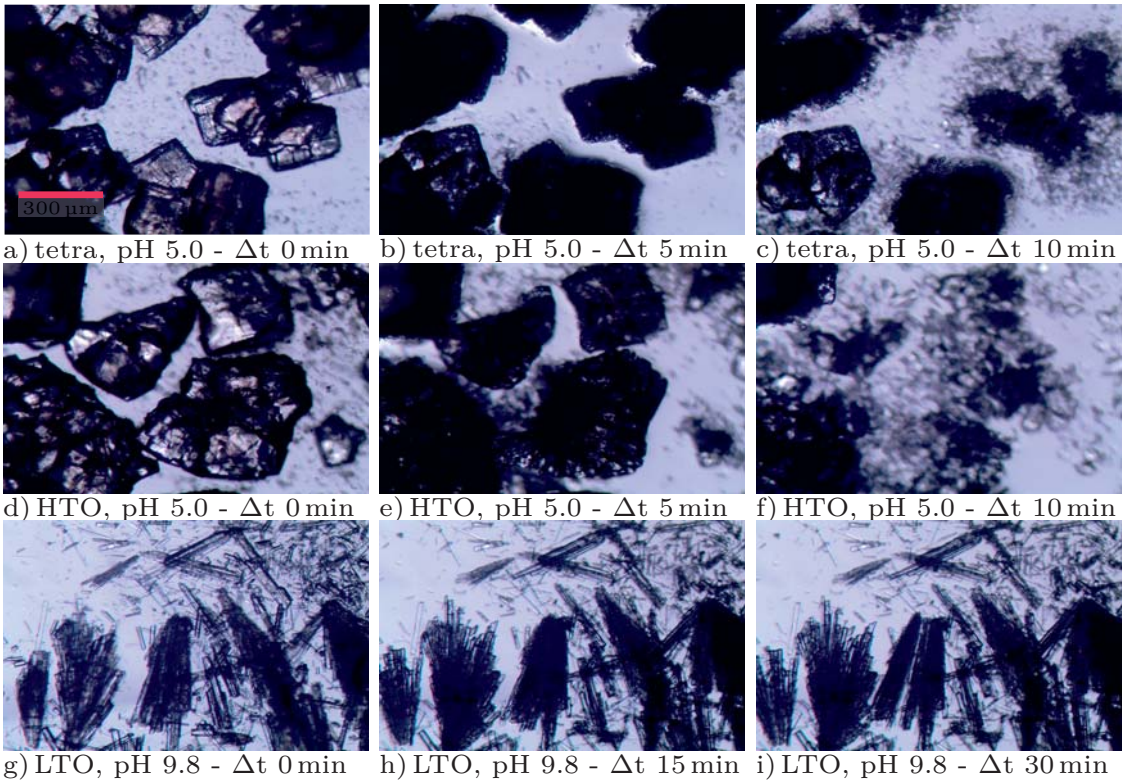

a) tetra, pH 5.0 - Δt 0 min b) tetra, pH 5.0 - Δt 5 min c) tetra, pH 5.0 - Δt 10 min
d) HTO, pH 5.0 - Δt 0 min e) HTO, pH 5.0 - Δt 5 min f) HTO, pH 5.0 - Δt 10 min
g) LTO, pH 9.8 - Δt 0 min h) LTO, pH 9.8 - Δt 15 min i) LTO, pH 9.8 - Δt 30 min

Figure 5.12: Dissolving in 2 wt% ethanol solution (scale-bar in Figure 5.12a is applicable for all images in this Figure)

5.1.4 Influence of the precipitant substance

In literature (e. g. Wiencek [Wie02], Lim et al. [Lim98], Harata and Akiba [Har06] and Forsythe et al. [For99b]), there are different precipitants for the crystallization of lysozyme crystals described. In this work sodium bromide, sodium nitrate, ammonium sulfate, polyethylene glycol (PEG_{6000}), ethanol and acetone were used. All of these precipitants are used in crystallization and purification of protein crystals of the different modifications.

Sodium bromide is used for the crystallization of tetragonal lysozyme crystals [Lim98]. The dissolution of the tetragonal lysozyme chloride crystals in a sodium bromide solution was not anymore rounding and shrinking with time (see Figures 5.7a to 5.7c). The crystals "falling into pieces" when dissolving at the pH values where they were crystallized. Sodium nitrate and ammonium sulfate will be used for the crystallization of lysozyme to achieve the modifications triclinic and monoclinic [Har06; For99b]. Both precipitants had also changed the dissolution mechanism to a "falling into pieces" (see Figures 5.8a to 5.8c and Figures 5.9a to 5.9c). PEG_{6000}, ethanol and acetone are generally used for protein crystallization and again the tetragonal crystals showed a "falling into pieces" dissolution mechanism for the three precipitants (see Figures 5.10a to 5.10c, Figures 5.12a to 5.12c and Figures 5.11a to 5.11c).

The High Temperature Orthorhombic (HTO) crystals showed for all of the six used precipitation agents the same dissolution behavior as the tetragonal crystals do. The images are shown in Figures 5.7d to 5.7f for NaBr, Figures 5.8d to 5.8f for $NaNO_3$, Figures 5.9d to 5.9f for $(NH_4)_2SO_4$, Figures 5.10d to 5.10f for PEG_{6000}, Figures 5.12d to 5.12f for ethanol and Figures 5.11d to 5.11f for acetone.

The Low Temperature Orthorhombic modification (LTO) showed a different behavior. Except for the ammonium sulfate (see Figures 5.9g to 5.9i), the crystals dissolved in the conventional way, they are rounding and shrinking homogeneously (Figures 5.7g to 5.7i for NaBr, Figures 5.8g to 5.8i for $NaNO_3$, Figures 5.10g to 5.10i for PEG_{6000}, Figures 5.12g to 5.12i for ethanol and Figures 5.11g to 5.11i for acetone. Especially, in the case of ammonium sulfate the LTO crystals showed sometimes lengthwise stripes (Figure 5.9h). The direction of the fascinated bars in case of other precipitants differs from the direction found by the change of the pH value.

5.1.5 Influence of the precipitant concentration

The precipitant concentration had no influence on the dissolution mechanism. It only affected the dissolution rate. An increase of precipitant concentration in the case of salting-out (see Chapter 2.2.2) for the protein lysozyme lowers the solubility. The decrease in solubility will afterwards decrease the dissolution rate, the crystals dissolve slower. This effect is huge, with low concentration of 1 wt% of sodium chloride the crystals dissolved within approximately 6 hours, with a concentration of 4 wt% the dissolving process already needed several days.

5.1.6 Influence of the temperature

The temperature level is another parameter enabling the control of the dissolution rate of protein crystals. With increasing temperature the dissolution rate was increasing. With a lowered temperature, the rate was slowed down. Due to the existence of the dissolution rate dispersion (already examined in Chapter 2.3.2), it was not possible to give a mean value for the dissolution rate using the microscope cell method. The number of examined crystals was not high enough to achieve a reliable mean value. Furthermore, the "falling into pieces" mechanism prevents the use of measurements of one characteristic length. The determination of the dissolution rate by microscope cell is not possible since the crystals do not shrink during dissolution.

5.1.7 Phase transition test

To check if there was a phase transition during the dissolution of one crystal modification, the following method was used. From the crystallization process (see Chapter 4.1) the mother liquor of the LTO modification was filled in the microscope cell. This liquid was chosen, according to the same temperature as other dissolution experiments 20 °C and the lower solubility of lysozyme at this pH range. The crystals were placed in the microscope cell prior the dissolution experiments. The images show the crystals changed and became opaque after some minutes (Figure 5.13b). This was already seen in dissolution experiments (Figures 5.6p to 5.6r). The crystal seems to be porous (Figure 5.13h) like a sponge. This means some parts of the crystals dissolved already! After certain time some needles are to be found

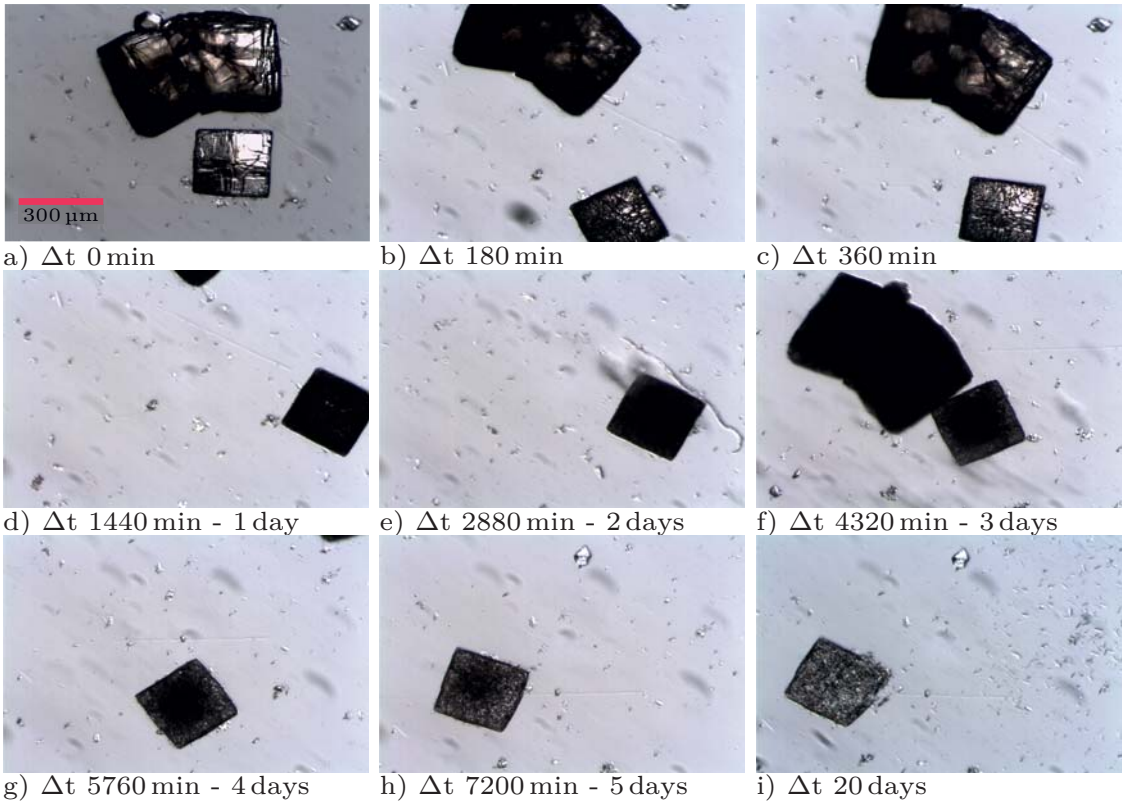

a) Δt 0 min b) Δt 180 min c) Δt 360 min

d) Δt 1440 min - 1 day e) Δt 2880 min - 2 days f) Δt 4320 min - 3 days

g) Δt 5760 min - 4 days h) Δt 7200 min - 5 days i) Δt 20 days

Figure 5.13: Long time phase transition test of tetragonal crystals inside pH 9.8 with LTO crystals saturated solution at T_{const} 20 °C (scale-bar in Figure 5.13a is applicable for all images in this Figure)

in the cell (see Figure 5.13i) but not on the surface or around the dissolving crystal, everywhere inside the cell (see Figure 5.13h).

5.1.8 Coloration experiment

Previous work (Müller [Mül12b]) gave some information on the colorization of lysozyme crystals. Afterwards the crystals were decolorized in some liquids without colorant. In this work, a pH active indicator colorant was chosen to see if a changed pH value is able to diffuse into the inside of a protein crystal. Calmagite is the substance which was able to colorize the crystals and gave some valuable results. The Figures 5.14a to 5.14f show this captured image series. It was shown that more than one process is running at the same time. The conditions will dissolve the crystals and from Chapter 5.1.2 it is known that the crystals become opaque after some minutes. From Müller [Mül12b] it is known that the crystals were decolorized with time. Furthermore, in these images the red color changed to blue from the outside to the inside of each crystal.

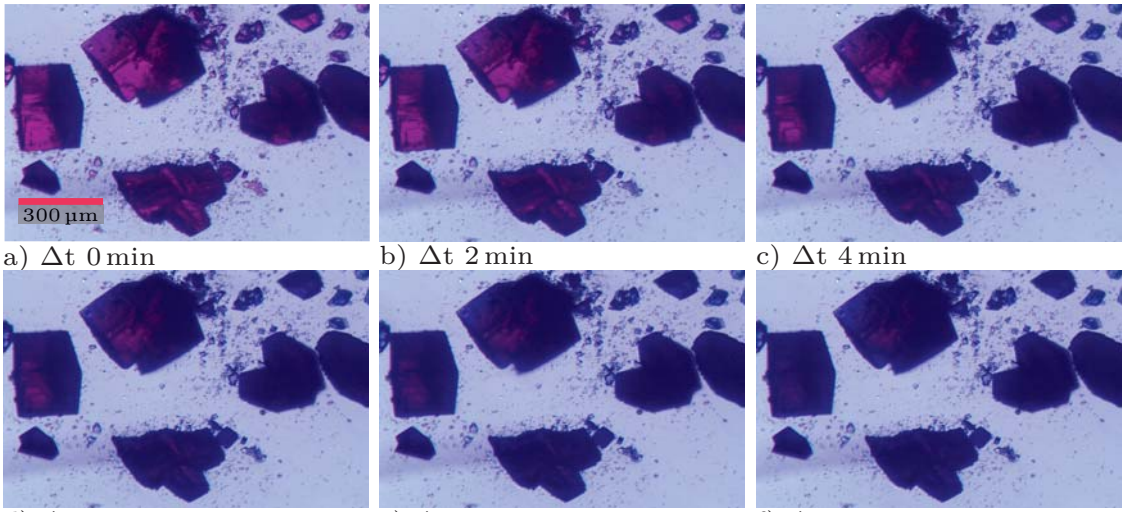

a) Δt 0 min b) Δt 2 min c) Δt 4 min

d) Δt 6 min e) Δt 8 min f) Δt 10 min

Figure 5.14: Discoloring of calmagite colorized tetragonal crystals in pH 9.8 (scale-bar in Figure 5.14a is applicable for all images in this Figure)

5.1.9 Summary of dissolution experiments

To sum up, Table 5.2 shows the dissolution phenomena of the different components of the mother liquor. In Chapter 5.1.2 it was shown that a changed pH condition from that of the crystallization condition will change the dissolution mechanism. A further test confirmed that there is no phase transition on the crystals surface to be found. The indicator colorization test showed that the liquid with the modified pH can diffuse into the crystals (where the non-bounded water, the buffer, is to be found).

Table 5.2: Summary of dissolution mechanisms

	tetragonal	HTO	LTO
water	fall apart	fall apart	ideal/individual lengthwise needles
NaCl - 5.0	ideal	ideal	fasciated bars/falling apart
NaCl - 9.8	fall apart	fall apart	ideal/individual lengthwise needles
NaBr - 5.0	fall apart	fall apart	-
NaBr - 9.8	-	-	ideal/individual lengthwise needles
$NaNO_3$ - 5.0	fall apart	fall apart	-
$NaNO_3$ - 9.8	-	-	ideal/individual lengthwise needles
$(NH_4)_2SO_4$ - 5.0	fall apart	fall apart/big particle	-
$(NH_4)_2SO_4$ - 9.8	-	-	ideal/individual lengthwise needles
PEG_{6000} - 5.0	fall apart	fall apart/big particle	-
PEG_{6000} - 9.8	-	-	ideal/individual lengthwise needles
acetone - 5.0	fall apart	fall apart/big particle	-
acetone - 9.8	-	-	ideal/individual lengthwise needles
ethanol - 5.0	fall apart	fall apart	-
ethanol - 9.8	-	-	ideal/individual lengthwise needles

5.2 Metastable zone

5.2.1 Influence of the pH value

The solubility line of lysozyme chloride was measured with 0.1 M acetate buffer and 4 wt% of sodium chloride as precipitant. The highest solubility by means of lowest temperature measured was at pH 5.0 (Figure 5.15). The nucleation line in Figure 5.16 shows a similar result. Here the nucleation occurred at the lowest temperature during the measurement of different pH values at pH 5.0. Additionally, the solubility line shows a step around 27 to 30 °C respectively 18 mg mL^{-1}.

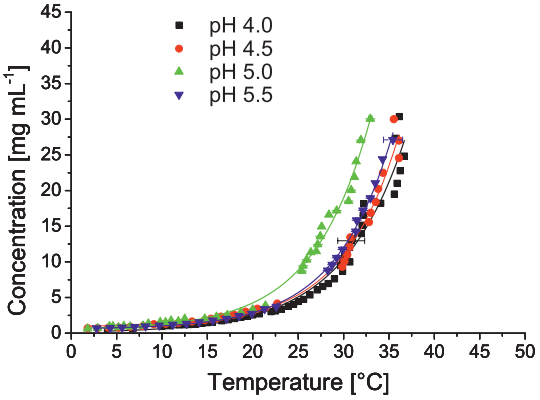

Figure 5.15: Solubility line of lysozyme chloride in the region of pH 5

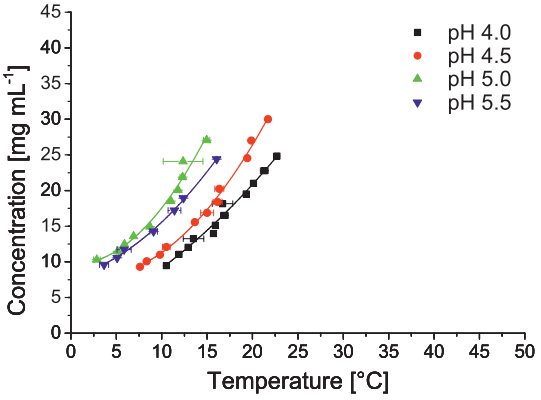

Figure 5.16: Nucleation line of lysozyme chloride in the region of pH 5

The metastable zone in the region of pH 7.0 was measured with use of a phosphate buffer at a concentration of 0.1 M. As precipitant sodium chloride with a concentration of 4 wt% was chosen. The solubility line (Figure 5.17) shows a significant split into two regions. Solutions with pH values 7.7 and 8.2 had a much higher solubility than those with the pH values in the range of 6.2 to 7.2. The nucleation lines are plotted in Figure 5.18 and show the lowest temperatures for the pH values of 6.7 and 7.2.

The metastable zone was measured in the region of pH 9.0 with use of a glycine buffer in a concentration of 0.05 M and sodium chloride as precipitant with a concentration of 4 wt%. The solubility line in Figure 5.19 shows a split into two regions. The lower solubility region for the pH values in range of 9.0 to 10.5 and the higher solubility for the pH range of 8.25 up to

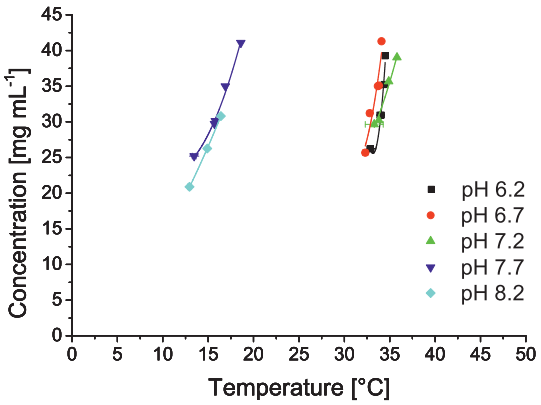

Figure 5.17: Solubility line of lysozyme chloride in the region of pH 7

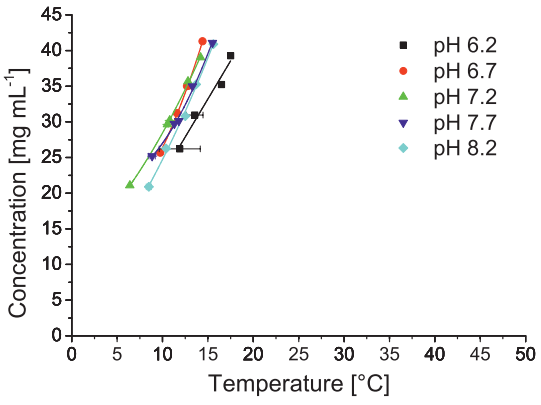

Figure 5.18: Nucleation line of lysozyme chloride in the region of pH 7

8.75. The nucleation line in Figure 5.20 shows also a split in two regions with the same pH values as the solubility line. As already shown in the solubility and nucleation line diagrams, the metastable zone width plot is a calculation of both diagrams. The resulting diagram of the metastable zone width versus concentration is shown in Figures 5.21, 5.22 and 5.23. As already expected in the region of pH 5 there is only one area where the points are pooled. In the diagram of pH 7 there is a split-up into two pooled regions and the curves of pH 9 are pooled into two to three regions. In Figure 5.24 a 3D plot is shown in order to see the highest local solubilities which can be found at certain pH values. The plane shape is like a wave with certain hills (maxima of solubility) versus pH value.

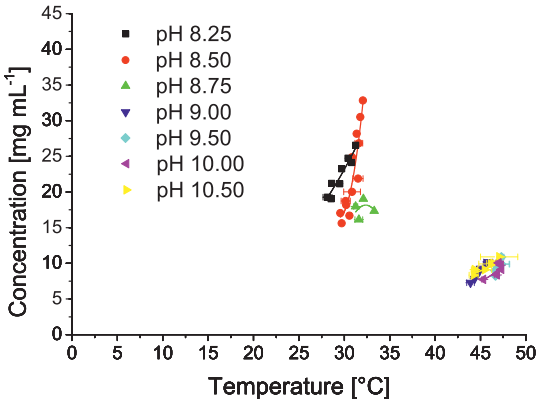

Figure 5.19: Solubility line of lysozyme chloride in the region of pH 9

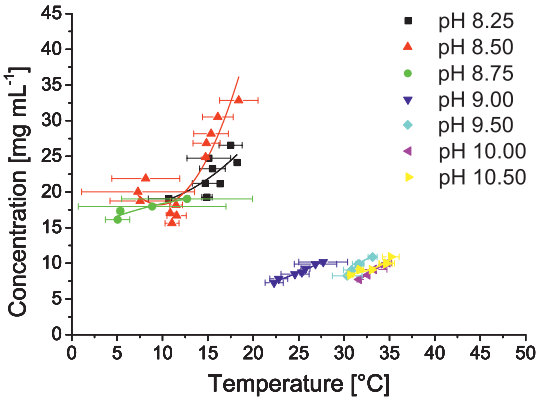

Figure 5.20: Nucleation line of lysozyme chloride in the region of pH 9

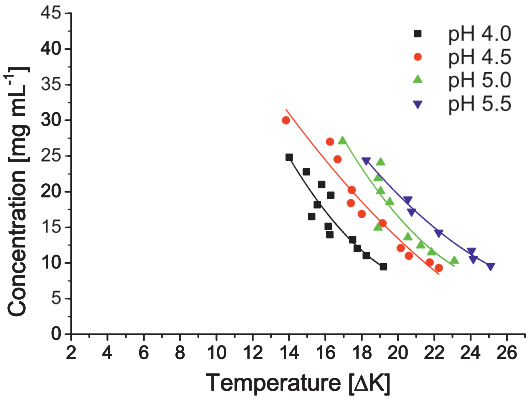

Figure 5.21: Metastable zone width of lysozyme chloride in the region of pH 5

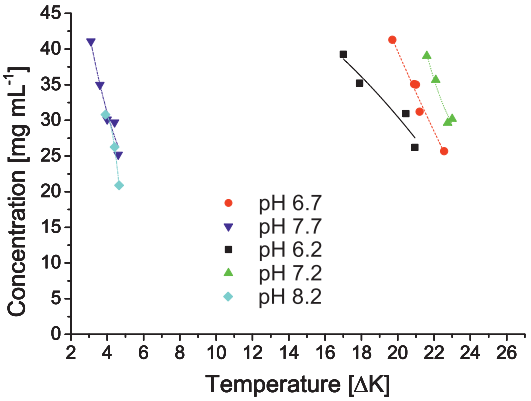

Figure 5.22: Metastable zone width of lysozyme chloride in the region of pH 7

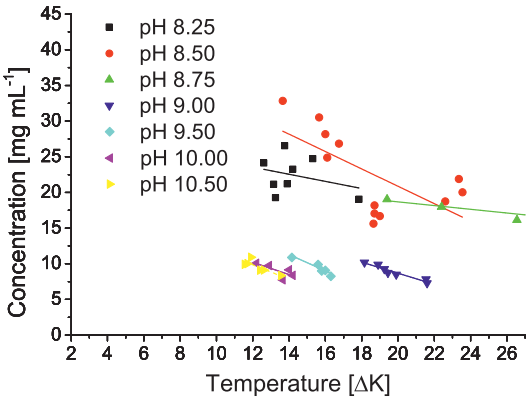

Figure 5.23: Metastable zone width of lysozyme chloride in the region of pH 9

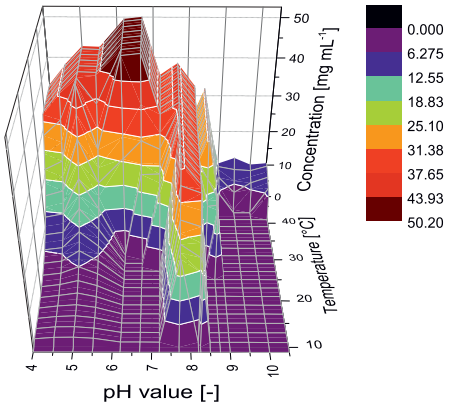

Figure 5.24: 3D plot of solubility of lysozyme chloride against the pH

5.2.2 Influence of the buffer components and buffer concentrations

In Chapter 5.1.3 the possibility to crystallize tetragonal lysozyme chloride crystals with the use of changed buffer components and concentrations was already introduced. Now the influence on the metastable zone width was investigated. Figures 5.25, 5.26 and 5.29 shows the solubility line, nucleation line and respectively the width of the metastable zone, if different buffer components (acetate, propionate and pyridine) were used. Figures 5.27, 5.28 and 5.30 shows the plots, if the concentration of the equal buffer composition (acetate) is changed.

It was shown that the buffer composition has almost no influence on the plots of the metastable zone, if compared to the deviation of the used method. The buffer concentration had a bigger influence on nucleation and solubility line. The width of the metastable zone was almost not affected at all.

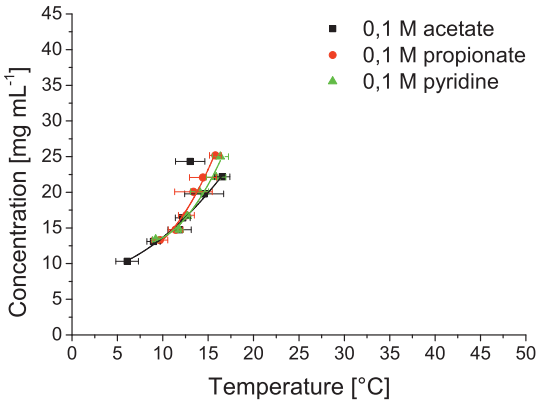

Figure 5.25: Nucleation line of lysozyme chloride at pH 5.0 and different buffer substance

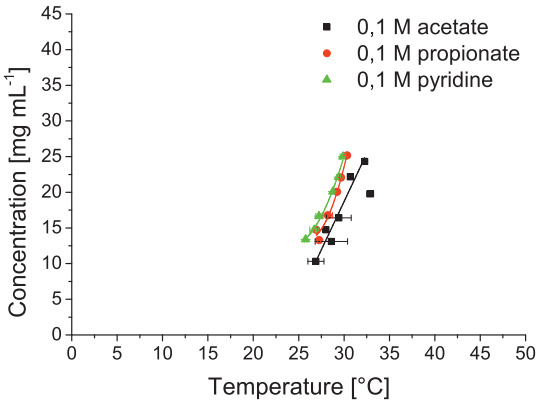

Figure 5.26: Solubility line of lysozyme chloride at pH 5.0 and different buffer substance

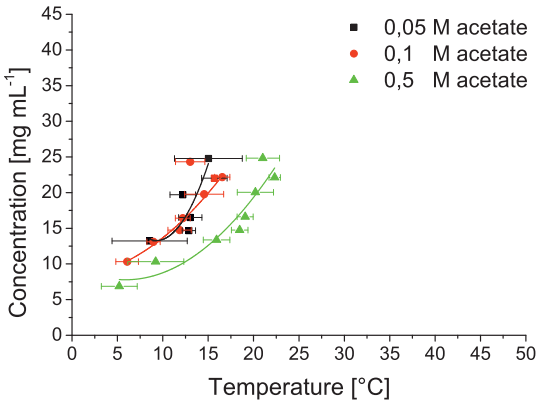

Figure 5.27: Nucleation line of lysozyme chloride at pH 5.0 acetate buffer of different concentration

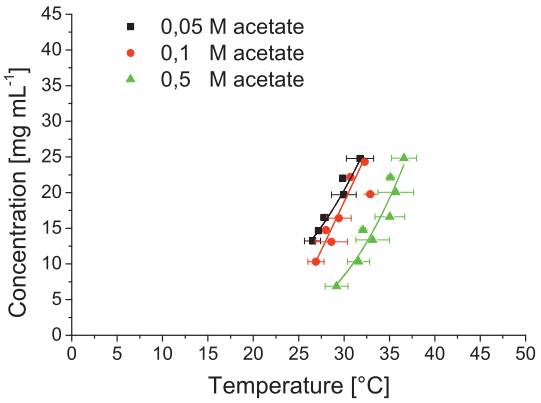

Figure 5.28: Solubility line of lysozyme chloride at pH 5.0 acetate buffer of different concentration

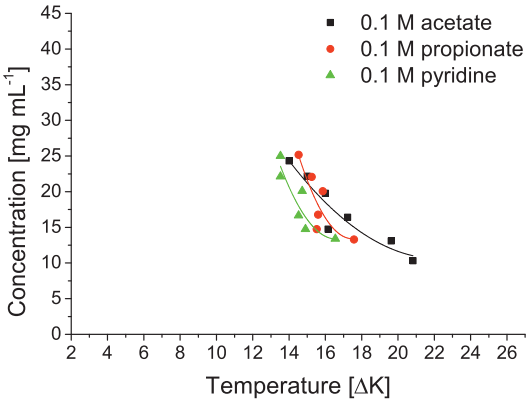

Figure 5.29: Metastable zone width of lysozyme chloride at pH 5.0 and different buffer substance

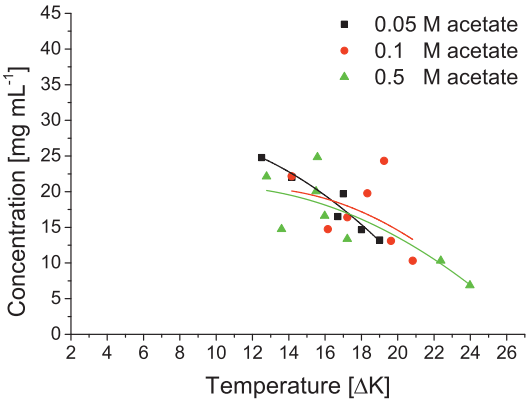

Figure 5.30: Metastable zone width of lysozyme chloride at pH 5.0 acetate buffer of different concentration

5.2.3 Influence by repeated dissolving and crystallizing cycles

The influence of repeated crystallizing and dissolving of crystals was observed in this Chapter. Here the pH values 5.0 (0.1 M acetate buffer with 4 wt% sodium chloride), 7.0 (0.1 M phosphate buffer with 4 wt% sodium chloride) and 9.0 (0.1 M glycin buffer with 4 wt% sodium chloride) were chosen as systems for long-time crystallization tests. At pH 5.0 two long-time tests were examined with different temperature profiles. The temperature profiles are shown and confronted in Figure 5.31. The first is a

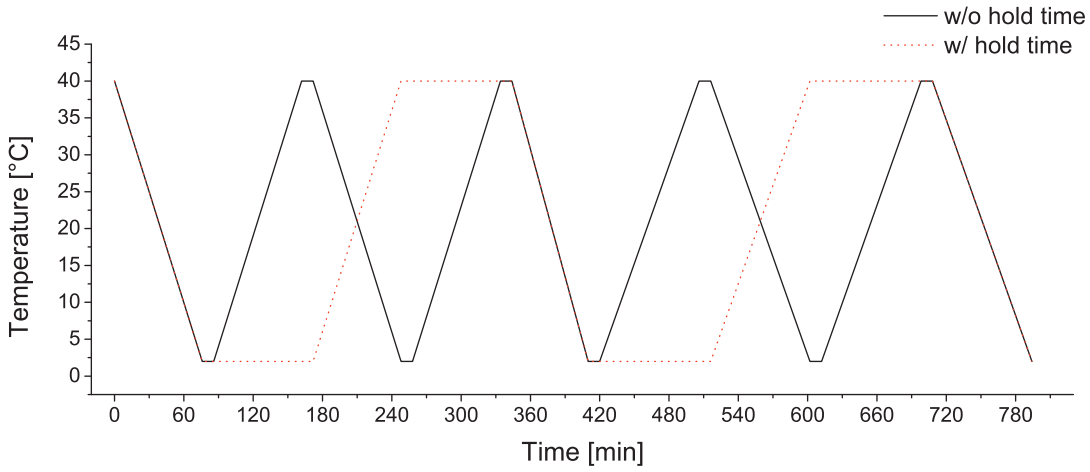

Figure 5.31: Comparison of temperature profile with and without hold time

temperature profile without retention time, and the second one uses some retention time at the end point of the heating and cooling curves. The appropriate buffer and lysozyme were weighed into the HPLC vessel and the crystallization cycles keep running until no further nucleation or solubility was detected by turbidity probe, or after a long period of time (several weeks!). It is shown in Figure 5.32 that the temperature of the solubility line at pH 5.0 remains constant while the nucleation line increases with time. In a comparison of Figures 5.32 and 5.33 a similar slope for the lines of the crystallization cycle count was found. The slope of the lines plotted versus time differs to each other. The measurement at pH 7.0 shown in Figure 5.34 shows a similar slope with increase of temperature versus time for the nucleation line. The last points of the pH 7.0 measurement shows a much lower temperature which ends with the state that the turbidity cannot dissolved anymore, and the measurement had to be stopped. The long-time measurement at pH 9.0 shown in Figure 5.35 gave a different and complex result. At the beginning the nucleation line versus time with respect to temperature was very close to the solubility line. This behavior was shown again after several points, after the nucleation occurs at a higher temperature than the solubility line is. Also, sometimes the nucleation line shows a much lower temperature than the solubility. It seems that the nucleation had varying points, but also the solubility line was sometimes slightly affected. Altogether, the temperature decreased with time for solubility and the nucleation line.

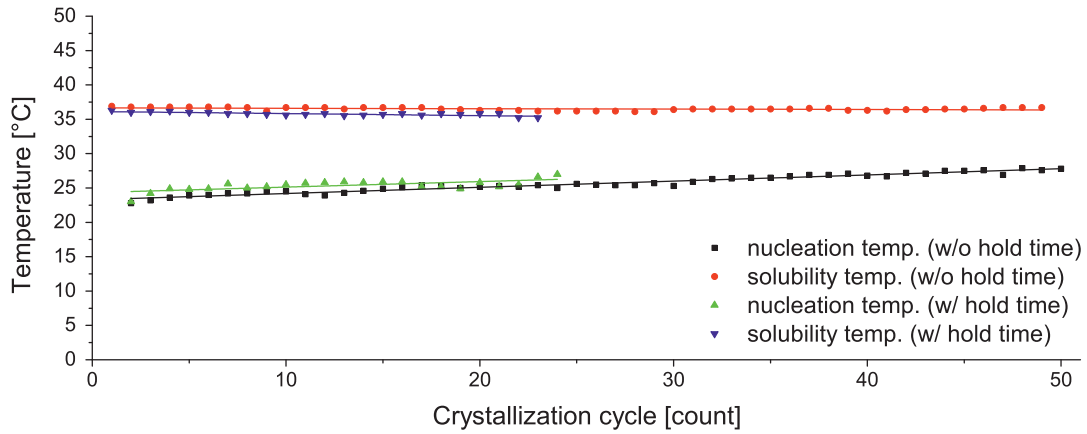

Figure 5.32: Metastable zone temperatures of lysozyme chloride at pH 5.0 plotted versus crystallization cycle counts

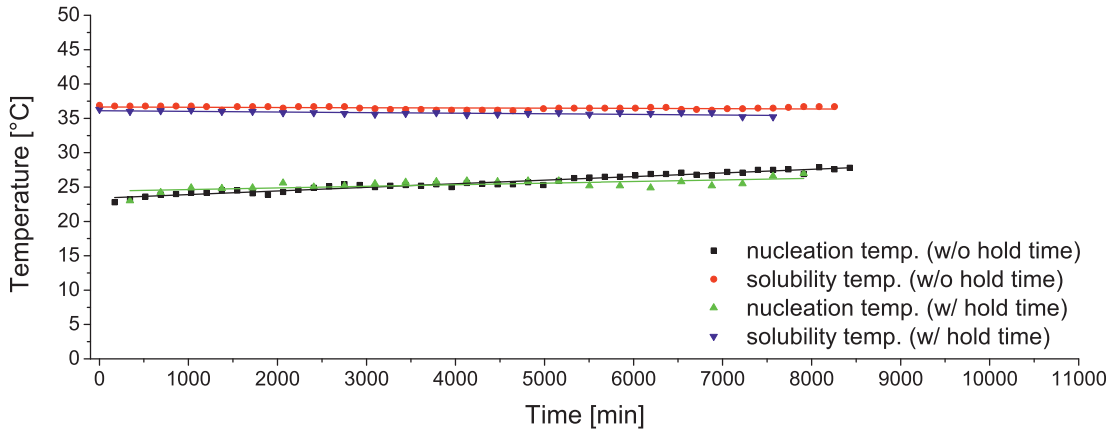

Figure 5.33: Metastable zone temperatures of lysozyme chloride at pH 5.0 plotted versus crystallization time

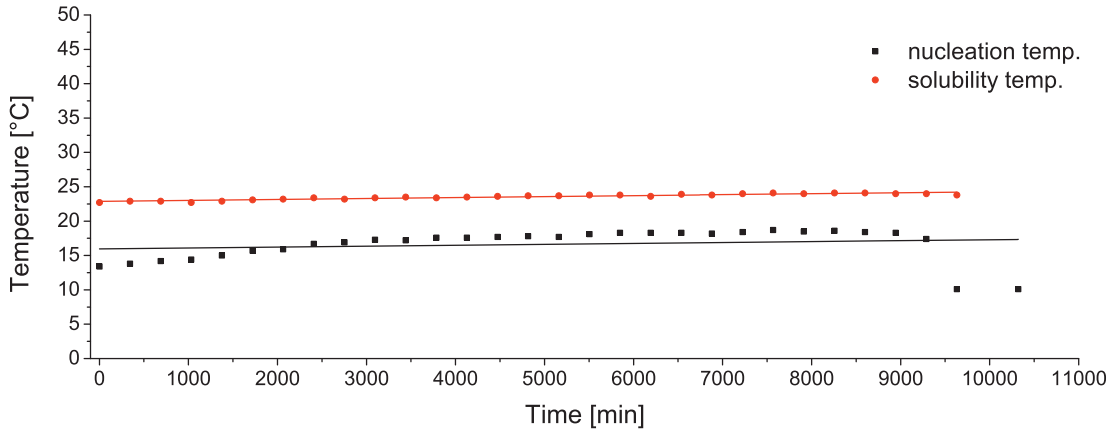

Figure 5.34: Metastable zone temperatures of lysozyme chloride at pH 7.0 plotted versus crystallization time

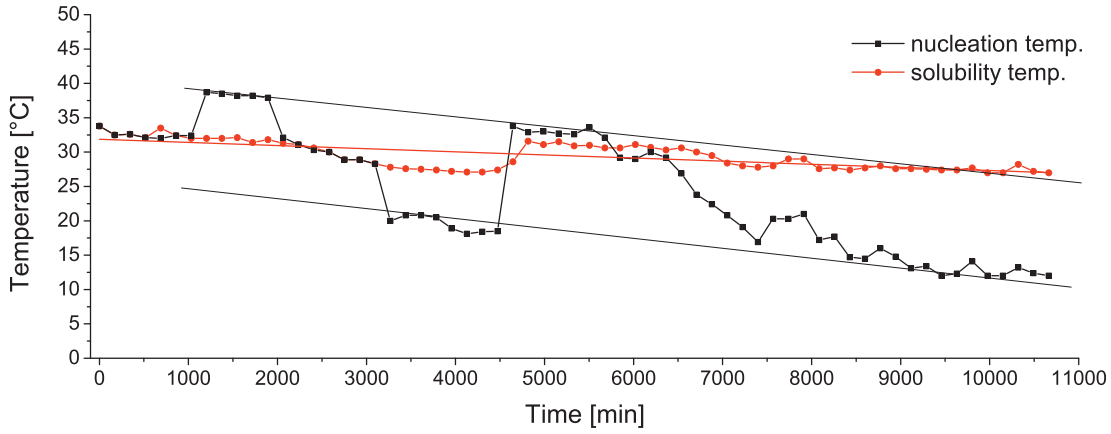

Figure 5.35: Metastable zone temperatures of lysozyme chloride at pH 9.0 plotted versus crystallization time

5.3 Kinetic measurements

5.3.1 Validation of methods

Prior to the results of the kinetic experiments, two new measurement set-ups were developed (presented in Chapter 4.3). For those measurements two prototype devices ("micro drop dispenser" and "Vision" probe) were used for a limited time. The measurements were rather used to validate these new measurement methods, than to measure the complete sets of data. The measured data with the use of those prototype devices is incorporated in the next Chapters. The modified solubility measurement set-up (shown in Chapter 4.3.1) gave reliable data within some days. After a long time, a white precipitate occurred and prevented the photometer to measure the protein concentration. The precipitate will block the light as used in the turbidity measurement. The "Vision" probe (shown in Chapter 4.3.2) delivered quite high-quality data. Due to the fact that the probe measures several wavelengths at the same time, the wavelengths will influence each other. One of the light sources varied in intensity after a short measurement time. The measurement was not possible anymore after this malfunction. Also gas bubbles under the sieve in the probe vessel had influenced the measurement and should be avoided by a modification in future experiments. The photometer method (shown in Chapter 4.3.3) was used for most of the data in this Chapter. A certain error in data due to the absence of stirring during the measurements is accepted since all mass transport distances are very short.

5.3.2 Influence of the dissolution mechanism (shrink homogeneous or fall into pieces) induced by pH

The measured data of the dissolution rate versus the pH value (the relevant for different dissolution mechanisms) are shown in Figures 5.36 to 5.38. The left axis are the direct measured data, the right side are calculations with the assumption that the crystals have an average size of 250 µm. The size is measured in a later Chapter in this work. All the three measured modifications showed a slower dissolution rate if dissolved at the pH condition used for crystallization of each modification. At higher concentrations at a certain point, the rate of dissolution of the "falling into pieces" pH

value was decreasing. The rate of dissolution after this concentration has then almost the rate of the shrink homogeneously pH value. This behavior is clearly to be seen in Figure 5.37.

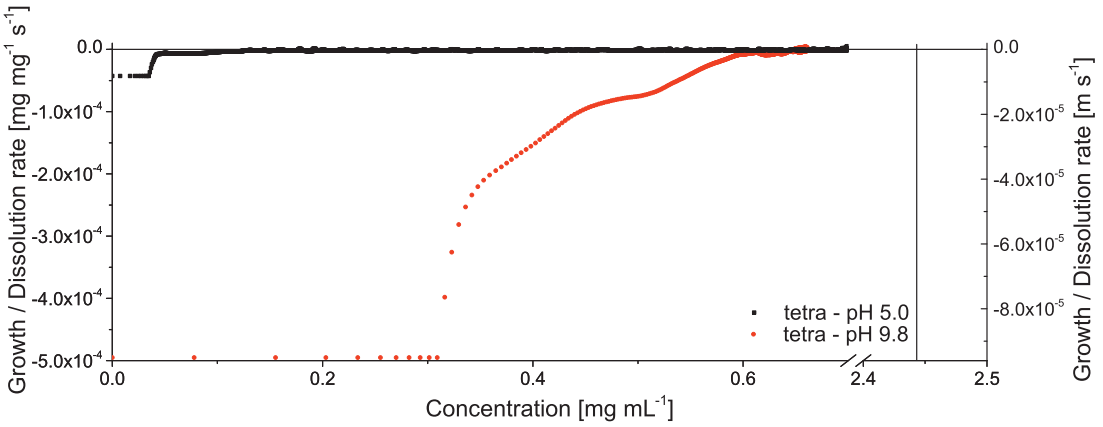

Figure 5.36: Dissolution rate of tetragonal lysozyme chloride crystals at varied pH (photometric method)

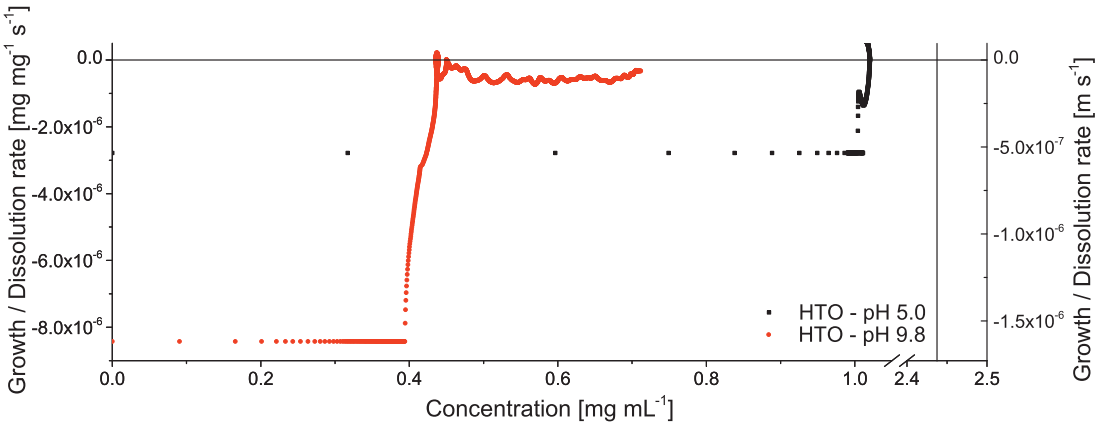

Figure 5.37: Dissolution rate of HTO lysozyme chloride crystals at varied pH (photometric method)

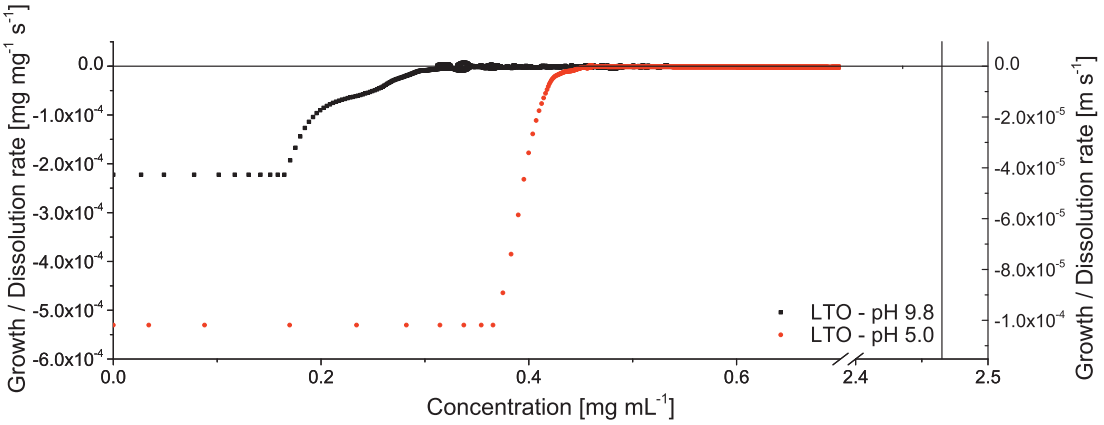

Figure 5.38: Dissolution rate of LTO lysozyme chloride crystals at varied pH (photometric method)

5.3.3 Influence of temperature

In Figure 5.39 the growth rate plot of the micro fluidized bed method is shown. The curve was created by B-spline, since no known fit is working for the kinetic measurement, to pass the growth rate of zero at a supersaturation level of zero. The data show a faster growth rate at 5 than at 10 °C. In Figure 5.40 the dissolution rate versus temperature was plotted. This data was measured by the photometric method. The highest dissolution rate was shown at 30 followed by 35 °C. Except of a later decrease of dissolution rate, the temperatures 15, 20 and 25 °C seems to had almost the same dissolution rate.

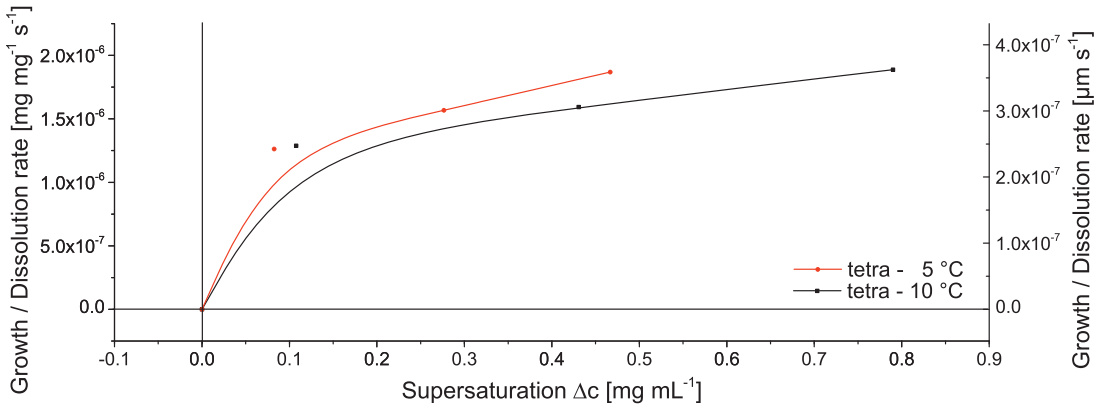

Figure 5.39: Growth rate of tetragonal lysozyme chloride crystals at varied temperature (micro fluidized bed method)

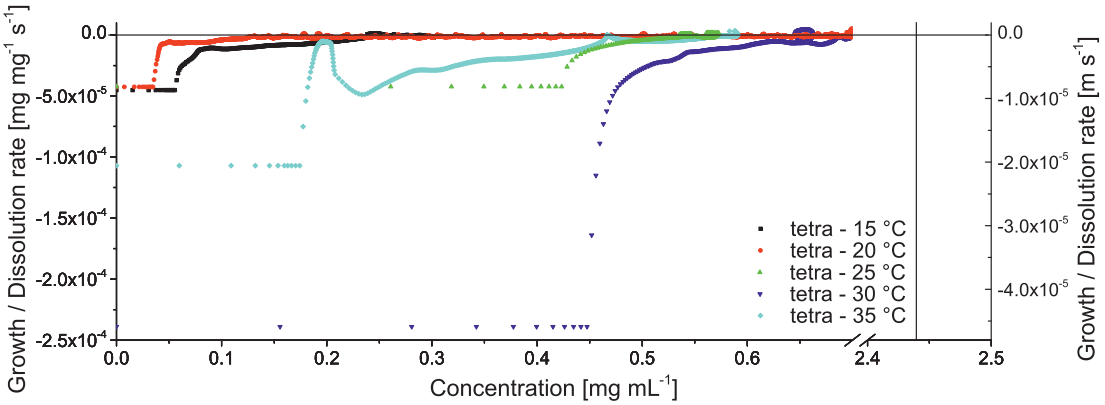

Figure 5.40: Dissolution rate of tetragonal lysozyme chloride crystals at varied temperature (photometric method)

5.3.4 Influence of the precipitant concentration

Figure 5.41 shows the data measured by the "Vision" probe. It shows that compared to data from the photometric method (see Figure 5.42) the data had a higher fluctuation. To make it easier to see the curve shape, linear fits were plotted into the diagram at data measured by "Vision" probe (Figure 5.41). A linear fit is not the right method to fit, since at zero concentration (the maximum in undersaturation), the dissolution rate should be as fast as possible. Between 0.5 wt% and 1.0 wt% there are no differences in dissolution rate. The dissolution rate with precipitate concentration of 2.0 wt% is faster at the beginning with a bigger slope to lower rates. In Figure 5.42, the data measured by photometric method look more clear. With an increase of the precipitant concentration, the dissolution rate decreased. This is the same behavior as found by the optical (not quantified) results in the microscope cell (shown in Chapter 5.1.5) measurements.

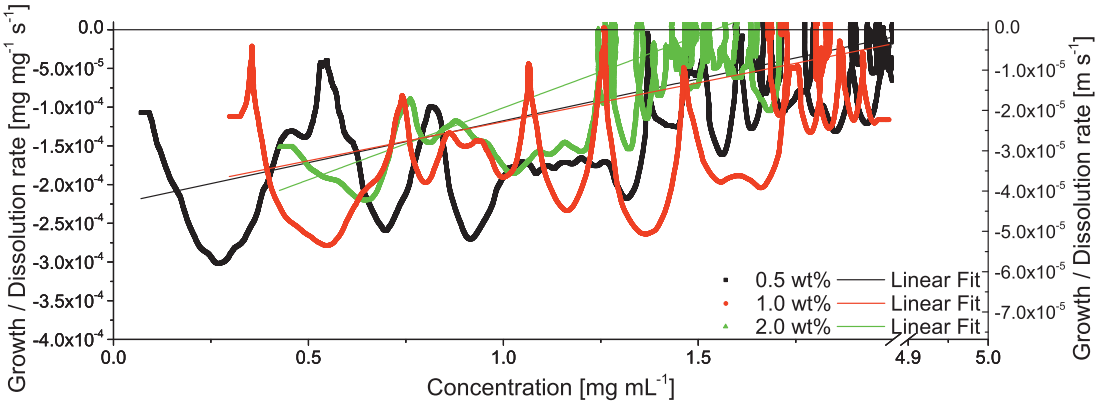

Figure 5.41: Dissolution rate of tetragonal lysozyme chloride crystals at varied precipitation concentration (Vision probe method)

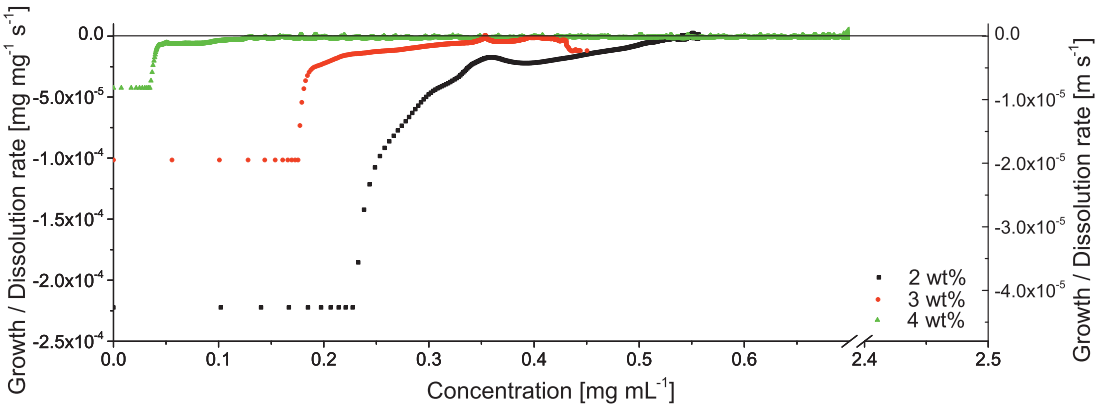

Figure 5.42: Dissolution rate of tetragonal lysozyme chloride crystals at varied precipitant concentration (photometric method)

5.4 Enzymatic activity measurements

5.4.1 Influence of the pH value

As already described in Chapter 2.1.5, the activity of a protein is affected by the pH value. For further discussions, it is helpful to quantify this behavior. In Chapter 4.6 the method of Shugar [Shu52] was described to measure the activity of the protein lysozyme. The standard operation procedure uses a pH value of 7.0. The pH influence on the enzymatic activity in this work was observed between pH of 5.0 to 8.0, to ensure that the same buffer substance for the whole measurement was used. The data are shown in Figure 5.43. The crystallized protein of different modifications were also dissolved in buffers with different pH values and are shown in Figure 5.44.

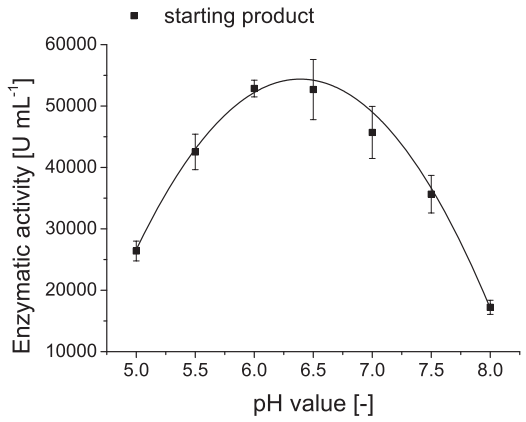

Figure 5.43: Plot of the starting product measured at different pH values with same buffer substance

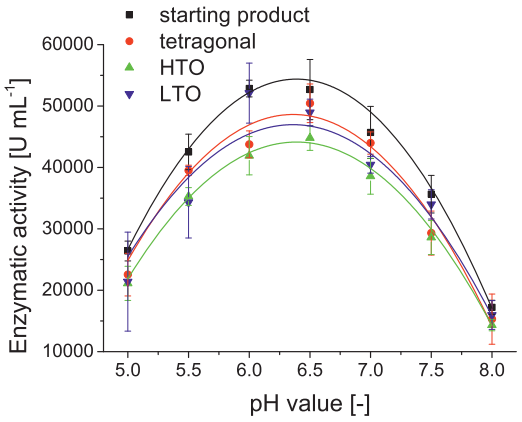

Figure 5.44: Plot of different crystal modification versus pH value

5.4.2 Influence of the dissolution mechanism

After observing the influence of the pH, the influence of the dissolution mechanism on the enzymatic activity was observed in the pH range of 5.0 up to 8.0. In Chapter 5.1.2 it was shown that there are different dissolution mechanisms in different ranges of pH values. The HTO and tetragonal modification dissolve by “falling into pieces” at higher pH values (approximately 7.0 to 8.0), and the LTO crystals at lower pH values of <7.0. The pH value of 5.0 was the crystallization condition of the tetragonal and HTO

modifications, and will result in the conventional rounding and shrinking homogeneous mechanism of dissolution. The LTO crystals, crystallized at pH 9.8 have this dissolution mechanism at the pH value of 8.0, too. The pH 8.0 lies in the region (±2.0 pH units) near to the crystallization conditions, which results in the rounding and shrinking homogeneous mechanism. In Figures 5.45 and 5.46 a factor was calculated between the crystal modification and the starting powder. It shows the differences between the curves. The standard deviation of both curves was calculated and is shown in the diagrams. An interesting fact is that the minima of the LTO modification are the maxima of the HTO/tetragonal modification and vice versa! The standard deviation compared to the factor is big, due to the method and mathematically division of two measurements. No significant change in the activity can be seen by this method to the different dissolution behavior.

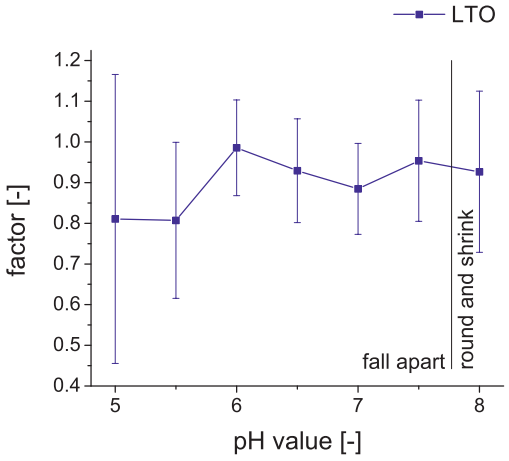

Figure 5.45: Plot of the factor between starting powder and crystallized product versus pH value

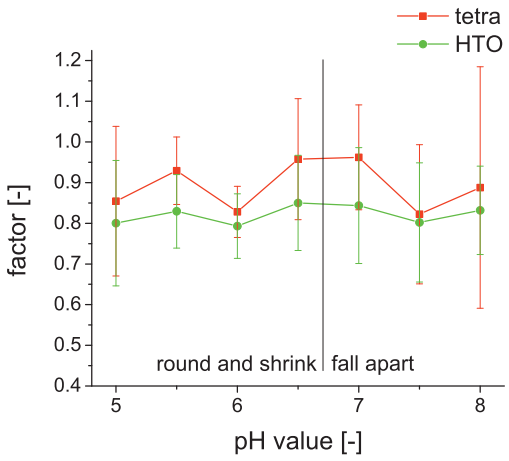

Figure 5.46: Plot of the factor between starting powder and crystallized product versus pH value

5.4.3 Influence of the buffer composition and buffer concentration

Due to the influence of the buffer concentration on the solubility of the metastable zone (see Chapter 5.2.2), the activity had to be observed for these influences. This measurement will give some information about the conformation in the *liquid phase*. In Figure 5.47 the plot of the enzymatic activity versus the acetate buffer concentration is shown. The pH value in

this measurement was kept constant, only the buffer capacity was changed. Due to the method, the standard deviation is giving no significant difference of enzymatic activity between the different buffer substance concentrations. In Figure 5.48 the concentration and pH value was kept constant, the buffer substance itself, however, was changed. Also in this measurement, there was no influence of the enzymatic activity on the buffer substance to be seen.

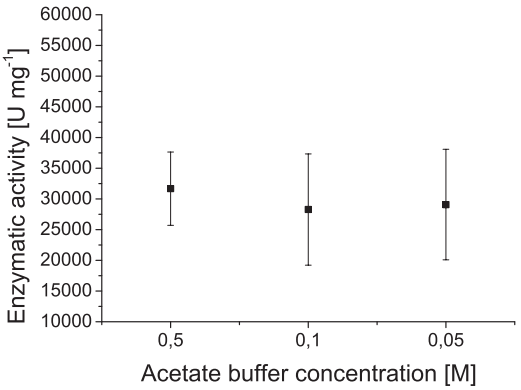

Figure 5.47: Enzymatic activity of lysozyme chloride at pH 5.0 acetate buffer of different concentration

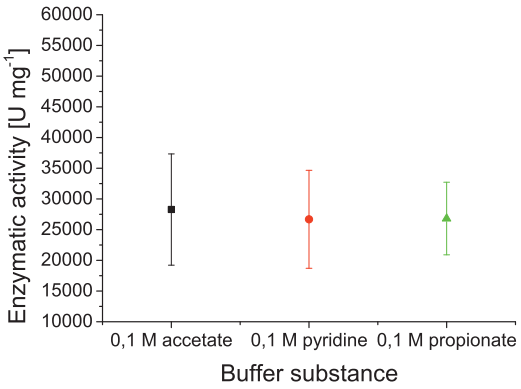

Figure 5.48: Enzymatic activity of lysozyme chloride at pH 5.0 and different buffer substance

5.4.4 Influence of repeated dissolving and crystallizing cycle

In Chapter 5.2.3 the influence of repeated crystallizing and dissolving of a protein on the metastable zone was observed. There are different states during the measurement. There is the dissolved protein in the *liquid phase* of different temperatures following the temperature profile and also the *crystalline phase* of the protein at different temperatures. In Figure 5.49 the loss in enzymatic activity in the *liquid phase* versus time was shown. Since the different crystal modifications were dissolved (in the *liquid phase*), there should be no differences between them. Between tetragonal/HTO (5.0) and LTO (9.8) the pH value is different. In Figure 5.50 the decrease of enzymatic activity versus time by repeated crystallizing and dissolving is plotted. The decrease in enzymatic activity with time was lower than in the measurement in the *liquid phase*.

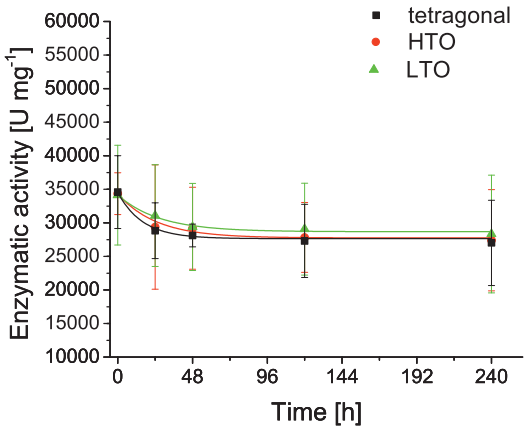

Figure 5.49: Enzymatic activity of lysozyme chloride crystal modifications dissolved in buffer

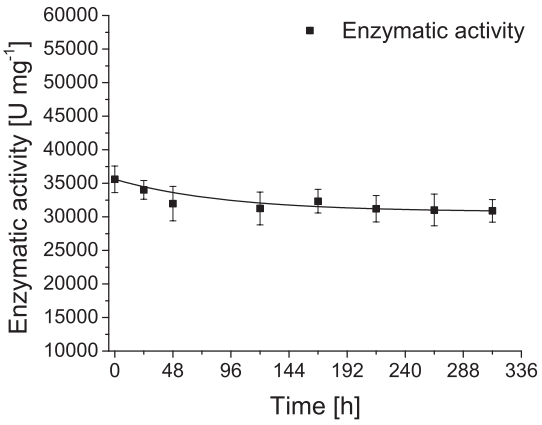

Figure 5.50: Enzymatic activity of lysozyme chloride out of the repeated crystallization cycles

5.4.5 Shelf life test in climate chamber

The enzymatic activity shelf life test was realized in a climate chamber. After every 7 days the conditions were changed and this is shown in the Figure 5.51 with varying results. Especially, the conditions at the end by this measurement method (80 % humidity and 50 °C) brought the dried crystals out of the save zone and thus the enzymatic activity decreased drastically. The enzymatic activity of the tetragonal modification decreased by −50 %, the HTO modification by −40 % and the LTO modification by −15 %.

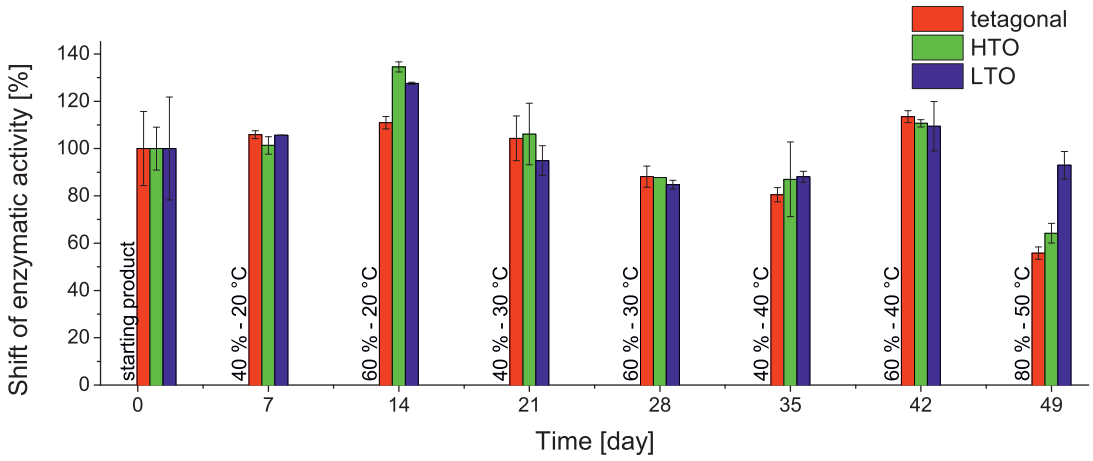

Figure 5.51: Enzymatic activity test of dryed powder

5.5 Fundamental measurements concerning structure and chemical composition

5.5.1 X-ray analysis

From the X-ray measurements in the range of 10 up to 50° 2θ (see Figure 5.52), only a broad peak around an angle of 31° was given. This peak correlates to sodium chloride which was used as precipitant. In the range of 1 up to 12° one significant peak was found at 2.77° and a smaller peak at 4.48°. There is no significant change in crystal lattice parameters by a changed pH value during the crystallization of the tetragonal crystals, at the pH value range of 4.70 and 5.30 (see Figure 5.53) by this method.

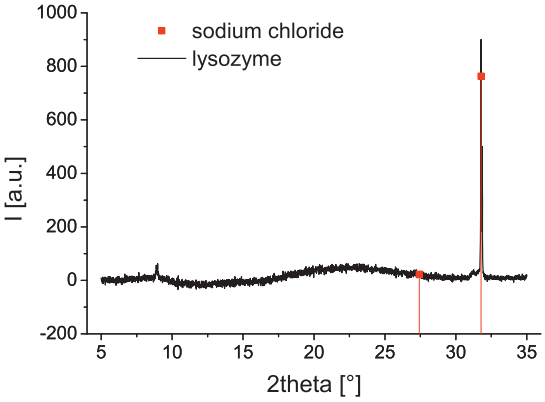

Figure 5.52: Comparison of lysozyme crystals and sodium chloride in range of 5 to 35° 2theta

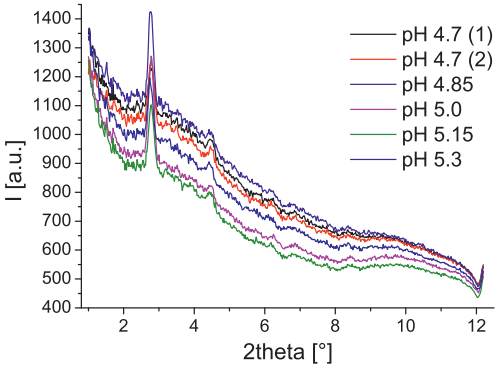

Figure 5.53: X-ray measurement in range of 1 to 12° 2theta

5.5.2 Water content

The amount of water evaporated from the different modification is shown in Table 5.3.

Table 5.3: Amount of the different "waters" in the lysozyme crystal modifications

	Tetra pH 4.0	Tetra pH 5.0	HTO	LTO
35 °C drying on air (48 h)	33.6 %	33.6 %	33.3 %	33.3 %
30 °C to 155 °C TGA/MS drying	1.25 %	1.11 %	1.94 %	0.28 %
155 °C to 225 °C TGA/MS drying	1.70 %	1.50 %	1.63 %	0.92 %

During the TGA/MS measurements, a correlation (linearity) between the mass of 28 (nitrogen) and 32 (oxygen) was observed. At the start of the measurements some air inside the device was detected, and the composition of air is known to have a ratio of approximately 20 : 80 (oxygen : nitrogen). During the heating, the gases will expanded but the ratio remains constant. No further nitrogen or oxygen was shown from decomposition of the protein sample. The decomposition of lysozyme crystals started at a temperature of around 220 °C. This temperature was defined by the first signals in mass spectrometer diagrams with a mass of 44, which is correlated to carbon dioxide by the decomposition of carbonic acid. This behavior is shown in Figure 5.55. The amount of the different "waters" can be seen and calculated from data of Figure 5.54 (TGA data) between the start temperature and the point of decomposition. It is possible to assume the two different waters (bound and free) as described by Ulrich and Pietzsch [Ulr15] by two broad peaks in the MS mass 18. In temperature, the range of 30 °C to 155 °C (drying on air and TGA/MS) correlates to the "non-bound water" ("free water"). The water which was released in the temperature range 155 °C to 225 °C correlates to the crystal water ("bounded").

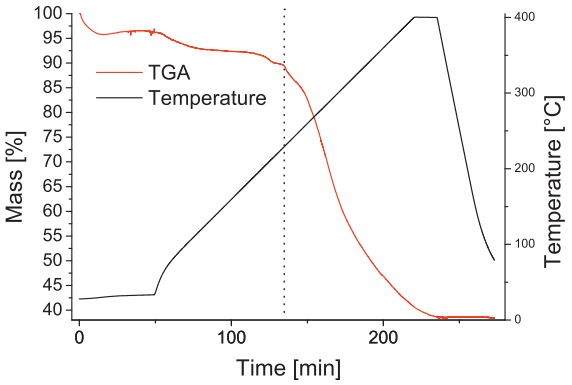

Figure 5.54: Temperature profile and mass loss of crystals during TGA measurement

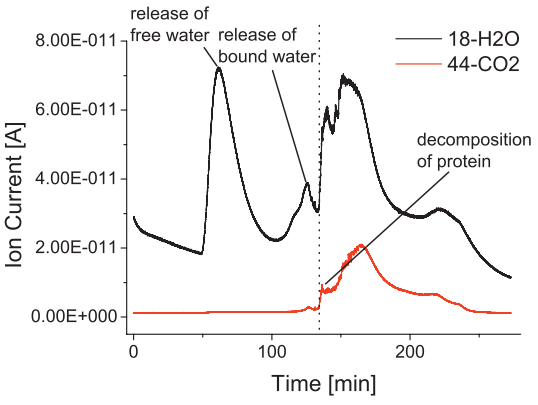

Figure 5.55: Mass spectrometer plot versus time, with notes on interpretation

5.5.3 Fundamental analysis

The fundamental analysis (Table 5.4) gives information on the composition of the protein crystals.

Table 5.4: Data in percent of mass given by the fundamental analysis

[%]	C	H	N	Cl	Na	S	O
Raw product	45.64	6.60	17.10	2.77	0.02	1.75	26.12
HTO	43.09	6.64	15.73	2.17	0.69	1.69	29.98
LTO	45.24	6.69	16.46	3.05	0.47	1.72	26.38
Tetragonal pH 4.0	42.94	6.73	15.54	3.59	0.92	1.62	28.66
Tetragonal pH 5.0	44.69	6.50	16.67	3.41	1.25	1.67	25.80

The crystallization was induced by sodium chloride as precipitant. A concentration of 4 and 6 wt% of sodium chloride was used for the crystallization of different crystals. During the filtration, some of the mother liquor will attach on the crystal surface. Due to the extreme high solubility of the protein lysozyme in pure water, it is not possible to rinse the crystals to remove the salt! Depending on the size of the crystals (surface area) the amount of adhering sodium chloride will change. With the known molecular mass of sodium and chloride, the amount of chloride can be subtracted if assumed that all the measured sodium will be bound to the appropriate stoichiometric amount of chloride. The amount of chloride after stoichiometric combination of sodium and chloride is shown in Table 5.5. Only one up to three percent in mass of a protein crystal is chloride as "counter ion". A calculation with molecular mass results in a range of 0.62 up to 1.55 chloride atoms, to each lysozyme molecule in a crystal.

Table 5.5: Recalculated chloride data after stoichiometric sodium chloride recombination

[%]	Raw product	HTO	LTO	Tetra pH 4.0	Tetra pH 5.0
Cl content w/o NaCl	2.74	2.32	1.11	1.48	2.17

5.5.4 Particle size analysis

The particle size distribution of the tetragonal lysozyme chloride crystals showed a trimodal distribution. The distribution is shown in Figure 5.56

and shows maxima at 70, 300 and 1200 µm in size. The Figures 5.57 and 5.58 show the corresponding particles. The 70 µm particles are broken-off parts. The particles 300 µm in size correspond to the appropriate grown crystals of the tetragonal modification and the size of 1200 µm corresponds to some agglomerates. If the particle size is compared to the particle volume, the 300 µm in size particles are the most frequent. The particle size distribution of the HTO lysozyme chloride crystals also showed a trimodal distribution. In Figure 5.59 the particle sizes are given as 70, 300 and 1200 µm. The volume amount of the distribution was different from the distribution of tetragonal crystals. The highest volume belongs to the 1200 µm sized particles. The HTO crystals are generally bigger in size and have often in one length an elongated shape. This was shown in the Figures 5.60 and 5.61. The particle size distribution of the LTO lysozyme chloride crystals is shown in Figure 5.62. Again a trimodal distribution was measured. The mean particle sizes are 70, 300 and 1200 µm. The LTO modification are needle shaped crystals. The measurement showed the size of 70 µm for the width of the needles and 1200 µm for the length. The 300 µm correspond to the average value if the crystals are spherical.

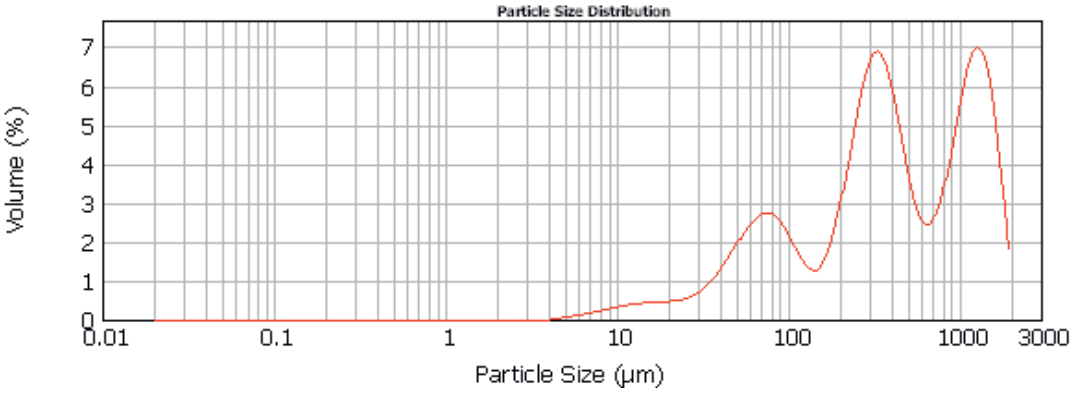

Figure 5.56: Average particle size distribution of tetragonal lysozyme chloride crystals by Mastersizer 2000

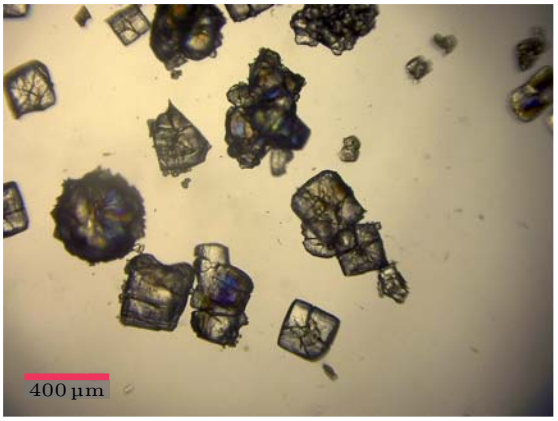

Figure 5.57: Tetragonal lysozyme chloride crystals from Mastersizer measurement

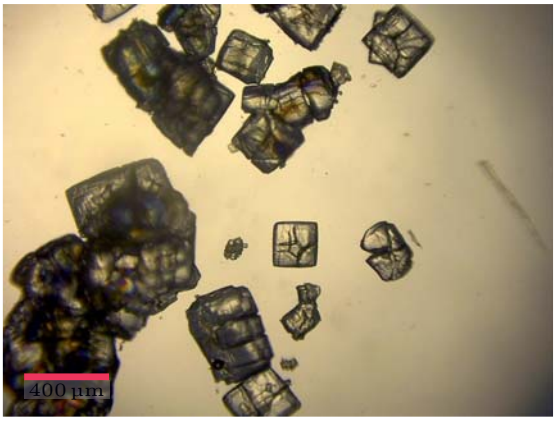

Figure 5.58: Tetragonal lysozyme chloride crystals from Mastersizer measurement

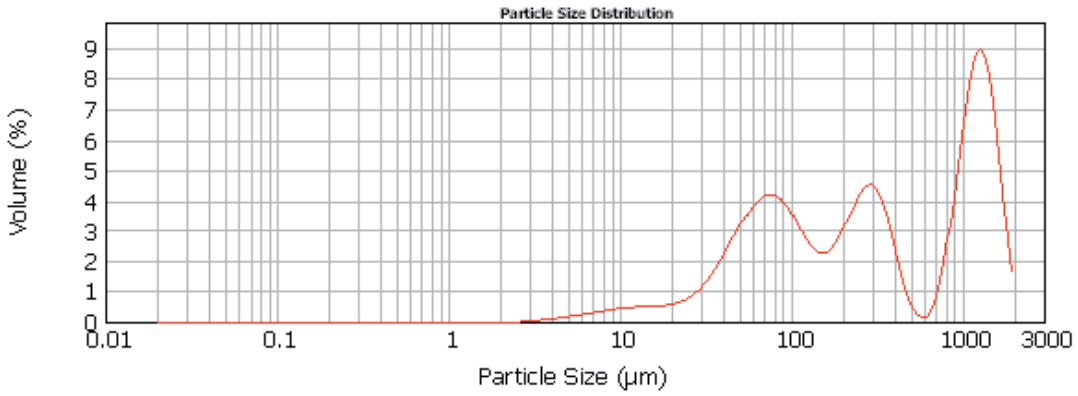

Figure 5.59: Average particle size distribution of HTO lysozyme chloride crystals by Mastersizer 2000

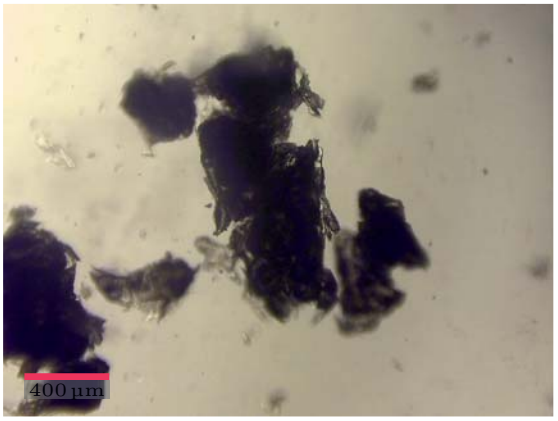

Figure 5.60: HTO lysozyme chloride crystals from Mastersizer measurement

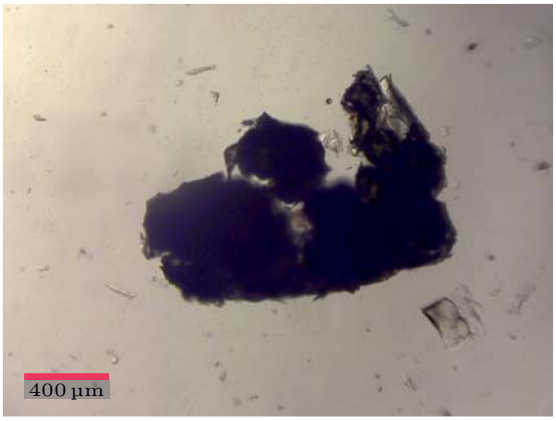

Figure 5.61: HTO lysozyme chloride crystals from Mastersizer measurement

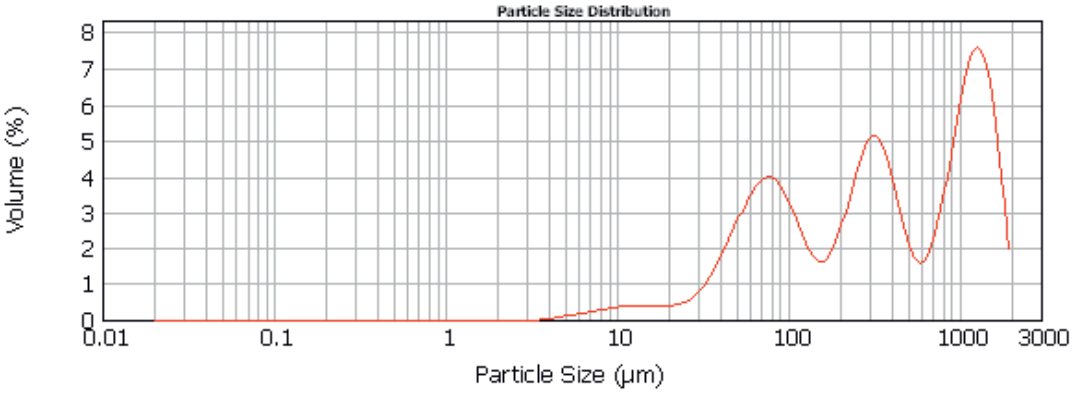

Figure 5.62: Average particle size distribution of LTO lysozyme chloride crystals by Mastersizer 2000

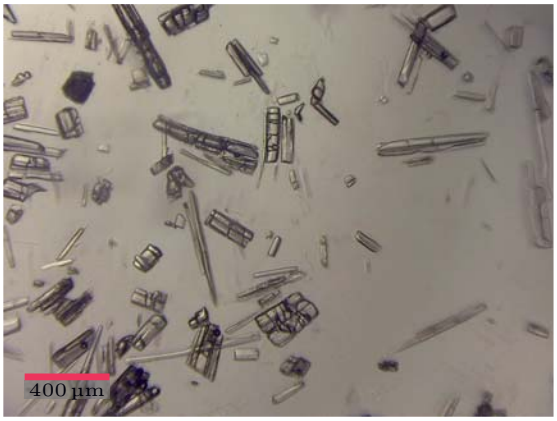

Figure 5.63: LTO lysozyme chloride crystals from Mastersizer measurement

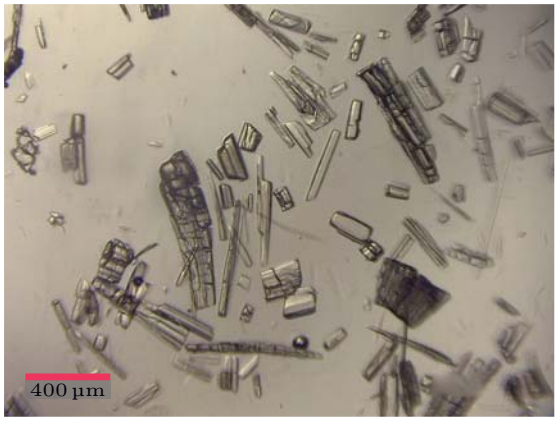

Figure 5.64: LTO lysozyme chloride crystals from Mastersizer measurement

6 Discussion

6.1 Fundamentals of protein crystals

For a better understanding the discussion of the measured fundamentals will be presented first. The discussion of dissolution mechanism, metastable zone and the dissolution rates will build up on the fundamentals discussed in the following.

6.1.1 Water content of protein crystals

It is important to have a clear idea of the nature of a protein crystal at this stage of the discussion. Many authors, especially, Jones [Jon14] as well as Ulrich and Pietzsch [Ulr15] clarified that protein crystals contain besides the protein itself, water, buffer and salt. This is different from conventionally known crystals which are, when pure, 100 % of the one material unless they are solvates (hydrates) or cocrystals. Matthews [Mat68] described that protein crystals contain between 27 and 65 % of water. The so-called "water", however, is not only pure water! There are two kinds of "water", a bounded water as known from hydrates (lattice water), and the so called "free water", which is actually the mother liquor without the protein that means buffer which contains dissolved precipitant agents (often salts). Due to this, buffer and the precipitant are included inside the protein crystal. In Chapter 5.5.2 the water contents of the crystals used in this work are given. As to be seen in Table 5.3 the lysozyme chloride crystals contain approximately 35 % of "free water" and one to two percent of "bound" lattice water.

6.1.2 Diffusional potential inside the water of protein crystals

Some experiments using coloration of the protein crystals support these statements as shown earlier by Müller [Mül12b]. The colorant is an im-

purity, but it will not disturb crystal growth. The experiments confirmed that diffusion into the crystals is possible, and that there is a “free water” inside the protein crystals. In this work a pH sensitive colorant was used, to colorize the protein crystals (see Chapter 5.1.8). It was shown by these experiments that the color inside of the protein crystals can change, due to a pH change in the solution. Also, the “free water” inside the protein crystals has clearly a diffusible exchange of protons, with the solution outside the crystals, in which the crystals are dispersed. The pH value inside the crystals, distributed due to the “free water” content will be changed.

6.1.3 “Counter ions” in protein crystals

The amount of chloride as “counter ions” (see Chapter 5.5.3) gives the certainty that a protein crystal is build up from ion bonds by coulomb interactions. In the *liquid phase* with hydration of ions by the solvent, the amount of chloride to neutralize protein molecules must increase with decreasing pH value, since all pKa values of the residues of amino acids (see Chapter 2.1) reacts in the same direction. Each functional group (each amino acid in the protein molecule chain) will increase or decrease their charges by a different value. Each functional group has a different pKa value and gives a different response to changes in pH value, since the pKa value is a value which marks the equilibrium. Some more information about the charges of lysozyme versus pH can be found in the paper of Spassov and Yan [Spa08]

The *solid state*, a crystal, is different compared to the same molecule in the *liquid phase*. Here, the charges of protein molecule surfaces must arranged in cooperation with “counter ions”. The attraction and repulsion forces between molecules need to reach an ideal value [Mat03]. Those “counter ions” will be statistically distributed and fixed in the crystal lattice [Lim98]. In simple ion crystals like sodium chloride, the coulomb attraction forces between positive and negative charged ions start with a value of zero, at a distance of zero. The repulsion forces increase if the electron shell of the ions starts to overlap. With protein crystals it is more complicated, since there is not only one charge on the molecule to generate an ion (which is assumed if the molecule is hydrated by solvent molecules in *liquid phase*), there are charges distributed over the whole surface of the large protein molecules.

The known type of modification exists, due to several ideal arrangements of molecules and "counter ions" to form a stable crystal [Mat03].

6.1.4 Structural justification in protein crystals

From X-ray measurements shown in Chapter 5.5.1 it is known that with only slightly changed pH values the lattice parameter remain the same. The same arrangement of molecules will still exist in a protein crystal within a certain small pH range. Due to the changed pH value, the charges of surfaces are changed, too. The amount of "counter ions" is also changed (to be seen in Table 5.5) but in opposite direction than in the *liquid phase*. This is possible due to the arrangement of protein molecules in the protein crystal, which have already some positive and negative charges. These charges are often able to compensate each other, so that a lower amount of "counter ions" is needed, to form a neutral crystal than calculated by pI in the *liquid phase*. The bound lattice water now acts as dipole-ion interactions, it is necessary to build up a neutral and stable crystal lattice (like hydrates). The amount of lattice water to form tetragonal crystals at e. g. pH 4.0 is higher than at pH 5.0 (see Chapter 5.5.2). This can also be seen by microscope images. If the outer shape of the crystals is the quality criteria, the tetragonal crystals crystallized at pH 4.0 is not as good as at pH 5.0. The not ideal surface charges, need more lattice water to form stable crystals. The amount of lattice water of other modifications cannot be compared, due to different lattice modification. This will also give a different X-ray pattern for the different modifications. Chapter 5.4.1 shows an influence of the pH value on the activity. It also shows a change in protein molecule conformation (see Chapter 2.1.5), due to slightly changed pH values. This results from a conformation change of the molecules in the *liquid phase*, during the change of the pH there.

6.1.5 Chemical composition of protein crystals

Besides the "counter ions", other components can be found by a fundamental analysis (see Chapter 5.5.3) and need to be discussed, too. If nitrogen will be used as a reference value for the calculation, according to the molecular composition of a lysozyme crystal with sodium chloride as precipitant

by amino acid sequence, probably all components can be explained in their amounts with respect to the fundamental analysis. Looking at the components used to crystallize the lysozyme proteins (see Chapter 4.1), the components forming the buffer can be neglected, since their concentration is negligible low. The main substances from the used components, if the concentration is considered (see Chapter 4.1), and also those substances found in the fundamental analysis, are three: lysozyme, sodium chloride (dissolved in "free water") and water (free and bound).

6.1.6 Particle size distribution after batch crystallization

In Chapter 5.5.4 the particle size distribution is observed. This measurement was chosen in order to get some information on the average size of lysozyme protein crystals from the batch crystallization process as shown in Chapter 4.1. This data is needed for the calculations in Chapter 5.3. The kinetic data are measured as increase of mass, and should be converted into values of a characteristic crystal length, which are more common in crystallization. The sizes of the trimodal distributions were already assigned to the crystals, broken parts of crystals, and agglomerates in Chapter 5.5.4.

6.2 Dissolution mechanism of lysozyme chloride

In literature (e.g. Matsuoka and Sumitani [Mat88], Beilles et al. [Bei01] and Pauchet and Coquerel [Pau07]), the "falling into pieces" mechanism of dissolution is only described in a similar way in case of binary systems, at conditions when only one of the components will be dissolved or will partially be molten. This situation is not faced here.
The point that there is a possibility to have a phase transition on the surface of crystals, while the dissolution takes place assumed due to the opacity prior the dissolution, is not valid. In Chapter 5.1.7 a test of induced phase transition due to optimal aligned parameters shows that crystals of the other modification would start to nucleate, and afterwards grow on the surface of the old modification. But this will not occur on the surface of the dissolving crystals. In the discussion of fundamentals (Chapter 6.1), a protein is a macromolecule built of different amino acids by polypeptide bonds. Distributed over these molecule chains, some functional groups

from different amino acids exist (see Chapter 2.1). These functional groups can hold charges [Wie02]. By protonation or deprotonation these charges, which depend on the pH value, can be changed (see Chapter 2.1). From those charges, also the protein molecules have an overall charge distribution on their total surface [Pus02], which results in attractive and repulsive forces between the protein molecules in a crystal lattice. The crystallization step incorporates some "counter ions", and alignment of the molecules to reach the lowest repulsion forces within the neutral crystal. From X-ray experiments, it is known that slightly changed pH values will result, in most cases, in the same lattice parameters. It needs a larger change in pH values until the modification will changes. Due to the large solvent content (the "free water") and the low binding energy, protein crystals are soft and sensitive to small changes in external conditions [Kam78].

6.2.1 Influence of the pH value

A driving force (a non-equilibrium situation) which is more than two units of pH value (see Chapter 5.1.2) is needed, before the crystals dissolve, and the repulsion forces between all molecules in a crystal will be increased enough, to push the protein molecules in case of a dissolution apart. This is also seen in the phase transition test in Chapter 5.1.7 for a saturated solution. The crystals become opaque, but a dissolution is not to be seen anymore. Only low forces are necessary to destroy a crystal lattice of a protein crystal, fixed during crystallization. Supported by the experimentally found results, the hypothesis is therefore that the repulsion forces generated by a pH value difference of more than two units, compared to the growth conditions of the crystals, delivers enough energy to disrupt the lattice so that the crystals can fall into smaller pieces. This holds, however, only for the case of the same precipitation agent.

6.2.2 Influence of the precipitant substance

The effect of the precipitant substances is more complex. The dissolution mechanisms of the HTO and tetragonal modification give a different result, compared to crystals of the LTO modification. For all dissolution experiments only the precipitant is changed. The pH values of the undersaturated solution is kept constant by the buffer. The pH value is kept on

the level of the solution used to crystallize the crystals, which are thereafter examined in the dissolution experiments. The first result is that the salts sodium bromide, sodium nitrate and ammonium sulfate change (substitute) the "counter ions" inside (the "free water"), and on the outer surface of the protein crystals. The "counter ions" are necessary to neutralize the protein molecules inside the crystal. Chapter 5.5.3 discusses on the incorporation of "counter ions". The "counter ions" can be changed for example from Cl^- to Br^- or $NO_3{}^-$. The "counter ions" do not have the same size. In the case that the new "counter ions" are sterically larger, this will result in a "falling into pieces" dissolution mechanism, in case of the dissolution of the lysozyme crystals. Due to the larger sterically size, the charged electron clouds will overlap, which results in changed attraction and repulsion forces in the crystal lattice. This is the second parameter to change the dissolution mechanism. The exchange of Cl^- by $SO_4{}^{2-}$ will result additionally in a different charge of the single ion, which results in different amounts of needed "counter ions". If $NO_3{}^-$ and $SO_4{}^{2-}$ will be used for the crystallization of lysozyme, it will result in a different crystal morphology, the triclinic and monoclinic form [Har06; For99b]. The usage of organic compounds or solvents shows the same dissolution mechanism, the "falling into pieces" of the crystals. These substances change the dielectric constant and react as anti-solvent, which lowers the solubility of proteins. These substances are not able to exchange "counter ion", but the use of all these substances will result in an undersaturation against the "counter ion", since the new solvent in its composition contains no chloride anymore. It seems the extraction of the "counter ions" by undersaturation generates again, the "falling into pieces" dissolution mechanism.

The LTO modification shows except ammonium sulfate, no "falling into pieces" dissolution behavior by an exchange of the incorporated "counter ions". An explanation is the position of the system with respect to the pI, the isoelectric point (see Chapter 2.1.4). At this point the charge of the protein molecule in its total, is neutral. At the pI, theoretically no "counter ions" are needed. As an example, in solutions with a pH value more acid than the pI, the molecules get a positive overall charge. In the *liquid phase*, there are several ions which result in a neutral charged solution. For the *solid state*, the protein crystal, it is necessary to incorporate some "counter ions" inside the crystal lattice to reach a neutral crystal. The gap between

the crystallization pH, and the pH equivalent to the amount of "counter ions" needed, make the difference between the different modifications. The pI for lysozyme is located between pH values of 9.3 and 11.3 units [Mor05; Tan72]. That means, for the LTO modification less "counter ions" are needed to create a neutral charge of the crystals. If a protein crystal needs only a reasonable small amount of included "counter ions" for the neutralization, the dissolution mechanism does not change, and the dissolution mechanism for HTO and tetragonal crystals on the one hand, and LTO lysozyme crystals on the other hand, differs from each other. It is the same effect which was observed for different pH values, which needs a difference in pH of about two pH units to change the dissolution mechanism.

6.2.3 Influence of other parameters

The temperature has its influence on the kinetics, but only in the sense of the Arrhenius correlation. The temperature has no influence on the dissolution mechanisms of lysozyme chloride. The precipitant again affects the thermodynamics, and by the resulting different driving forces, the kinetics of the dissolution due to the influence on the solubility line (see salting-in/out in Chapter 2.2.2). The buffer substance and concentration are to be neglected values since the concentration is very low (see the frame conditions of lysozyme crystallization in Chapter 4.1). The buffer substance and concentrations have no effect on the dissolution mechanism. Furthermore, the fundamental data give no information on the incorporation of buffer molecules into the protein crystals. No incorporation of buffer molecules into the protein crystals can be seen, and no effects from the change due to the different buffer can be seen either. But there is the "free water" and the ability of diffusion of the solvent molecules into this water. Therefore, the buffer substance is not proven by the fundamental analysis since the concentration is low.

6.3 Metastable zone width of lysozyme chloride

6.3.1 Influence of the pH value

As already presented in Chapter 5.2.1, the plot of concentration versus time shows a ranking of the curves (Figures 5.15, 5.17 and 5.19). This means for

each concentration, there is one pH value which gives the lowest temperature for the solubility. But what does it mean, if the lowest temperature is needed for the solubility line of one pH value? From Chapter 6.1.4 it can be seen that for slightly modified pH values the crystal lattice parameter remain the same. The effects of the pH value on the solubility line is to be found in the *liquid phase*, since the lattice is fixed in case of only slightly modified pH values. The lowest temperature is needed for the solubility, this means the driving force (Gibbs free energy) is the highest! The data can be seen in Chapter 5.2.1, especially, in the 3D plot in Figure 5.24. If a constant concentration will be observed, there are some pH values which need the lowest temperature. The values of pH 5.0, pH 6.7, pH 7.7 and pH 9.0 show those lowest temperatures.

The pH value 5.0 will fit best to the crystallization conditions of tetragonal and HTO modifications of lysozyme, see e. g. [Mül12b; Jud99]. Also, the quality of the prepared crystals in relation to the outer habit at pH 5.0 is the best. By a step like behavior in the solubility curve around 18 mg mL^{-1} respectively 27 to 30 °C at pH 5.0 (Figure 5.15) is possible, to mark the transition point of the different modifications. For lower temperatures the tetragonal modification will exist, and for higher temperatures the HTO modification. Closest to pH 7 (Figure 5.17) the lowest solubility is at pH 6.7 and 7.7. Harata [Har94] used a pH value of 7.6 in his works for the monoclinic modification of lysozyme crystals. In the pH range of 9 (Figure 5.19) there is a local minimum in temperature around pH of 9.0 and 8.25 to 8.5. The pH of 9.0 correlates with the crystallization conditions for the LTO modification. Here to be seen e. g. in the work of Aldabaibeh et al. [Ald09b] which gives a pH value between 8.6 and 10 for LTO modification of lysozyme. A pH value of 8.4 was used by Brinkmann et al. [Bri06] for the crystallization of hexagonal lysozyme, but in the presence of sodium nitrate as precipitant, and not sodium chloride which was used for solubility measurement in this work. At the minima in the saturation temperature at a pH range of 4.0 to 10.5, respectively, the ideal crystallization conditions (correlated to literature data) can be found.

Figure 5.17 also shows a split in two regions of the solubility curve. Two modifications will exist with different values of solubility (except one point). But the point of nucleation stays almost the same according to Figure 5.18.

That means during the measurement process a phase transition occurs. This is a disadvantage for a fast turbidity measuring method when used to determine the metastable zone width. Because it is possible that the nuclei will be dissolved again and the new nuclei for a different modification will be crystallized. Or it is possible that the crystal itself fulfills a phase transition. In both cases the turbidity technique is not able to give any reliable information during measurements since in case an opaque media occurs, no further information can be gathered. For a value of pH near to pH 9, two modifications will exist with their nucleation and solubility curves.
The width of the metastable zone is plotted in Figures 5.21 to 5.23, respectively. Except of the lower concentrations next to pH 9 (pH 9.0 to 10.5), all of the domains (pH 4.0 to 5.0, pH 6.2 to 7.7, pH 7.7 to 8.2, pH 8.25 to 8.75 and pH 9.0 to 10.5), respectively modifications, have the same sequence. The width of metastable zone increases with increasing pH. The inversed order for the lower concentration and beyond pH 9 (pH 9.0 to 10.5) is not understood yet. The pI for lysozyme is located between pH values of 9.3 and 11.3 [Mor05; Tan72], which could explain the behavior. The sequence of metastable zone width is inversed, if the pH value is higher than 9.0. But therefore, the pI has then to have the value of 9.3 or lower, and not other values as given by Moritz and Simpson [Mor05] with pH 9.3 and Tanford and Roxby [Tan72] with pH 10.20!

6.3.2 Influence of other parameters

As written in Chapter 5.2.2, there is no influence of the buffer substance on the metastable zone. The buffer concentration, especially, at a higher concentration, has an influence on the nucleation and solubility line. If compared to the discussion of the chemical composition of protein crystals (Chapter 6.1.5), the buffer itself is not to be found in the protein crystals. Due to the coloration experiments in Chapter 4.10, the buffer substance is sterically not too big that it is impossible to incorporated in the “free water”. But the concentration of the used buffer substance is almost too low to be recognized in the data. If the buffer concentration for the same buffer substance is changed, the nucleation and solubility line will be changed. The width of metastable zone remains almost the same. It can be assumed

that the buffer itself is also able to act as precipitant (see e. g. Chapter 2.2.2) if the concentration is high enough.
The precipitant substance is not changed in this work in the metastable zone measurements, since if the precipitant is changed, also a different crystal will be crystallized. The concentration of the precipitant concentration is already well explained in literature (see e. g. Maosoongnern et al. [Mao12], Forsythe et al. [For99a] and Howard et al. [How88]).

6.4 Growth and dissolution rate

6.4.1 New methods for kinetic measurement

Due to the fact that in protein crystallization only low amounts of material is available for testing, and growth and dissolution rate dispersion is existing, new methods for the determination of the growth and dissolution rates have to be developed. This is possible by the use of some new devices. One of such devices is a "micro drop dispenser" with a very high accuracy (approximately $\pm 1\,\mu L$) to dispense volumes from $7\,\mu L$ down to intervals of $1\,\mu L$. It is possible to mix a supersaturated solution, if salting-out (see Chapter 2.2.2) is possible for the measured substance. With this technique, it is possible to reduce big equipment (in substance hold up) by an small ($3\,mL$ in volume) circuit only. The second device is a new probe which is able to detect concentrations in small volumes starting from $2\,mL$. The measurements make use of the possibility of concentration calculation for proteins in solvents at a wavelength of $280\,nm$. Here a deviation of concentration occurs, due to the extinction coefficient. Especially, from Chapter 5.5.2 it is known that protein crystals contain not only protein. A big portion of mass of a protein crystal is water (approximately 30 % in mass!) and some salt. Here is a big calculation error possible from the calculation of the absorbency to the concentration. It is not known, if the extinction coefficients are measured by weight of the "protein crystals" (which contain beside the protein itself e. g. water and salt in big amounts), or if those calculations are of pure protein? Since the concentration measurement at wavelength of $280\,nm$ is also used for solubility measurement in the micro column method, here the same error can be expected! It is better, however, to measure some data with a systematic error than to

have no usable data at all. Furthermore, the calculation of the measured data units ($\mathrm{mg\,mg^{-1}\,s^{-1}}$), into more common in crystallization, is not free of some deviations. Is the crystal composition at the start and the end of growth rate measurements the same, or will it change during crystal growth? Due to only limited amounts of available protein crystals (high costs), it is not possible to use sieving to get a small size fraction. The particle size distribution measurement (Chapter 5.5.4) shows that there are crystals of different sizes. Only the average value of size is used to calculate the more common units ($\mathrm{mg\,s^{-1}}$).
The "Vision" probe was in an early stage of development. The measured data contain a deviation due to electrical noise. The deviation of the measured points is bigger than from the measurements with a standard UV/Vis photometer.

6.4.2 Growth and dissolution rates versus temperature

The growth rate of lysozyme chloride at pH 5.0 of the tetragonal modification shows a faster growth rate at 5 than at 10 °C. Following the Arrhenius equation, the growth rate should increase with an increase in temperature. Here it is different. Comparing the data of Chapter 5.2.1, there is a step in the solubility curve (see Figure 5.15) around 27 to 30 °C. Therefore, the existing of two modifications at pH 5.0, the tetragonal for temperatures lower than 27 to 30 °C, and the HTO for higher temperatures must be assumed. The concentration in both measurements are the same, and so are the level of supersaturation. Both temperatures are in the ideal range of crystallizing the tetragonal modification. The data show, however, that the driving force (Gibbs free energy) is bigger for lower temperatures and thus the growth rate increases for the modification of the lower temperatures.
The dissolution rates show similar results. There is no linear ranking of the curves by temperature. The fastest dissolution occurs at 30 °C. This is the transition point of the modifications tetragonal and HTO as shown in Chapter 5.2.1. Temperatures lower or higher than this will decrease the dissolution rate. This is due to the fact that the tetragonal modification is crystallized best at 4 °C and the HTO modification at 40 °C (see Chapter 4.1). This is the same behavior as discussed in Chapter 6.3.1 for the influence of the pH on the metastable zone. There are temperatures, at

which the influence by temperature is ideal to form the desired modification by means of biggest Gibbs free energy. An increase in temperature for the tetragonal modification means an decrease of the Gibbs free energy, and thus a decrease in growth and increase of dissolution rate. The same occurs for the HTO modification starting from 40 °C. A lowering of the temperature decreases the Gibbs free energy and thus the stability to form stable crystals. The crystals will dissolve faster at lower temperatures. The fastest dissolution rate is approximately at 30 °C. There is the transition point between the tetragonal and HTO modification.

6.4.3 Dissolution rate versus dissolution mechanism (induced by pH)

In Chapter 5.3.2 the influences of the dissolution mechanisms, which are influenced by the pH value, are shown for the dissolution rate. As already known from Chapter 5.1.2, the pH value is a parameter to control the resulting dissolution mechanism. For the tetragonal and HTO modification at pH 9.8 the crystals will "fall into pieces". At a pH 5.0 the crystals will shrink homogeneously. For the LTO modification at pH 5.0 the crystals "fall into pieces". At a pH 9.8 the crystals shrink homogeneously. The resulting data show that the "falling into pieces" mechanism increases the dissolution rate significantly. For the HTO modification it starts from a concentration of $0.4\,\mathrm{mg\,mL^{-1}}$ on, the dissolution rate is slower than the homogeneous shrinking crystals. This effect is explainable by a diffusion problem of the "falling into pieces" mechanism. The small particles will increase the available surface area and therefore the dissolution rate. However, around the small crystals with respect to time, the concentration reaches the solubility concentration quite fast. This will decrease the dissolution rate (unless there is some mixing or stronger convection), until the diffusion of molecules has reached a state of homogeneous mixing in the full volume of the solution. Here, an error in the measured results with the photometric method without stirring can be found.

6.4.4 Dissolution rate versus precipitant concentration

In Chapter 5.3.4, the measured dissolution rates are plotted versus precipitant concentration. Due to the increase of precipitant concentration in the *liquid phase*, the solubility of lysozyme will be lowered, and due to this the solubility curve will be moved to lower concentrations. Therefore, the absolute level of undersaturation is lower, and thus the driving force (Gibbs free energy) is lower. The resulting dissolution rate is slower if the precipitant concentration will be increased.

6.5 Enzymatic activity measurements

6.5.1 Measurement versus pH value

The shown results (see Chapter 5.4.1), give the biggest enzymatic activity at pH 6.5. At this pH value the conformation of the protein molecules in the *liquid phase* seems to be ideal, to catalyze the specific reaction which is used to determine the enzymatic activity (see Chapters 2.1.5 and 4.6). With a different pH value the conformation changes, and thus the complex mechanism which is used to perform such specific catalytic reactions are inhibited.

6.5.2 Measurement versus dissolution mechanism

There is no significant influence of the chosen dissolution mechanism to be seen on the remaining enzymatic activity of proteins after dissolution of the crystals (see Chapter 5.4.2). This opens the ability to choose the dissolution mechanism, with the desired properties depending on the wanted application of protein crystals.

6.5.3 Measurement versus buffer substance and concentration

In Chapter 5.4.3 the conditions of crystallized lysozyme chloride crystals were varied. The buffer substance and concentration were changed during the crystallization process, to observe the potential influences on the enzymatic activity. As to be seen by the results, the crystals stay “the same”. This means as already seen in the measurements of the metastable

zone (Chapter 5.2.2), and the discussion about the fundamentals in protein crystallization (Chapter 6.1), the buffer substances and concentrations are neglectable in the protein crystals. The enzymatic activity is, therefore, the same for lysozyme crystals prepared from different buffer substances or concentrations.

6.6 Shelf life of protein crystals

6.6.1 Shift in the nucleation and solubility curve during crystallization

As to be seen in Chapter 5.2.3, the slope of the solubility and nucleation curves at pH 5.0 (the measurement with retention time compared to the measurement without retention time, see the temperature profiles in Figure 5.31), shows a similar slope in Figure 5.32, if the retention time is subtracted and only the absolute crystallization cycle counts are plotted on the x axis. The plot in Figure 5.33 shows a changed slope. The retention time is now included in the x axis that the measured points are plotted versus time. This means that each crystallization cycle will change the metastable zone, and not the absolute time of the crystals inside the mother liquor, the running time. The average temperature and time for the dissolved protein and crystallized protein in the mother liquor is the same in both temperature profiles, shown in Chapter 5.2.3. The temperature of solubility remains constant during the measurements, the nucleation temperature shifts towards higher temperatures with time/cycle counts.
At pH 7.0 again, the solubility temperature during the measurement remains constant. The nucleation temperature will shift towards higher temperatures, too. There are two points which might change during the measurements. The first, is a loss of water in the measurement sample. This will also affect the solubility temperature, and is not to be seen in these results. The second, is the protein will denaturized due to the continuous crystallizing and dissolving. But in this case, the denaturation process has no effect on the protein concentration, and thus the solubility temperature. Those denaturized protein molecules are only be able to promote primary heterogeneous nucleation! This will support the temperature of nucleation. At the end of the measurement run (pH 7.0), there is a nucleation at

much lower temperature than in the previous cycles of this measurements. If there is no solubility seen anymore due to the change in modification, and the solubility is out of the temperature range used in this measurement, the substance in the measurement vessel remains opaque. At pH 9.0 some more processes occur during the measurements. The nucleation temperature seems to shift unpredictably between two or three temperatures. Obviously, here is a problem in the IR measurement technique which is already discussed in Chapter 6.3.1. The problem results from the fact, that when the probe is detecting opaque, no further nucleation or phase transition can be detected anymore! It is, however, possible that nucleation occurs at approximately 32 °C (temperature in the plot of Figure 5.35, where nucleation and solubility line have the same temperature) due to the fact that the temperature profile, the cooling, keeps running towards much lower temperaturwerees. If there is a further modification present, it is possible that there is also a second point of nucleation which is not to be seen by this technique. Or, the nucleated and growing crystals will undergo a phase transition into another modification. In both cases the turbidity devices will not detect any change in the IR signal! When heated up again, then the new (transformed) modification will dissolve according to the changed solubility temperature. This solubility temperature can have the same value as well as the nucleation temperature!

From the data in Chapter 5.2.1 it can be seen that for the pH values 9.0 to 10.5 the concentration range is chosen in a very close range. With a greater concentration range, often no nucleation appeared, or the crystals would not dissolve in a comparable temperature profile. It is shown that there are, especially at the measurement at pH 9.0, some unpredictable phase transitions which make problems during crystallization.

6.6.2 Enzymatic activity during crystallization

There is a loss of enzymatic activity in the *liquid phase* with time (see Chapter 5.4.4). Due to this, the work on the crystallization is under development. The crystallization is a method of storage of proteins with preservation of the enzymatic activity. The metastable zone width measured, is therefore increasing with cycle counts e. g. time.

6.6.3 Enzymatic activity under changing storage conditions

Chapter 5.4.5 shows the data of the enzymatic activity long-time stability tests. There are some small changes in the measured enzymatic activities after every week (e. g. changed humidity and temperature conditions), but those changes are not significant. No storability problems can be detected, except in the case of the most extreme conditions tested, 80 % humidity and 50 °C. In the range of the tested conditions of 40 to 60 % humidity and 20 to 40 °C temperature, the enzymatic activity can be defined "stable" for storage. The small changes are more to be seen at different levels of "free water" (see e. g. Chapter 5.5.2), and thus a different weight portion of the pure protein, which is able to catalyze the enzymatic activity test. Also between the three measured modifications there are no significant differences to be seen in enzymatic activity while being stored. At the above-mentioned extreme conditions, the enzymatic activity decreases significantly. At those conditions, protein crystals get a yellowish color which shows the denaturation.

6.7 Conclusions

Some points identified as not clear in literature up to today with respect to growth and dissolution of protein crystals, are clearer after the discussion in the last Chapters. The results are related to Chapter 3 the following points:

- There is an optimal pH value for the crystallization of each different protein modification (here presented based on the protein lysozyme). There is an influence of the pH value on the solubility line. There is a maximum in solubility at certain pH values. This can, especially, be seen in a 3D plot (Figure 5.24). Those pH values, at which the maximum occurs, correlate to those conditions named in literature, which lead to be the best crystals of each lysozyme crystal modification. From X-ray analyses in this work (see Chapter 5.5.1), it is known that slightly modified pH values will still lead to the same crystal lattice of the protein, until at certain deviation in pH will lead to a change in modification. The influence of the pH value on the solubility is to be found in the *liquid phase*, e. g. forces between molecules. With a maximum solubility, the released Gibbs free energy is on the highest level, and therefore the driving force to form stable crystals the biggest. At the end, the pH value will change the proton concentration. The protons are part of the equilibrium constant of the proteins.

- New methods to determine the protein crystal growth and dissolution kinetics, taking the necessity of the availability of only low amount of substances, and the dispersions into account are presented.
  The first method is a micro fluidized bed using a “micro drop dispenser” to measure crystal growth rates. Very small dosing’s of two equivalent volumes of salt and protein solutions are mixed. Due to the salting-out effect a supersaturated solution is created. The crystals inside the fluidized bed will be floated by the supersaturated solvent. The level of supersaturation will be detected by an UV/Vis photometer at 280 nm wavelength. From the volume flow rate, and the known concentrations in the dosing unit, as well as the measured

concentrations in the measurement circuit, the growth rate with respect to the growth rate dispersion can be calculated. The volume of the circuit is approximately 3 mL, and crystal masses of 10 to 200 mg have to be used in the flow cell.
The dissolution rate will be measured by a second method (set-up). A batch vessel is filled with some crystals of fixed mass, and the appropriate dissolution solvent will be added as fast as possible. The concentration in the dissolving liquid will be detected by a new measurement probe ("Vision" probe), or a UV/Vis photometer at 280 nm. From these measurements versus time, the concentration versus time can be calculated. By some calculations, the first deviation creates a plot of dissolution rate versus concentration. All the three set-ups, use a mass of crystals (10 to 200 mg) and not only one crystal. Due to this, the growth and dissolution rates will be measured not forgetting the dispersion rates.

- The "falling into pieces" dissolution mechanism as discovered and described by Müller [Mül12b] has been explained. The two different dissolution mechanisms (the new and the conventionally) for the lysozyme crystals, can be explained by repulsion forces between the protein molecules in the crystal lattice. **Due to this new knowledge, it is possible to tailor the dissolution mechanism for protein crystals with respect to fast or slow dissolution. For pharmaceutical use, this is of key importance!** A protein molecule contains of several amino acids, and thus functional groups which are loadable. If some of the conditions in the *liquid phase*, where the crystals will be dissolved are changed differently than compared to the crystallization conditions, the charges will be changed. Changed charges will change the interactions between molecules in the crystal lattice. If the interactions will be changed that the Gibbs free energy is big enough, the crystal lattice is not stable anymore, and thus the crystals will "fall into pieces". The parameter to induce the modified mechanism are determined as the pH value. A change of the pH value of two units compared to the crystallization conditions is enough, to leave the metastable zone and change the dissolution mechanism. The precipitant substance, and solvent effects from ad-

ditives and different solvents, can also be the source of the changed charges in a protein crystal. Due to "falling into pieces", rather than just shrinking and rounding, the dissolution rate will be increased. If the dissolution conditions are kept the same as used for crystallization except of course of the saturation level, the lysozyme crystals dissolve in the conventionally form, known as rounding of the edges and afterwards shrinking homogeneous mechanism.

- The enzymatic activity in the protein crystals remains constant for normal ambient temperatures and humidity's (20 to 40 °C and 40 to 60 %) according to the measured data. Between different crystal modifications, there seems to be no differences in the preservation of their enzymatic activity. Extreme conditions (80 % of humidity and 50 °C of temperature) will decrease the enzymatic activity drastically, and will results in a yellowish color of the crystals due to denaturation. Especially, the enzymatic activity of the tetragonal modification decreased by 50 %.

- Protein crystals need to be named much more precisely with much more information in their name, in order not to lead to problems in their usage with respect to their chemical and physical composition behavior. Based on X-ray measurements it could be shown that the crystal lattice parameters for slightly changed pH values in the liquid, where the crystals were grown from, did not change. In the pH range of 4.7 to 5.3, the X-ray data give no indication that the crystal lattice is changed. This means, it is the same lattice (the same crystal modification), with the same lattice parameters, found within a certain small pH range. The water content of lysozyme chloride crystals is confirmed to be approximately 35 %.
  From the fundamental analysis, it could be shown that there are some "counter ions" incorporated in the lysozyme crystals, but with varying content different from the calculated content which could be given by the pI in the *liquid phase*.
  Furthermore, the chemical composition of a protein crystal is explained. It can be confirmed that a protein crystal contains two kinds of "water" (the bounded and the "free water", the last is a

buffer rather than pure water), the protein itself with the appropriate amount of "counter ions", and salt as precipitant in the "free water". The buffer substance in the "free water" within the protein crystal is neglectable in a composition of a protein crystal, due to the low concentration in mother liquor.

As a result of this work the naming of protein crystals as e. g. lysozyme crystal has to be modified due to the fact that several parameters will affect the produced crystals (pH value, modification, precipitant as "counter ions" etc.), and as to be seen by the different dissolution mechanisms. According to the protein crystal growth process respectively their growth conditions, these can be different crystals, too. To be able to describe a protein crystal precisely enough, the following information must be included: pH value of the solution at which the protein crystals are grown, the generated modification, the kind of protein, the precipitant substance and its concentration. The pH value and the modification belong together, and the precipitant substance and concentration belong together. The "counter ion" substance is already described by the precipitant concentration. As an example for a naming of a lysozyme crystal as used in this work: "HTO(5.0)-lysozyme-(6 wt%)sodium chloride" or "LTO(9.8)-lysozyme-(4 wt%)sodium chloride"

7 Outlook

As an outlook it is possible to suggest that there is a big potential in the field of molecular modeling in the field of protein crystallization. With modeling, it should be possible to calculate the electrostatic forces between the protein molecules in the crystal lattice. With such a technique, the assumptions presented in this work could be verified or improved. As an example, in the case of an approval of all the assumptions, the needed pH value difference can be calculated to induce the "falling into pieces" mechanism of the crystals for a desired application. A key problem in the field of pharmaceutical application. Also, the ideal pH value could be predicted, if the surface charges can be calculated from the pKa values of the amino acid residuals.

There is a need of much more measurements of the kinetics of protein crystals. In this work, some new techniques to determine the dissolution and growth rate with respect to the dispersion were presented, but the measurement range is still very small. After the measurements of the protein lysozyme of this work, other proteins have to be measured with this technique to bring the crystallization of proteins one step closer to industrial mass production.

Dissolution phenomena should be examined for other proteins, than the ones examined here. Do the assumptions and findings of this work hold in other fields? Will other protein crystals also dissolve with a "falling into pieces" mechanism? Of special interest is here, the lattice energy of the protein crystals. If this energy is much higher than of the lysozyme chloride crystals, it might be possible that no "falling into pieces" mechanism is to be seen with those protein crystals.

The shelf life tests started in this work of the lysozyme chloride crystals must be carried on over a much longer period of time, since the results in this work of maximum two months is short for industrial needs.

8 Summary

The partly unusual dissolution behavior of lysozyme crystals as presented by Müller [Mül12b] were systematically investigated. Two dissolution mechanisms were found. The first dissolution mechanism is, the conventionally known rounding of the edges and homogeneous shrinking. The second mechanism is a "falling into pieces" mechanism, where new much smaller particles dissolve afterwards independently, and therefore a much faster dissolution rate can be achieved. The dissolution mechanisms can be transferred via a pH adjustment, change of "counter ions" or solvent parameters (influenced by added polymers and solvents). The two different dissolution mechanisms can be explained by repulsion forces between the protein molecules in the crystal lattice. If the dissolution conditions are kept the same as used for crystallization except of course of the saturation level, the lysozyme dissolve in the conventionally form. A change of only one parameter is enough, to induce the "falling into pieces" mechanism. With this new knowledge, it is possible to tailor the dissolution mechanism for protein crystals, with respect to fast ("falling into pieces") or slow (rounding and shrinking homogeneously) dissolution. For pharmaceutical use, e. g. this is of key importance! Several fundamental measurements, like water content, structural X-ray analysis, amount of "counter ions" etc. promote the given explanation of these mechanisms.

The effect of the pH on the metastable zone (solubility line and nucleation line) was investigated. In literature (see e. g. [Gol04; McN07; Wie02; Car92]), and from amino acids it is known that the lowest solubility occurs at the pI value. This is due to, at pH values lower than pI the molecules are positively charged, at pH values higher than pI they are negatively charged. In either case, the molecules push each other away (by Colombian repulsion), and therefore they wont to stick together. The substance is then more soluble. However, no prediction how the solubility curve shape pro-

ceeds at other points is known. Forsythe et al. [For99a] wrote: *"The effect of pH is not clearly seen and varies unpredictably with pH"*. The presented data show a decrease in solubility of higher pH values to the direction of pI. But there are also points with a local maximum of solubility at a certain pH value. The results of the X-ray analyses show that only slightly modified pH values still make the crystals crystallize with the same lattice parameters. The pH value has then, obviously, only an influence on the forces (Colombian repulsion) between molecules in the *liquid phase*. The molecules in *solid state* define lattice parameters and are fixed for each modification. If the solubilities at certain pH values show a maximum, the released Gibbs free energy at this pH is also on the maximum level. This means here are the best conditions for crystallization, and therefore for the best crystals concerning perfectness. The found pH values are exact those used in literature to crystallize the different known modifications (tetragonal and HTO at pH 5.0 [Mül12b] and [Jud99], monoclinic at pH 7.6 [Har94], LTO at pH 8.6-10.0 [Ald09b] and hexagonal at pH 8.4 [Bri06]).

Furthermore, new methods (techniques) to determine the growth and dissolution rates keeping in mind the low availability of substance, as well as the growth and dissolution rate dispersion, are developed. An average rate of growth and dissolution, which is important for industrial applications, needs to be determined.

A micro fluidized bed with a substance consumption of less than 3 mL and 10 to 200 mg of crystals in the column was developed, for the growth rate measurements. For measuring the dissolution rates, a new probe which is able to determine the concentration of protein in liquids, was used. A method using a conventional UV/Vis photometer is added to increase the amount of measured data. As a result, it was possible to show that in the case of crystals "falling into pieces", during dissolution the rate is higher.

It is clear that in case the pH value and the used "counter ions" have an influence on the dissolution mechanism, then a naming like "lysozyme crystal" is definitely not precise enough. Nobody knows from the currently used name the crystallization conditions (e. g. incorporated "counter ions", pH value, modification etc.) which, however, are essential for a predic-

tion of the dissolution mechanism of those crystals. Those parameters describe automatically the properties of the protein crystals, and a lysozyme grown in sodium chloride solution is different from a lysozyme grown e. g. in sodium bromide! A new example to give protein crystals systematic and better clarifying names is presented. In this work used crystals can be named: "HTO(5.0)-lysozyme-(6 wt%)sodium chloride" or "LTO(9.8)-lysozyme-(4 wt%)sodium chloride"

The influence of the dissolution mechanism on the enzymatic activity was investigated. There is no significant influence of the dissolution mechanism on the remaining enzymatic activity. It should be therefore possible, to tailor protein crystals with respect to their dissolution mechanism for the desired applications (fast or slow dissolution).

The enzymatic activity in the *liquid phase* measured in this work is exponentially decreasing with time. Therefore, a crystalline form is necessary to store and at the same time to preserve the activity. All shelf life tests in a climate chamber, with changing conditions in the range of 20 to 40 °C and 40 to 60 % humidity, show no change in enzymatic activity. Except the extreme conditions (80 % humidity and 50 °C), where the enzymatic activity of all measured modifications decrease significant (by up to 50 %) within one week, and the crystals get a yellowish in color. At this conditions the crystals will be decomposed.

9 Zusammenfassung

Das erstmals von Müller [Mül12b] präsentierte ungewöhnliche Auflösungsverhalten von Lysozym Kristallen wurden systematisch untersucht. Es wurden zwei voneinander unterschiedliche Auflösungsverhalten gefunden. Der bereits bekannte Auflösungsmechanismus verläuft über ein Verrunden der Ecken, gefolgt von einem Schrumpfen der Kristalle mit der Zeit. Beim zweiten Auflösungsmechanismus zerfallen die Kristalle in kleinere Fragmente, welche sich danach separat weiter auflösen. Durch die Erhöhung der Oberfläche wird die Auflösungsgeschwindigkeit beim zweiten Auflösungsmechanismus erhöht. Das Auflösungsverhalten hängt ab von der Änderung des pH-Wertes, Änderung der im Kristall eingebauten Gegenionen oder Änderung von Lösungsmittelparametern (durch Zugabe von Polymeren oder mischbaren organischen Lösungsmitteln). Das Auftreten der unterschiedlichen Auflösungsmechanismen lässt sich damit erklären, dass Abstoßungskräfte zwischen den Proteinmolekülen im Kristallgitter sich unter gewissen Bedingungen voneinander abstoßen. Werden also die Bedingungen (natürlich muss die Löslichkeit entsprechend angepasst werden) entsprechend denen während der Kristallisation der Kristalle verwendet, lösen sich die Kristalle unter abrunden der Ecken und folgendem Schrumpfen auf. Bereits die Änderung eines Parameters genügt um ein Zerfallen der Proteinkristalle zu initiieren. Es ist somit möglich, maßgeschneiderte Kristalle für die entsprechenden Anwendungen (schnelles oder langsames Auflösen) zu erzeugen. Für z. B. pharmazeutische Anwendungsgebiete nimmt diese Möglichkeit eine Schlüsselrolle ein! Zusätzlich wurden viele für das weitere Verständnis wichtige Grundlagenmessungen durchgeführt, wie z. B. die Röntgenbeugung, Wassergehalte im Kristall, sowie die Menge der im Kristall eingebauten Gegenionen.

Der Einfluss des pH-Wertes auf den metastabilen Bereich (Löslichkeits- und Keimbildungskonzentration) wurde untersucht. Entsprechend der Lit-

eratur (z. B. [Gol04], [McN07], [Wie02] und [Car92]) ist: Die niedrigste Löslichkeit dort zu finden, wo der IEP-Wert dem pH-Wert entspricht. Vom Isoelektrischen Punkt (IEP-Wert) aus in Richtung niedrigen pH-Werten erfolgt eine positive Ladung der Moleküle, in Richtung zu höheren pH-Werten erfolgt eine negative Ladung der Moleküle. In beiden Fällen führt dies zu einer abstoßenden Wechselwirkung untereinander (Coulomb Wechselwirkungen), die Moleküle wollen sich nicht gegenseitig annähern (einen Kristall bilden) und die Löslichkeit ist daher höher. Jedoch gibt es in der Literatur keine Angaben dazu, wie die Kurven vom Isoelektrischen Punkt in beiden Richtungen weiter verlaufen. Forsythe et al. [For99a] schrieb dazu, dass der Einfluss des pH-Wertes nicht klar zu bestimmen war bzw. die Kurve unvorhersehbar verläuft. Die in dieser Arbeit ermittelten Messwerte zeigen, dass die Löslichkeit vom isoelektrischen Punkt aus in beide Richtungen abfällt. Es gibt aber zusätzlich diverse lokale Löslichkeitsmaxima verteilt über die gesamte Kurve. Von der Messung der Röntgenbeugung zur Kristallstrukturaufklärung ist bekannt, dass kleine Änderungen im pH-Wert nicht dazu führen, dass sich die Gitterparameter für das Kristallisieren der entsprechenden Modifikation ändern. Daraus lässt sich schlussfolgern, dass der Einfluss des pH-Wertes auf den metastabilen Bereich in Eigenschaften der flüssigen Phase zu finden sind, denn die Gitterparameter im Kristall bleiben dabei konstant. Die durch lokale Maxima gefundenen pH-Werte korrelieren bezüglich der Bedingungen für die perfektesten Kristalle größtenteils mit den in der Literatur zu findenden bekannten Kristallmodifikationen, hier für den Fall des Proteins Lysozym (tetragonal und HTO beim pH-Wert 5.0 [Mül12b] und [Jud99], monoklin beim pH-Wert 7.6 [Har94], LTO beim pH-Wert 8.6 bis 10.0 [Ald09b] und hexagonal beim pH-Wert 8.4 [Bri06]).

Es wurden neue Methoden (Versuchstechniken) entwickelt um die Wachstums- und Auflösungsgeschwindigkeit von Proteinkristallen zu vermessen. Dies ist notwendig um die für industrielle Anwendungen so wichtigen mittleren Werte für das Wachstum und das Auflösen zu ermitteln. Dabei ist die Verfügbarkeit von nur kleinen Mengen an Substanz und die Berücksichtigung der Wachstums- und Auflösedispersion zu beachten.

Es wurde eine kleine Fließbettapparatur entwickelt, welche mit einem Produktvolumen von 3 mL und nur 10 bis 200 mg an Kristallen in der Säule zur Messung der Wachstumsraten auskommt. Für die Messung der Auflösungsgeschwindigkeit wurde eine neue Messsonde verwendet, welche eine Konzentrationsbestimmung der Proteine innerhalb der Lösung ermöglicht. Diese Methode wurde unter Verwendung eines UV/Vis Photometers erweitert um auch Messwerte ohne Prototypmesssonde zu generieren. Der Zerfallmechanismus der Proteinkristalle führt zu einer signifikanten Beschleunigung der Auflösungsgeschwindigkeit.

Da der pH-Wert und die im Kristall verbauten Gegenionen einen Einfluss auf den resultierenden Auflösungsmechanismus ausüben wird klar, dass die Bezeichnung z. B. eines "Lysozym Kristalls" nicht die nötigen Informationen enthält um diesen präzise beschreiben zu können. Die verwendeten Kristallisationsbedingungen (pH-Wert, eingebaute Gegenionen, Modifikation etc.) werden nicht ersichtlich. Diese werden allerdings benötigt um den Auflösungsmechanismus voraussagen zu können. Diese Parameter beschreiben automatisch bestimmte Eigenschaften der Kristalle, denn ein Lysozym Kristall gewachsen in einer Natriumchlorid Lösung ist ein anderes Kristall, als ein in Natriumbromid gewachsener. Als Beispiel könnte die zukünftige Beschreibung lauten: "HTO(5.0)-Lysozym-(6 wt%)Natriumchlorid" oder "LTO(9.8)-Lysozyme-(4 wt%)Natriumchlorid"

Es wurde überprüft, ob das erzwungene "Zerfallen" der Proteinkristalle in kleine Fragmente zu einer Verringerung der resultierenden enzymatischen Aktivität führt. Die Ergebnisse zeigen keine signifikanten Unterschiede in der resultierenden enzymatischen Aktivität zwischen den untersuchten Auflösungsmechanismen. Somit ist es möglich durch gezielte Wahl der Kristallisations- bzw. Auflösebedingungen der Proteinkristalle, den Auflösungsmechanismus und somit die Auflösungsraten gezielt maßzuschneidern.

Die gemessene enzymatische Aktivität über die Zeit nimmt in flüssigen Medien exponentiell ab. Aus diesem Grund findet die Kristallisation Anwendung um die Lagerstabilität (enzymatische Aktivität) zu erhöhen. Die

Lagerungsstabilitätsmessungen (enzymatische Aktivität unter wechselnden Umweltbedingungen in einer Klimakammer zwischen 20 und 40 °C und 40 bis 60 % Luftfeuchtigkeit) der Lysozymchlorid Kristalle verschiedener Modifikationen zeigen, dass sich die Aktivität der Kristalle über die Messdauer von zwei Monaten nicht verändert. Erst unter extremen Bedingungen (80 % Luftfeuchtigkeit und 50 °C Temperatur) zeigt sich innerhalb einer Woche eine signifikante Verringerung der enzymatischen Aktivität aller vermessener Modifikationen. Besonders stark fällt diese Verringerung für die tetragonale Modifikation mit 50 % aus. Die Kristalle verfärben sich gelb und zersetzen sich.

List of symbols and abbreviations

$\Delta A450$	– absorbance at 450 nm
ΔK	– temperature difference in kelvin
Δm_{cryst}	– mass increase of crystals
Δt	– measurement time interval
°C	– degree celsius
3D	– third dimension
A	– ampere
a.u.	– atomar unit
$\beta_{circuit}$	– mass concentration of circuit
$\beta_{solution}$	– mass concentration of solution
cm	– centi meter
conc.	– concentration
d	– distance between lattice planes
e. g.	– exempli gratia
et al.	– et alii - and others
GRD	– growth rate dispersion
h	– hour
HPLC	– high pressure liquid chromatography
HTO	– High Temperature Orthorhombic
ICP	– inductive coupled plasma
IEP	– Isoelektrischer Punkt, german translation of pI
IR	– infrared
κ	– Debye length
KG	– Kommanditgesellschaft
LALLS	– low angle laser light scattering

λ	– wavelength
LTO	– Low Temperature Orthorhombic
µL	– micro liter
m_{cryst_0}	– mass of crystals at time zero
mg	– milli gramm
min	– minute
mL	– milli liter
mm	– milli meter
MS	– mass spectometer
n	– order of diffraction
nm	– nano meter
OD_{450}	– optical density at wavelenght 450 nm
OES	– optical emission spectroscopy
PEG	– polyethylen glycol
PEG_{6000}	– polyethylen glycol mass number 6000
pH	– potential of hydrogen
pI	– isoelectric point
pKa	– dissociation constant
R	– organic residue
tetra	– tetragonal
TGA	– thermogravimetric analyse
θ	– theta, bragg angle
USB	– universal serial bus
UV	– ultra violett
$\dot{V}_{dos}$	– volume rate of dosing
$V_{solution}$	– volume of solution
Vis	– visible
wt%	– weight percent
w/	– with
w/o	– without
w_{cryst}	– mass fraction of crystals

Bibliography

[Ald09a] N. Aldabaibeh. "Towards an improved understanding of the variables controlling crystal modification and phase transition in protein crystals". PhD thesis. Illinois Institute of Technology, 2009.
URL: http://gradworks.umi.com/34/17/3417924.html.

[Ald09b] N. Aldabaibeh, M. J. Jones, A. S. Myerson, and J. Ulrich. "The Solubility of Orthorhombic Lysozyme Crystals Obtained at High pH". *Crystal Growth & Design* 9 (2009) 7, 3313–3317.
ISSN: 1528-7505.
DOI: 10.1021/cg900113e.

[Art82] P. J. Artymiuk, C. C. F. Blake, D. W. Rice, and K. S. Wilson. "The structures of the monoclinic and orthorhombic forms of hen egg-white lysozyme at 6 Å resolution". 38 (1982) 3, 778–783.
DOI: 10.1107/s0567740882004075.

[Aun69] K. C. Aune and C. Tanford. "Thermodynamics of the denaturation of lysozyme by guanidine hydrochloride. I. Dependence on pH at 25°". *Biochemistry* 8 (1969) 11, 4579–4585.
DOI: 10.1021/bi00839a052.

[Bei01] S. Beilles, P. Cardinael, E. Ndzié, S. Petit, and G. Coquerel. "Preferential crystallisation and comparative crystal growth study between pure enantiomer and racemic mixture of a chiral molecule: 5-ethyl-5-methylhydantoin". *Chemical Engineering Science* 56 (2001) 7, 2281–2294.
ISSN: 0009-2509.
DOI: 10.1016/s0009-2509(00)00442-5.

[Bre08] A. Breda, N. Valadares, and O. Norberto de Souza. "Protein Structure, Modelling and Applications." Ed. by A. Gruber, A. Durham, and C. Huynh. 2008.
URL: https://www.ncbi.nlm.nih.gov/books/NBK6824/.

[Bri06] C. Brinkmann, M. S. Weiss, and E. Weckert. "The structure of the hexagonal crystal form of hen egg-white lysozyme." eng. *Acta Crystallogr D Biol Crystallogr* 62 (2006) Pt 4, 349–355.
DOI: 10.1107/S0907444906000825.

[Bud12] H. Budzikiewicz and M. Schäfe. *Massenspektrometrie*. Wiley VCH Verlag GmbH, 2012.
ISBN: 3527329110.
URL: http://www.ebook.de/de/product/18118201/herbert_budzikiewicz_mathias_schaefer_massenspektrometrie.html.

[Cac91a] E. Cacioppo, S. Munson, and M. L. Pusey. "Protein solubilities determined by a rapid technique and modification of that technique to a micro-method". *Journal of Crystal Growth* 110 (1991) 1-2, 66–71.
DOI: 10.1016/0022-0248(91)90867-5.

[Cac91b] E. Cacioppo and M. L. Pusey. "The solubility of the tetragonal form of hen egg white lysozyme from pH 4.0 to 5.4". *Journal of Crystal Growth* 114 (1991) 3, 286–292.
DOI: 10.1016/0022-0248(91)90043-5.

[Car92] C. Carter Jr, A. Ducruix, and R. Giegé. *Crystallization of Nucleic Acids and Proteins*. 1992.

[Cli39] D. R. Clippinger and C. W. Foulk. "Electrometric Indicators with the Dead-Stop End-Point System: Applications to Neutralization and Precipitation Reactions". *Industrial & Engineering Chemistry Analytical Edition* 11 (1939) 4, 216–218.
DOI: 10.1021/ac50132a016.

[Des11] M. A. Dessau and Y. Modis. "Protein Crystallization for X-ray Crystallography". *Journal of Visualized Experiments* (2011) 47.
DOI: 10.3791/2285.

[Dur86] S. Durbin and G. Feher. "Crystal growth studies of lysozyme as a model for protein crystallization". *Journal of Crystal Growth* 76 (1986) 3, 583–592.
DOI: 10.1016/0022-0248(86)90175-2.

[Dur96] S. D. Durbin and G. Feher. "Protein Crystallization". *Annual Review of Physical Chemistry* 47 (1996), 171–204.
DOI: 10.1146/annurev.physchem.47.1.171.

[Fab93] J. Fabian and J. Ulrich. "Dissolution Like Crystal Growth - a Two Step Process-Presentation of Experimental Evidence". *proceeding 12th Symposium on Industrial Crystallization*. Ed. by Z. H. Rojkowski. Vol. 2. 12. 1993, pp. 41–46.

[For96] E. L. Forsythe and M. L. Pusey. "The effects of acetate buffer concentration on lysozyme solubility". *Journal of Crystal Growth* 168 (1996) 1-4, 112–117.
DOI: 10.1016/0022-0248(96)00368-5.

[For99a] E. L. Forsythe, R. A. Judge, and M. L. Pusey. "Tetragonal Chicken Egg White Lysozyme Solubility in Sodium Chloride Solutions". *Journal of Chemical & Engineering Data* 44 (1999) 3, 637–640.
DOI: 10.1021/je980316a.

[For99b] E. L. Forsythe, E. H. Snell, C. C. Malone, and M. L. Pusey. "Crystallization of chicken egg white lysozyme from assorted sulfate salts". *Journal of Crystal Growth* 196 (1999) 2-4, 332–343.
ISSN: 0022-0248.
DOI: 10.1016/s0022-0248(98)00843-4.

[Gil89] S. C. Gill and P. H. von Hippel. "Calculation of protein extinction coefficients from amino acid sequence data". *Anal. Biochem.* 182 (1989) 2, 319–326.

[Gol04] A. P. Golovanov, G. M. Hautbergue, S. A. Wilson, and L.-Y. Lian. "A simple method for improving protein solubility and long-term stability". *Journal of the American Chemical Society* 126 (2004) 29, 8933–8939.

[Gro12] J. H. Gross. *Massenspektrometrie*. Spektrum-Akademischer Verlag, 2012.
ISBN: 3827429803.
URL: http://www.ebook.de/de/product/19189592/juergen_h_gross_massenspektrometrie.html.

[Har06] K. Harata and T. Akiba. "Structural phase transition of monoclinic crystals of hen egg-white lysozyme". *Acta Cryst D* 62 (2006) 4, 375–382.
ISSN: 0907-4449.
DOI: 10.1107/s0907444906001314.

[Har14] D. C. Harris. *Lehrbuch der Quantitativen Analyse*. Springer-Verlag GmbH, 2014. XV pp.
ISBN: 3642377874.
URL: http://www.ebook.de/de/product/20649935/daniel_c_harris_lehrbuch_der_quantitativen_analyse.html.

[Har94] K. Harata. "X-ray structure of a monoclinic form of hen egg-white lysozyme crystallized at 313 K. Comparison of two independent molecules". *Acta Crystallographica Section D: Biological Crystallography* 50 (1994) 3, 250–257.

[Hof88] F. Hofmeister. "Zur Lehre von der Wirkung der Salze". *Archiv für Experimentelle Pathologie und Pharmakologie* 24 (1888) 4-5, 247–260.
DOI: 10.1007/bf01918191.

[Hol07] A. F. Holleman and E. Wiberg. *Lehrbuch der anorganischen Chemie*. Ed. by N. Wiberg. Berlin [u.a.], 2007.
URL: http://www.reference-global.com/action/showBook?doi=10.1515/9783110177701.

[How88] S. B. Howard, P. J. Twigg, J. K. Baird, and E. J. Meehan. "The solubility of hen egg-white lysozyme". *Journal of Crystal Growth* 90 (1988) 1-3, 94–104.
DOI: 10.1016/0022-0248(88)90303-x.

[Hun03] C. Hunte, G. von Jagow, and H. Schagger, eds. *Membrane Protein Purification and Crystallization: A Practical Guide*. ACADEMIC PR INC, 2003. 316 pp.
ISBN: 0123617766.
URL: http://www.ebook.de/de/product/4256795/membrane_protein_purification_and_crystallization_a_practical_guide.html.

[Jon14] M. Jones. *On the Industrial Crystallization of Proteins*. Berichte aus der Verfahrenstechnik. Shaker Aachen, 2014.
ISBN: 9783844033557.
URL: https://books.google.de/books?id=qR4ZrgEACAAJ.

[Jud99] R. A. Judge, R. S. Jacobs, T. Frazier, E. H. Snell, and M. L. Pusey. "The Effect of Temperature and Solution pH on the Nucleation of Tetragonal Lysozyme Crystals". *Biophysical Journal* 77 (1999) 3, 1585–1593.
ISSN: 0006-3495.
DOI: 10.1016/s0006-3495(99)77006-2.

[Kam78] Z. Kam, H. Shore, and G. Feher. "On the crystallization of proteins". *Journal of Molecular Biology* 123 (1978) 4, 539–555.
ISSN: 0022-2836.
DOI: 10.1016/0022-2836(78)90206-1.

[Kar94] P. Karlson, D. Doenecke, and J. Koolman. *Kurzes Lehrbuch der Biochemie für Mediziner und Naturwissenschaftler*. 14., neub. Aufl. Stuttgart [u.a.]: Thieme, 1994. XV, 580.
ISBN: 3133578146.

[Kec12] C. M. Keck and H. H. Müller. *Moderne Arzneiformen und Pharmazeutische Technologie - die aktuelle Ergänzung zu den "Standardbüchern"*. 2012.

[Lim98] K. Lim, A. Nadarajah, E. L. Forsythe, and M. L. Pusey. "Locations of bromide ions in tetragonal lysozyme crystals." eng. *Acta Cryst D* 54 (1998) Pt 5, 899–904.

[Mao12] S. Maosoongnern, V. Diaz Borbon, A. E. Flood, and J. Ulrich. "Introducing a Fast Method to Determine the Solubility and Metastable Zone Width for Proteins: Case Study Lysozyme". *Ind. Eng. Chem. Res.* 51 (2012) 46, 15251–15257.
ISSN: 1520-5045.
DOI: 10.1021/ie300799d.

[Mat03] Y. Matsuura and A. A. Chernov. "Morphology and the strength of intermolecular contacts in protein crystals." eng. *Acta Crystallogr D Biol Crystallogr* 59 (2003) Pt 8, 1347–1356.

[Mat68] B. W. Matthews. "Solvent content of protein crystals." eng. *J Mol Biol* 33 (1968) 2, 491–497.

[Mat88] M. Matsuoka and A. Sumitani. "Rate of composition changes of organic solid solution crystals in sweating operations." *J. Chem. Eng. Japan* 21 (1988) 1, 6–10.
ISSN: 0021-9592.
DOI: 10.1252/jcej.21.6.

[McN07] E. J. McNally and J. E. Hastedt. *Protein formulation and delivery*. CRC Press, 2007.

[McP90] A. McPherson. "Current approaches to macromolecular crystallization". *European Journal of Biochemistry* 189 (1990) 1, 1–23.
ISSN: 1432-1033.
DOI: 10.1111/j.1432-1033.1990.tb15454.x.

[Moh96a] H. A. Mohameed and J. Ulrich. "Influence of the pH-Value on the Growth and Dissolution Rate of Potassium Chloride". *Crystal Research and Technology* 31 (1996) 1, 27–31.
DOI: 10.1002/crat.2170310107.

[Moh96b] H.-A. Mohameed. "Wachstumskinetik in der Lösungskristallisation mit Fremdstoffen". PhD thesis. Universität Bremen, 1996.

[Mor05] R. L. Moritz and R. J. Simpson. "Liquid-based free-flow electrophoresis-reversed-phase HPLC: a proteomic tool". *Nature Methods* 2 (2005) 11, 863–873.
ISSN: 1548-7105.
DOI: 10.1038/nmeth1105-863.

[Mul01] J. W. Mullin. *Crystallization*. Elsevier Science, 2001.
URL: http://www.ebook.de/de/product/15167552/j_w_mullin_crystal-%20lization.html.

[Mül12a] C. Müller and J. Ulrich. "The dissolution phenomenon of lysozyme crystals". *Crystal Research and Technology* 47 (2012) 2, 169–174.
ISSN: 0232-1300.
DOI: 10.1002/crat.201100553.

[Mül12b] C. Müller. "How to describe protein crystals correctly? -case study of lysozyme crystals-". PhD thesis. Martin-Luther-Universität Halle-Wittenberg, 2012.
URL: http://digital.bibliothek.uni-halle.de/hs/content/titleinfo/1177647.

[Nad96] A. Nadarajah and M. L. Pusey. "Growth Mechanism and Morphology of Tetragonal Lysozyme Crystals". *Acta Crystallographica Section D Biological Crystallography* 52 (1996) 5, 983–996.
DOI: 10.1107/s0907444996004532.

[Nöl02] J. Nölte. *ICP Emissionsspektrometrie für Praktiker*. Wiley VCH Verlag GmbH Weinheim, 2002.
ISBN: 3527303510.
URL: http://www.ebook.de/de/product/1402923/joachim_noelte_icp_emissionsspektrometrie_fuer_praktiker.html.

[Oki99] H. Oki, Y. Matsuura, H. Komatsu, and A. A. Chernov. "Refined structure of orthorhombic lysozyme crystallized at high temperature: correlation between morphology and intermolecular contacts". *Acta Crystallographica Section D Biological Crystallography* 55 (1999) 1, 114–121.
DOI: 10.1107/s0907444998008713.

[Oma10] W. Omar, J. Chen, and J. Ulrich. "Reduction of seawater scale forming potential using the fluidized bed crystallization technology". *Desalination* 250 (2010) 1, 95–100.
ISSN: 0011-9164.
DOI: 10.1016/j.desal.2009.03.013.

[Pau07] M. Pauchet and G. Coquerel. "Polar Dissolution and Regrowth of (±)-Modafinil Twins Grown in Gels". *Crystal Growth & Design* 7 (2007) 9, 1612–1614.
ISSN: 1528-7505.
DOI: 10.1021/cg070115f.

[PhI1] *General Chemistry Online! - Acid-Base Indicators*.
URL: http://antoine.frostburg.edu/chem/senese/101/acidbase/indicators.shtml.

[PhI2] *Lexikon der Chemie - Indikatoren*.
URL: http://www.spektrum.de/lexikon/chemie/indikatoren/4426.

[Pod06] R. Podgornik and M. Ličer. "Polyelectrolyte bridging interactions between charged macromolecules". *Current Opinion in Colloid & Interface Science* 11 (2006) 5, 273–279.
DOI: 10.1016/j.cocis.2006.08.001.

[Pus02] M. L. Pusey and A. Nadarajah. "A Model for Tetragonal Lysozyme Crystal Nucleation and Growth". *Crystal Growth & Design* 2 (2002) 6, 475–483.
ISSN: 1528-7505.
DOI: 10.1021/cg0200107.

[Pus88] M. L. Pusey and K. Gernert. "A method for rapid liquid-solid phase solubility measurements using the protein lysozyme". *Journal of Crystal Growth* 88 (1988) 3, 419–424.
DOI: 10.1016/0022-0248(88)90017-6.

[Pus93] M. L. Pusey. "A computer-controlled microscopy system for following protein crystal face growth rates". *Review of Scientific Instruments* 64 (1993) 11, 3121.
DOI: 10.1063/1.1144318.

[Ric92] D. Rice. "Crystallization of nucleic acids and proteins". *Trends in Biochemical Sciences* 17 (1992) 9, 364.
DOI: 10.1016/0968-0004(92)90316-2.

[Rie04] E. Riedel. *Anorganische Chemie*. 6. Aufl. Berlin [u.a.]: de Gruyter, 2004. XVI, 935.
ISBN: 3110181681.

[Riè91] M. M. Riès-Kautt and A. F. Ducruix. "Crystallization of basic proteins by ion pairing". *Journal of Crystal Growth* 110 (1991) 1-2, 20–25.
DOI: 10.1016/0022-0248(91)90861-x.

[Rud02] A. K. Rudolf Allmann. *Röntgenpulverdiffraktometrie*. Springer-Verlag GmbH, 2002. VI pp.
ISBN: 3540439676.
URL: http://www.ebook.de/de/product/2048126/rudolf_allmann_a_kern_roentgenpulverdiffraktometrie.html.

[Sab] R. Sabnis. *Handbook of Acid-Base Indicators. 2008*.

[Saz99] G. Sazaki, Y. Nagatoshi, Y. Suzuki, S. D. Durbin, S. Miyashita, T. Nakada, and H. Komatsu. "Solubility of tetragonal and orthorhombic lysozyme crystals under high pressure". *Journal of Crystal Growth* 196 (1999) 2-4, 204–209.
DOI: 10.1016/s0022-0248(98)00861-6.

[Sch55] W. Schöniger. "Eine mikroanalytische Schnellbestimmung von Halogen in organischen Substanzen". *Mikrochim Acta* 43 (1955) 1, 123–129.
ISSN: 1436-5073.
DOI: 10.1007/bf01220660.

[Sch84] E. Scholz. "Karl Fischer". *Karl Fischer Titration* (1984).
DOI: 10.1007/978-3-642-69989-4_1.

[Shu52] D. Shugar. "The measurement of lysozyme activity and the ultra-violet inactivation of lysozyme". *Biochimica et Biophysica Acta* 8 (1952), 302–309.
ISSN: 0006-3002.
DOI: 10.1016/0006-3002(52)90045-0.

[Som06] P. Somasundaran and A. T. Hubbard, eds. *Encyclopedia of surface and colloid science. P.* 2. ed. Vol. Vol. 1. [Absorption - adsorption]. Literaturangaben. New York, NY [u.a.]: Taylor & Francis, 2006. LXVIII, 814, 100.
ISBN: 9780849396085.

[Spa08] V. Z. Spassov and L. Yan. "A fast and accurate computational approach to protein ionization". *Protein Science* 17 (2008) 11, 1955–1970.
DOI: 10.1110/ps.036335.108.

[Sul08] S. M. Sullivan and T. Holyoak. "Enzymes with lid-gated active sites must operate by an induced fit mechanism instead of conformational selection". *Proceedings of the National Academy of Sciences* 105 (2008) 37, 13829–13834.
DOI: 10.1073/pnas.0805364105.

[Sun14] Sunspeanzler. 2014.
URL: https://creativecommons.org/licenses/by-sa/3.0/deed.en.

[Tan72] C. Tanford and R. Roxby. "Interpretation of protein titration curves. Application to lysozyme". *Biochemistry* 11 (1972) 11, 2192–2198.
ISSN: 1520-4995.
DOI: 10.1021/bi00761a029.

[Ulr11] J. Ulrich and T. Stelzer. "Crystallization. Kirk-Othmer Encyclopedia of Chemical Technology." John Wiley & Sons, Inc. Hoboken, 2011, pp. 1–63.
ISBN: 9780471238966.
DOI: 10.1002/0471238961.0318251918152119.a01.pub3.

[Ulr15] J. Ulrich and M. Pietzsch. "What is a protein crystal? Can we apply the terminology of classical industrial crystallization to them?" *Crystal Research and Technology* 50 (2015) 7, 560–565.
ISSN: 0232-1300.
DOI: 10.1002/crat.201500057.

[Ulr87] J. Ulrich and M. Stepanski. "Einfluß der Oberflächen-Beschaffenheit auf das Kristallwachstum aus Lösungen". *Chemie Ingenieur Technik* 59 (1987) 5, 402–404.
DOI: 10.1002/cite.330590508.

[Ulr89] J. Ulrich. "Growth rate dispersion — a review". *Crystal Research and Technology* 24 (1989) 3, 249–257.
DOI: 10.1002/crat.2170240302.

[Wal13] H. S. Walter Borchardt-Ott. *Kristallographie*. Springer-Verlag GmbH, 2013. XIV pp.
ISBN: 3642348106.
URL: http://www.ebook.de/de/product/19990398/walter_borchardt_ott_heidrun_sowa_kristallographie.html.

[Wan07] J. Wang, M. Dauter, R. Alkire, A. Joachimiak, and Z. Dauter. "Triclinic lysozyme at 0.65 Å resolution". 63 (2007) 12, 1254–1268.
DOI: 10.1107/s0907444907054224.

[Wie02] J. Wiencek. "Protein crystallization". *Handbook of Industrial Crystallization, Second Edition*. Ed. by A. Myerson. Butterworth-Heinemann Oxford, 2002. Chap. 12, pp. 267–285.
ISBN: 0750670126.

[Zha09] Y. Zhang and P. S. Cremer. "The inverse and direct Hofmeister series for lysozyme". *Proceedings of the National Academy of Sciences* 106 (2009) 36, 15249–15253.
DOI: 10.1073/pnas.0907616106.

Statement of authorship

I declare under oath that this is my own work entirely and has been written without any help from other people. I used only the sources mentioned and included all the citations correctly both in word and content.

This thesis has not been used previously at this or any other university in order to achieve an academic degree.

Halle (Saale), June 7^{th}, 2017

Ronny Oswald

Curriculum vitae

Ronny Oswald

date of birth:	April 25^{th} 1982 in Dessau
citizenship:	Germany
degree:	Certified chemist (Diplom-Chemiker)
e-mail:	ronny.oswald <at> web.de

Career and education

since 10/2012	Research associate at the Chair of Thermal Process Technology, Martin Luther University Halle-Wittenberg
09/2005-03/2012	Study of Chemistry Martin Luther University Halle-Wittenberg
01/2002-08/2005	Chemical technician DHW Deutsche Hydrierwerke GmbH Rodleben
09/1998-01/2002	Apprenticeship as chemical technician DHW Deutsche Hydrierwerke GmbH Rodleben
09/1988-08/1998	Secondary school Gesamtschule Dessau Kleinkühnau

List of publications

2014 R. Oswald and J. Ulrich. "The dissolution behavior of lysozyme crystals". *Proceedings of the 19th International Symposium on Industrial Crystallization*. Ed. by B. Biscans and M. Mazzotti. University of Toulouse, Toulouse, France. 2014, pp. 331–333

2015 R. Oswald and J. Ulrich. "Changing the pH-value in crystallization and dissolution of lysozyme crystals". *Proceedings of the BIWIC 2015, 22th International Workshop on Industrial Crystallization*. Ed. by K.-J. Kim and K. Lee. Hanbat National University, Daejeon, South Korea. 2015, pp. 92–98.
ISBN: 978-89-97590-15-5

2015 R. Oswald and J. Ulrich. "Dissolution Behavior of Lysozyme Crystals". *Crystal Growth & Design* 15 (2015) 9, 4556–4562.
ISSN: 1528-7505.
DOI: 10.1021/acs.cgd.5b00821

2016 R. Oswald, M. Pietzsch, and J. Ulrich. "A view inside the nature of protein crystals". *Proceedings of the Asian Crystallization Technology Symposium 2016*. Ed. by D. Wei. Tianjin University, Tianjin, China. 2016, pp. 84–86

2016 R. Oswald and J. Ulrich. "New Techniques to Determine Growth and Dissolution Kinetics of Protein Crystals". *Proceedings of BIWIC 2016, 23th International Workshop on Industrial Crystallization*. Ed. by bibinitperiod Lorenz and H. Buchholz. Cuvillier Verlag Göttingen, Germany, 2016, pp. 138–143.
ISBN: 978-3-7369-9322-8

2016 R. Oswald, M. Pietzsch, and J. Ulrich. "A view inside the nature of protein crystals". *Journal of Crystal Growth* 469 (2017) 9, 176–179.
DOI: 10.1021/acs.cgd.5b00821

List of conference contributions

2014 Poster. "The dissolution behavior of lysozyme crystals". *ISIC19 - 19th International Symposium on Industrial Crystallization*, 16.-19.09., Toulouse, France.

2014 Lecture. "The dissolution behavior of lysozyme crystals". *University of Szeged, Faculty of Pharmacy*, 04.11., Szeged, Hungary.

2015 Lecture. "Untersuchungen des metastabilen Bereichs vom Protein - Lysozym in Abhängigkeit des pH-Wertes". *ProcessNet Fachausschuss - Jahrestreffen des Fachausschuss Kristallisation*, 18.-20.03., Magdeburg, Germany.

2015 Lecture. "Determination of the average growth rates of protein crystals for equipment design". *Achema 2015*, 15.-19.06., Frankfurt am Main, Germany

2015 Lecture and Poster. "Changing the pH-value in crystallization and dissolution of lysozyme crystals". *BIWIC 2015, 22th International Workshop on Industrial Crystallization*, Hanbat National University, 09.-11.09., Daejeon, South Korea.

2016 Lecture and Poster. "A view inside the nature of protein crystals". *ACTS 2016 - Asian Crystallization Technology Symposium*, 25.-27.05., Tianjin, China.

2016 Poster. "New methods to determine the kinetics of protein crystal growth and dissolution". *BIWIC 2016, 23th International Workshop on Industrial Crystallization*, Max Planck Institut, 06.-08.09., Magdeburg, Germany.